Structure and Function of *Tetrahymena thermophila* Telomerase RNA

by
Jason Donald Legassie

A dissertation submitted to the faculty of the University of North Carolina at Chapel Hill in partial fulfillment of the requirements for the degree of Doctor of Philosophy in the School of Pharmacy (Pharmaceutical Sciences).

Chapel Hill
2007

Approved By:

Advisor: Professor Michael B. Jarstfer

Reader: Professor Thomas A. Kunkel

Reader: Professor Andrew Lee

Reader: Professor Jian Liu

Reader: Professor Rihe Liu

This dissertation is dedicated to

my mom and dad who always believed in me and told me

I could do anything I put my mind to,

my sisters, Sherry and Lisa, who have provided more support

in every aspect of my life than I could have ever asked for,

and my loving wife and son, Tanya and Austin, who have provided

a nurturing environment for me to grow as a person.

ACKNOWLEDGEMENTS

The author wishes to express his sincere gratitude to:

Dr. Michael B. Jarstfer for his guidance, patience and friendship throughout my graduate career

Drs. Thomas A. Kunkel, Andrew Lee, Jian Liu, and Rihe Liu for their valuable insight and mentorship to this endeavor

Dr. Cathy D. Thaler for her mentorship during my early research career

Dr. Kevin Weeks and his lab members for their assistance and collaboration

The UNC School of Pharmacy Graduate Education Committee and GlaxoSmithKline for their fellowship during my graduate career

Lab members from the Jarstfer laboratory for their comments, assistance, and friendship

ABSTRACT

Jason Donald Legassie: Structure and Function of the *Tetrahymena thermophila* Telomerase RNA
(Under the Direction of **Michael B. Jarstfer, Ph.D.**)

Telomerase is a specialized reverse transcriptase, which synthesizes telomeric repeats to the 3' ends of linear chromosomes. By helping to maintain adequate telomere length, telomerase ensures chromosomal and genetic stability. Telomerase represents a possible universal cancer target as its expression and activity are upregulated in >85% of all cancers. This thesis describes two major areas of investigation of important structural aspects of the RNA subunit of a model telomerase enzyme from the unicellular ciliate, *Tetrahymena thermophila.*

In the first major area of research, we engineered two mutant forms of the *Tetrahymena* telomerase RNA, tTER, that contain DNA only in the templating region. These chimeric template telomerase mutants were able to extend telomeric DNA primers, though with reduced efficiency compared to wild type. Additionally, the DNA dependent telomerases were RNase sensitive confirming that non-template portions of tTER are critical for maintaining activity of the assembled telomerase complex.

The second major study utilized a novel chemical footprinting approach termed SHAPE for Selective 2′-Hydroxyl Acylation analyzed by Primer Extension. SHAPE employs the small molecule *N*-methylisatoic anhydride, which selectively acylates the 2′-hydroxyl of unconstrained or non-base paired ribonucleotides. This approach was

employed to analyze the solution structure of the essential stem IV of tTER. The SHAPE chemistry of stem IV exhibited excellent correlation with high resolution NMR structures. Stem IV mutants were also SHAPE analyzed and their proposed structures were confirmed.

SHAPE chemistry was further employed to analyze the structure of tTER in solution and in the telomerase complex. SHAPE was able to recapitulate most of the phylogenetically predicted secondary structure of tTER. However, SHAPE chemistry suggests that the solution structure of tTER deviates substantially within the pseudoknot region, which instead forms a 12-base pair stem with a 4-base bulge and 6-member apical loop. SHAPE analysis of tTER in the telomerase complex suggests the formation of a pseudoknot that is similar to the phylogenetically predicted structure. This study allows us to propose a model for telomerase assembly where the RNA undergoes one or more structural reorganizations upon holoenzyme maturation.

These studies illustrate the complexity of structure and function of tTER. The novel investigative approaches and intimate knowledge generated of the *Tetrahymena* telomerase RNA should guide future research of more clinically relevant telomerase enzymes.

TABLE OF CONTENTS

LIST OF TABLES

LIST OF FIGURES

LIST OF ABBREVIATIONS

1M7	1-methyl-7-nitroisatoic anhydride
DAT	Dissociated activities of telomerase
DEPC	Diethylpyrocarbonate
DMS	Dimethylsulfate
DNA	Deoxyribonucleic acid
DTT	Dithiothreitol
Est	Ever shorter telomeres
GFP	Green fluorescent protein
hsp90	Heat shock protein 90 kDa
IA	Isatoic anhydride
NMIA	*N*-methyl isatoic anhydride
NMR	Nuclear Magnetic Resonance
RID	RNA interaction domain
RNA	Ribonucleic acid
RNP	Ribonucleoprotein
RT	Reverse Transcriptase
TEN	Telomerase essential N-terminal domain
TER	Telomerase RNA
TERT	Telomerase Reverse Transcriptase
tlc1	Saccharomyces telomerase RNA component
TRF	Telomeric repeat-binding factor

Chapter I. Introduction

A. Telomere Function and Cancer

Cancer is the second leading cause of death in America today and is a diverse disease with a variety of tumors with an equally variable physiology. The variations of different cancers make the development of universal treatments a difficult task. However, one possible unifying target is the enzyme telomerase (Shay and Wright 2006). Telomerase expression and activity is upregulated in greater than 85% of all described cancer types (Shay et al. 2001) and its inhibition leads to decreased tumorigenicity and inhibition of tumor growth (Hahn et al. 1999). This makes telomerase modulation a highly researched area as it may yield a near universal cancer drug.

1. Telomere protection and structure

Linear chromosomes present a unique problem in biological systems by virtue of their ends (Lingner et al. 1995). Chromosome ends must be carefully guarded against unwanted recognition by normal DNA repair enzymes and be protected against nucleolytic degradation. Furthermore, the mechanism of DNA replication leads to the loss of telomeric DNA after each round of the cell cycle (Olovnikov 1971; Watson 1972). These problems have been circumnavigated in eukaryotes by telomeres. Telomeres are specialized protein-DNA complexes that protect the ends of eukaryotic chromosomes and serve as a substrate for the specialized enzyme telomerase, which extends the 3'-end of

each chromosome strand. The 3'-strand of the telomere is G-rich and contains several tandem repeats of the simple telomeric DNA sequence 5'-TTAGGG in vertebrates (Moyzis et al. 1988) and 5'-TTGGGG in the unicellular ciliate *Tetrahymena thermophila* (Blackburn and Gall 1978). Proper telomere maintenance is critical for genetic stability and plays an essential role in aging and tumorigenesis, making the study of telomere biology integral to understanding these processes (Blasco 2005; Blasco 2007).

Telomere structure is complex and dynamic, involving a number of different proteins and changing with the cell cycle. The three main protein players in telomere structure are double stranded DNA binding proteins (TRF1 and TRF2 in humans (Smogorzewska et al. 2000), Rap1p in budding yeast (Kyrion et al. 1992), Taz1 in fission yeast (Cooper et al. 1997)), and single stranded DNA binding proteins (Pot1 in vertebrates (Baumann and Cech 2001), *Arabidopsis* (Jacob et al. 2007), and *Tetrahymena* (Shakirov et al. 2005), Cdc13p in yeast (Nugent et al. 1996), and TEBP in ciliates (Gottschling and Cech 1984)). In the well studied human system, TRF1 complexes with a TRF2 dimer, POT1, TRF1-interacting nuclear factor 2 (TIN2) (Kim et al. 1999), TPP1 (Cristofari et al. 2007; Xin et al. 2007), repressor/activator protein 1 (RAP1) (Li et al. 2000), and Tankyrase 1 and 2 (TANK1, TANK2) (Smith et al. 1998), which are poly(ADP)-ribosylases, to form a telomeric DNA binding unit that helps form the telomere. This complex is telomere specific and is known as shelterin (de Lange 2005). During phases of the cell cycle when DNA is not being replicated it is believed that the ends of telomeres form a T-loop by insertion of the 3'-G-rich overhang back into the telomere forming a loop (Griffith et al. 1999). TRF2 appears to aid in forming or stabilizing this structure (Griffith et al. 1999). The displaced G-strand, termed the D-

loop, is bound by POT1 (Yang et al. 2005). It is postulated that the T-loop structure protects the telomere from break repair enzymes and from telomerase elongation. During S-phase the T-loop is hypothesized to open up to allow for DNA replication and telomerase extension of the 3' end (de Lange 2005). A second complex that is also found at the telomere is TRF2 mediated and contains an array of DNA damage repair proteins that appear to be important for telomere structure and stability (Crabbe and Karlseder 2005).

2. End replication problem

The end replication problem is the inability of DNA polymerase to completely copy linear, duplex DNA (Olovnikov 1971; Watson 1972). Lagging strand DNA replication requires an RNA primer and after the ultimate RNA primer is removed the sequence at the very end of the chromosome is lost. This occurs after each round of DNA replication. After a number of replications the telomeres reach a critically short level known as the Hayflick limit (Hayflick 1965), which signals the cell to senesce. However, if telomerase is expressed, telomere length is maintained and the cell can become immortal (Bodnar et al. 1998), which is an essential step in tumorigenicity. Telomerase activity is important for cancer biology since it promotes cellular immortality. It does so by extending the chromosomal 3' ends after each round of DNA replication.

The telomerase enzyme is a specialized reverse transcriptase that catalyzes the addition of telomeric repeats onto the 3'-ends of linear chromosomes using an internal RNA as the template. This function allows for the DNA replication machinery to then

synthesize additional complementary DNA thereby extending the ends of the chromosomes. This prevents the loss of vital genetic information associated with the end replication problem. In humans, normally only germ-line cells and stem cells are considered telomerase positive, while somatic cells do not express its activity (Cong et al. 2002).

B. Telomerase

1. Telomerase catalytic activity

Telomerase is a reverse transcriptase that utilizes its RNA subunit as a template. Telomerase is composed of several subunits including TERT (TElomere Reverse Transcriptase), which is the catalytic subunit and TER (TElomerase RNA), which is the template containing RNA subunit. TERTs contains sequence motifs that are hallmarks of reverse transcriptases (RT) as well as distinct telomerase-specific motifs (Lingner et al. 1997; Nakamura et al. 1997; Bryan et al. 2000). In agreement with past RT studies, mutation of the conserved RT amino acids in TERTs either abolishes or greatly affects enzymatic activity (Lingner et al. 1997; Bryan et al. 2000). The active site of telomerase is thought to consist of a solvent accessible nucleic acid binding pocket, containing the necessary amino acids to catalyze nucleotide addition, and the telomerase RNA template (Cech et al. 1997). The Blackburn lab made the important discovery that telomerase could add several telomeric repeats to a single primer in vitro (Greider and Blackburn 1989). Telomerase typically demonstrates two types of catalytic activity, deoxynucleotide addition (Greider and Blackburn 1985) and nuclease cleavage (Collins

and Greider 1993; Oulton and Harrington 2004). The basic steps of catalysis, which include primer binding, nucleotide addition, translocation, and dissociation (Figure 1.1), have been identified, though accurate kinetic, biochemical, and structural descriptions are missing. Telomerase also demonstrates two types of processivity: Type I processivity describes the continuous nucleotide addition to a primer until the end of the template is reached, while Type II processivity results from primer translocation and realignment on the template followed by further nucleotide addition (Huard et al. 2003; Bosoy and Lue 2004) (Figure 1.1). This second type of processivity, sometimes referred to as repeat addition processivity, results in the repeated addition of the telomeric sequence and is a process unique to telomerase. While Type I processivity is relatively well understood, the mechanism of Type II processivity and nuclease cleavage is less well defined. Type

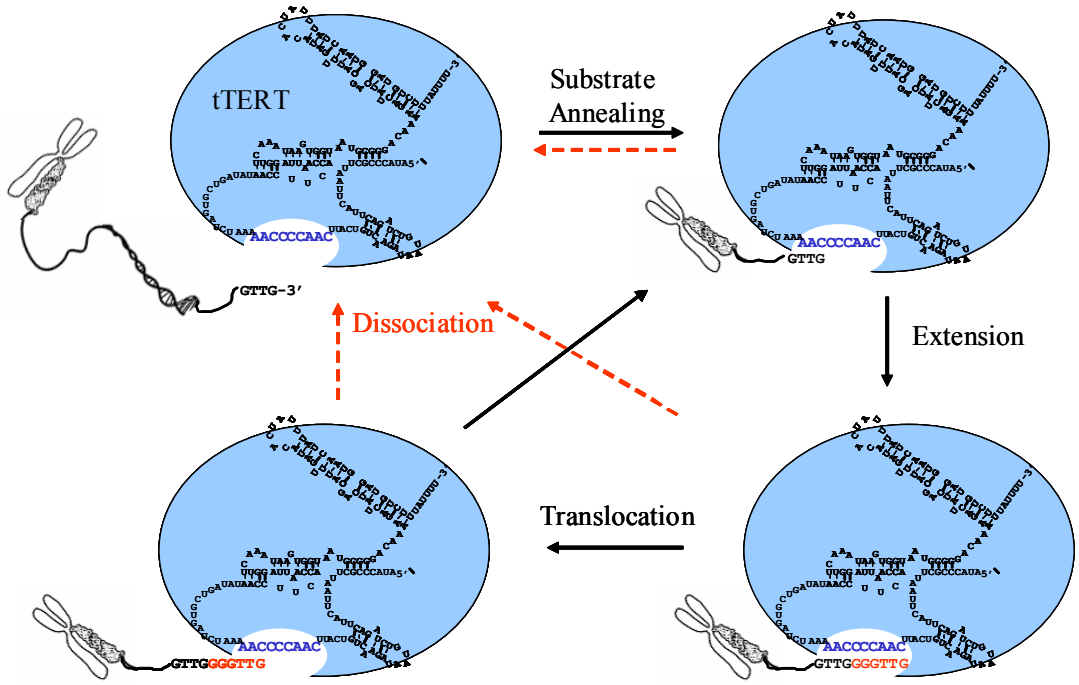

Figure 1.1 Telomerase catalytic cycle. (a) Telomerase ribonucleoprotein and substrate (3' telomere end) unbound. (b) Annealing of telomere 3' end to telomerase template (blue), which positions the telomere 3' end in the telomerase active site. (c) Extension of telomeric DNA (Type I processivity) by the addition of dNTPs (red) using RNA as the template for reverse transcription. (d) Translocation and realignment of substrate (or dissociation) followed by further extension (Type II processivity). Adapted from Jarstfer and Cech, (2002).

II processivity is believed by some to be a least partly protein and RNA subunit mediated (Collins 1999; Lai et al. 2003; Mason et al. 2003), while there is also evidence of product-assisted translocation (Jarstfer and Cech 2002).

This thesis focuses on the study of *Tetrahymena thermophila* telomerase, which is a valuable model system to study the mechanism and structure of all telomerases. Aided by the abundance of telomerase enzyme in the unicellular *Tetrahymena* macronucleus, which contains over 40,000 linear mini-chromosomes, Greider and Blackburn first discovered telomerase activity in 1985 (Greider and Blackburn 1985). *Tetrahymena* telomerase subsequently became a popular telomerase model system since it is amenable to genetic manipulation allowing detailed analysis of the telomerase complex. Later the RNA subunit, tTER, (Greider and Blackburn 1989; Bhattacharyya and Blackburn 1994; Zaug and Cech 1995) and the protein subunit, tTERT, were discovered, cloned and expressed in vitro in RRL to yield active telomerase enzyme (Bryan et al. 1998; Collins and Gandhi 1998). Detailed studies relating the primary and secondary structure of tTER with telomerase activity have been performed using the in vitro reconstituted *Tetrahymena* telomerase as well as the native complex (Autexier and Greider 1998; Gilley and Blackburn 1999; Sperger and Cech 2001; Lai et al. 2003). The template region, one of the most studied portions of tTER (Greider and Blackburn 1989; Wang et al. 1998; Miller et al. 2000), is defined by nine nucleotides, 3′-AACCCCAAC-5′. The first three 3′ nucleotides within this template domain function in aligning the telomeric primer, while the following six nucleotides function as the coding residues. Past experiments have revealed that telomerase can tolerate many changes within its template region while retaining catalytic ability. More specifically, the Blackburn laboratory

showed that telomerase with a template composed entirely of AU repeats or only poly-U was capable of extending a primer by adding the proper complementary sequence (Ware et al. 2000). Furthermore, the Collins laboratory demonstrated that the template could be added entirely in trans to the remainder of the RNA subunit and still yield a functional telomerase, though with severely reduced activity (Miller and Collins 2002). These key studies suggest that telomerase is an obligate RNP that requires specific elements of the RNA both within and away from the template to establish activity.

2. Telomerase components

The only telomerase subunits that are universally conserved among telomerase positive organisms are TERT and TER (Cech 2004). TERT contains conserved reverse transcriptase motifs that confirm its role as a DNA polymerase. The RNA subunits vary greatly in size and secondary structure with only a few common structures including a possible pseudoknot, a trans activating domain, and the template. In the three general groups of telomerase studied, each have a specific set of accessory or holoenzyme proteins in addition to the universal TERT and TER components (Harrington 2003; Collins 2006).

a. Vertebrate

A number of proteins appear to associate with vertebrate telomerase and have been co-purified using various methods. At this time, it appears that only TERT and TER are required for activity, while the other proteins are likely involved in RNA processing, holoenzyme assembly, and telomerase activity regulation (Collins 2006).

The box H/ACA domain of hTER interacts with dyskerin, which is a snoRNP processing RNA (Meier 2005). The human La protein appears to associate with telomerase in some purification schemes (Ford et al. 2001), similar to the obligate La homologues p43 and p65 in *Euplotes aediculatus* and *Tetrahymena thermophila*, respectively. The heat shock protein chaperone complex hsp90/p23 appear to be required for proper telomerase folding or activation and is in some experiments observed to be directly associated with the enzyme, presumably through an interaction with TERT (Keppler et al. 2006). Several RNA-binding proteins called hnRNPs, which are involved in RNA splicing and RNP assembly, have been shown to associate with telomerase as well, but do not appear to be obligate for activity (Collins 2006). A recent mass spectroscopy study shows that highly purified, catalytically active human telomerase is composed only of hTERT, hTER, and dyskerin (Cohen et al. 2007). The large assortment of vertebrate telomerase-associated proteins illustrates the complexity of both telomerase biogenesis and telomerase regulation that is required for proper telomerase function (Collins 2006).

b. Yeast

The yeast telomerase holoenzyme appears to be far more complex than other telomerase systems. In all species of yeast, the telomerase RNA component (tlc) is very large spanning from ~1,200 nts in *S. cerevisiae* to over 1,400 nts in *K. lactis*, and there appear to be a large number of obligate proteins associated with the active telomerase complex (Collins 2006). A genetic screen for short yeast telomeres identified three proteins that both copurify with the yeast telomerase complex and are required for telomere maintenance (Lendvay et al. 1996). They were termed ever shorter telomeres 1,

2, and 3 (Est1, 2, 3), after their telomere depletion-imposed phenotype. Est2p is the yeast version of TERT containing all of the requisite RT domains while Est1p and Est3p are directly associated with the telomerase complex and may be involved in modulating activity or telomerase access to the telomere (Lingner et al. 1997; Taggart and Zakian 2003). Two additional proteins are known to directly associate with tlc1, the Ku heterodimer (Featherstone and Jackson 1999) and the Sm protein heteroheptamer (Wolin and Wurtmann 2006). In addition to Est1p, these bind to three separate arms of tlc1 (Zappulla and Cech 2006).

c. Ciliate

Like vertebrate telomerase, ciliate telomerase minimally requires TERT and TER for activity. Many ciliate species have been studied and a second, seemingly obligate protein is required at least for telomerase biogenesis and remains associated with in vivo purified ciliate telomerases. They are both distant La homologues, p43 in *Euplotes* (Aigner et al. 2003) and p65 in *Tetrahymena* (Prathapam et al. 2005), and appear to mediate proper RNA folding and nuclear retention of telomerase (Mollenbeck et al. 2003). Additional proteins have been copurified with *Tetrahymena* telomerase, p75, p45 and p20, that demonstrate telomeric effects upon depletion, however, their exact function is not known at this time (Witkin and Collins 2004; Witkin et al. 2007).

3. Telomerase structure

Telomerase structure has been studied by a variety of techniques and at a variety of levels of resolution. The primary sequences of TERT and TER has offered insights

into evolutionarily conserved residues, which has led to the identification of critical residues involved in telomerase function (Romero and Blackburn 1991; ten Dam et al. 1991; Lingner et al. 1997). The structure of TER has also been extensively studied by computational folding experiments in addition to chemical and enzymatic footprinting (Chen et al. 2000). These studies have helped establish secondary structure models of the RNAs (Chen and Greider 2004). Higher resolution studies including NMR spectroscopy, X-ray crystallography, and electron microscopy have recently been used to study telomerase and are beginning to shed light on the fine structure of telomerase (Legassie and Jarstfer 2006; Theimer and Feigon 2006).

a. Telomerase Reverse Transcriptase (TERT)

Early sequence alignment studies placed TERTs in the reverse transcriptase family of polymerases (Lingner et al. 1997; Nakamura et al. 1997). Diverse TERTs from ciliates, vertebrates, and yeast were found to contain the seven conserved RT motifs that form the fingers, palm, and thumb structures, which has been solved for other RTs by X-ray crystallography (Cech et al. 1997). Presumably the telomerase active site looks similar and positions the TER template within this hand motif. Selective mutation of any of TERTs catalytic triad of aspartic acids results in a catalytically inactive TERT (Lingner et al. 1997). TERTs (~120 kD) are rather large RTs (Nakamura et al. 1997) and collectively share sequence conservation outside of the RT domains in both the N- and C-terminal portions of the polypeptide (Kelleher et al. 2002; Autexier and Lue 2006). Two RNA interacting domains (RID1 and 2) have been defined in the N-terminus. RID1, also known as TEN or DAT, spans approximately the first 200 residues of TERT and contains

a weak RNA-binding region and possibly a DNA anchor site (Lee et al. 2003; Moriarty et al. 2005). A highly variable region separates RID1 and RID2. The boundaries of RID2 are not tightly defined but this region appears to bind TER with high affinity (Bryan et al. 2000; Bachand and Autexier 2001; O'Connor et al. 2005). The C-terminal region has been implicated in promoting repeat addition processivity (Huard et al. 2003).

There is a wealth of data on the dimerization states of different telomerases. It appears after much investigation that human (Wenz et al. 2001; Ly et al. 2003), *Euplotes crassus* (Wang et al. 2002), and yeast telomerases are present as dimers or multimers (Kelleher et al. 2002; Autexier and Lue 2006). Extensive purification of active human telomerase followed by mass spectrometry analysis revealed the presence of only hTERT, hTER, and dyskerin in a complex with a molecular weight consistent with a dimer of these subunits (Cohen et al. 2007). *Euplotes aediculatus* telomerase has been shown to sediment as a dimer (Aigner et al. 2003) and has been viewed directly by electron microscopy as a dimer and multimer (Fouche et al. 2006). The situation with yeast is complex as there is evidence of two active sites in each yeast telomerase complex (Prescott and Blackburn 1997), but other investigations have suggested that dimerization is not obligate for yeast telomerase activity (Livengood et al. 2002; Friedman et al. 2003). *Tetrahymena* telomerase appears to purify as a functional monomer (Bryan et al. 2003). Despite all of these studies it is still not clear how dimerization is important functionally. Functional studies of human telomerase dimers using template mutants combined with obligatory trans-dimer forming pseudoknot mutations show that dimerized hTER can form a functional telomerase enzyme complex. In this complex, only one template is used, suggesting either the absence of template switching or the absence of two

functional active sites in the dimer (Rivera and Blackburn 2004). Interestingly, HIV RT is actually a heterodimer protein with both protein subunits containing an active site, but only the larger subunit (p66) exhibits activity (Kohlstaedt et al. 1992). Speculation on the functional significance of dimerization (Kelleher et al. 2002; Autexier and Lue 2006) postulates that telomerase is processive because of template switching between the two active sites, which has been partially ruled our for human telomerase (Rivera and Blackburn 2004), that telomerase may extend two telomeres at the same time following DNA replication (Prescott and Blackburn 1997; Wenz et al. 2001), or that one telomerase particle in the dimer acts as the anchor site for the telomere while the other telomerase extends the 3' end (Rivera and Blackburn 2004).

Recently, a high throughput screen for soluble GFP-tagged *Tetrahymena* TERT fragments found an N-terminal region suitable for structural analysis (Jacobs et al. 2005). This fragment spanned the majority of the GQ region of TERT (Xia et al. 2000), residues 2-191. This 23.5 kDa telomerase essential N-terminal (TEN) domain was crystallized and analyzed to a final resolution of 2.22 Å (Jacobs et al. 2006). The solved structure represented a novel protein fold that was organized around a central β-sheet with seven surrounding α-helices. Even though there is only 20% sequence conservation between TERTs in the region spanned by the TEN domain, the structure is likely a universal TERT fold as three invariant amino acids appear in key structural areas. Specifically, Gly144 and Gly171 adopt extreme angles only attainable by glycine residues and orchestrate tight turns between α5 and α6, and β6 and α7, respectively and Gln168 is located on the surface of the structure on β6 and is required for activity. Other pertinent features include a deep groove that runs from the C-terminal tail into the core of the

structure that contains a number of similar or conserved residues (Met13, Leu14, Phe158, Gln168, Val169, and Leu174). This region is postulated to form the primer anchor site (Romi et al. 2007) since it can be photo cross-linked to primers in a sequence specific manner and mutations of Trp187, Phe178, and Gln168 eliminate primer cross-linking. The TEN domain also binds tTER at near 100 nM affinity, but non-specifically as the P4-P6 domain of the *Tetrahymena* group 1 intron and hTER binds with similar affinity. Mutations that removed the positively charged C- and N-terminal regions of the TEN domain abolished tTER binding suggesting the interaction is mostly electrostatic, which is further suggested by the pH dependence of binding (10 nM at pH 6.0; 100 nM at pH 7.0; 275 nM at pH 8.0).

b. Telomerase RNA (TER)

Telomerase RNA is essential both because it supplies the template for reverse transcription and because its specific structure is important for protein binding, including TERT and accessory proteins, and catalysis (Autexier and Lue 2006; Legassie and Jarstfer 2006; Theimer and Feigon 2006). Since the RNA component plays such a crucial role to telomerase function, it is puzzling that there is such a great divergence in size, primary sequence, and overall structure. Three major groups of folding topologies of telomerase RNA have been observed (Figure 1.2). The ciliate RNAs are the smallest (160-200 nts) and all contain a long 3' stem IV, a putative pseudoknot (stem III) (ten Dam et al. 1991), and a large single stranded loop containing the template that is closed by stem I (Romero and Blackburn 1991; Lingner et al. 1994). The vertebrate RNAs are intermediate in size (400-500 nts) and also contain a large 3' stem or stems (p4-p8), a

pseudoknot (p2 and p3), and a single stranded loop containing the template that is closed by a stem (p1) in most species (Chen et al. 2000). The yeast RNAs are the largest telomerase RNAs observed to date (~1200-1400 nts) and contain a central core that houses the template and a putative pseudoknot (Tzfati et al. 2003) (Stem V and VI). The core has three stems or arms that branch out and function to bind the accessory proteins Sm7 (Stem I and VII), Ku (Stem II), and Est1p (stem IV) (Chen and Greider 2004). The

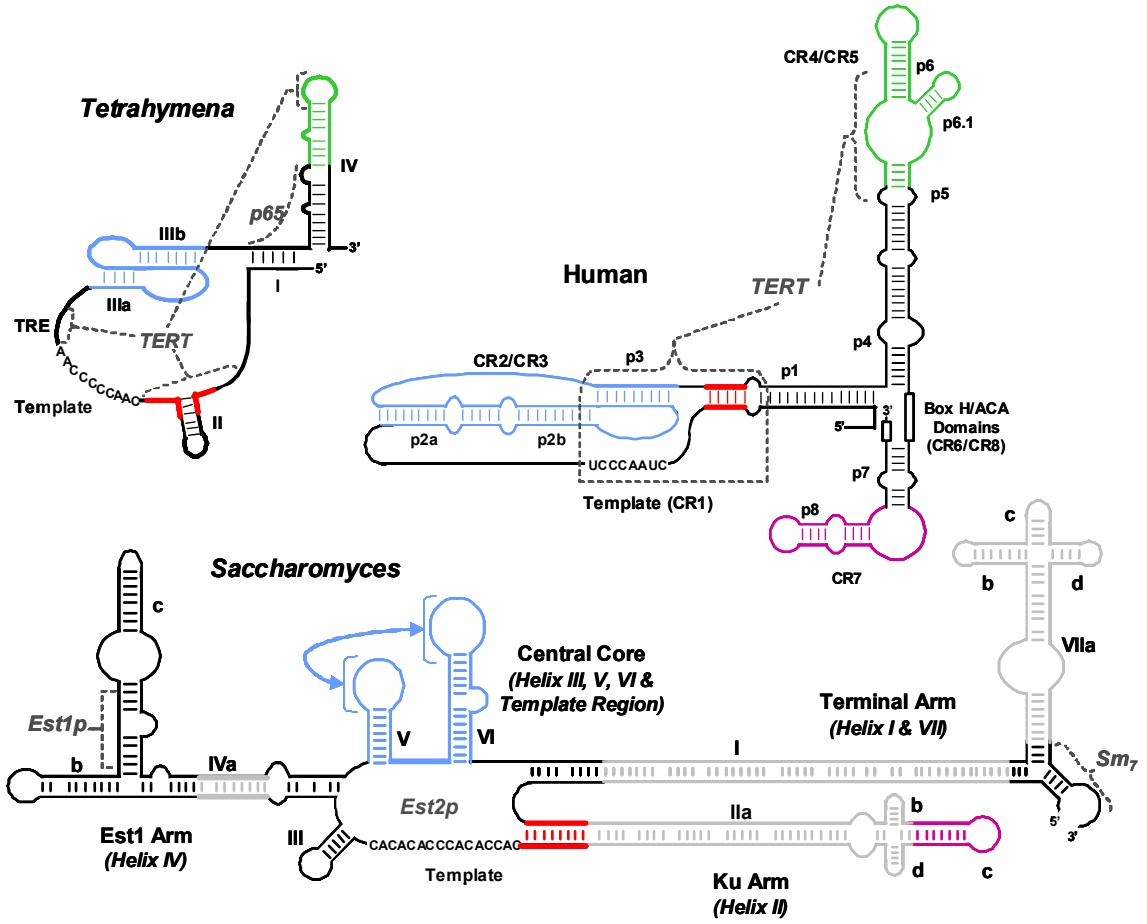

Figure 1.2 Secondary structure of telomerase RNAs. Elements common between at least two of the RNAs are highlighted by color as follows: blue – putative pseudoknot, red – template boundary element, green – trans activation domain, cyan – Ku binding region. Template sequences are provided. Dark grey brackets and text illustrate regions defined to interact with a specific protein. The putative *Saccharomyces* TER pseudoknot is depicted as two conserved stem-loops with a connector linking the possible pseudoknot forming interaction. The light grey regions of yeast TER are dispensable for forming an active telomerase particle *in vivo* and *in vitro* as determined by Zappulla and Cech (2005). The yeast TER nomenclature is as previously reported (Dandjinou et al., 2004; Lin et al., 2004; Zappulla and Cech, 2004). Adapted from Legassie and Jarstfer, (2006).

large difference in telomerase RNA size is likely the key determinant in the difference in telomerase activity and regulation between these disparate phyla.

i. Yeast Telomerase RNA

Recently, the yeast telomerase RNA secondary structure was independently proposed by four different research groups (Chappell and Lundblad 2004; Dandjinou et al. 2004; Lin et al. 2004; Zappulla and Cech 2004). Two groups utilized RNA folding programs combined with phylogenetic analysis to propose secondary structures for the entire RNA (Dandjinou et al. 2004; Zappulla and Cech 2004). The other two groups also utilized computer folding programs and phylogenetic analysis, but further tested some of the predicted pairings experimentally (Chappell and Lundblad 2004; Lin et al. 2004). All four studies reported a similar, unique structure with three long arms that are involved in telomerase cofactor protein binding (Est1p, Ku, and Sm7). The template region is long (16 nt) and the template boundary is defined by the proximal portion of stem II (Tzfati et al. 2000). More recently, a synthetic version of the RNA that was dramatically smaller in size was produced. This construct contained only the pertinent accessory protein binding regions, and yielded a robustly active enzyme that could be reconstituted in vitro, unlike the full length RNA (Zappulla et al. 2005). This has led to the beads on a string model for this large RNA where most of the RNA is non-essential and is only present to tether together necessary holoenzyme proteins (Zappulla and Cech 2006).

A recent study by the Tzfati laboratory utilized site directed mutation and in silico modeling to propose a U-A•U major grove triple helix in the pseudoknot of *K. lactis* telomerase RNA (Shefer et al. 2007). The pseudoknot region encompasses residues 856-

883 and 956-972 to form stem I and II and CS3 and CS4 (Lin et al. 2004; Shefer et al. 2007) with the triple helix involving residues U862-U866, A958-A963 (U959 bulged), and U872-U876. The triple helix structure was evaluated by selectively mutating different strands and either destroying the helix along with telomerase activity in vivo or rescuing it with pH dependent G-C•C^+ base triples. This triple helix appears to be conserved among *Kluveromyces* species. This finding is not unusual as many pseudoknot solution and crystal structures form triple helices (Su et al. 1999; Michiels et al. 2001; Nixon et al. 2002) including the hTER pseudoknot (Theimer et al. 2005). If the yeast and vertebrate TERs contain pseudoknots that form triple helices, it leads to speculation that the ciliate TERs may also contain a triplex forming pseudoknot.

Dimethylsulfate (DMS) footprinting (Table 1.1) of endogenous *S. cerevisiae* telomerase RNA showed a unique mechanism of 5' primer unwinding as it was extended and supported the recently proposed secondary structure as well as a pseudoknot (Forstemann and Lingner 2005). When a short telomeric primer was added to the telomerase without dNTPs, 7 bases of the template were protected from DMS modification. Upon addition of dNTPs the primer was extended to the template boundary, but only 7 bases remained protected. This experiment provides convincing evidence that yeast telomerase unwinds its nascent primer-template duplex during elongation keeping a maximum of 7 base pairs intact. Other studies have suggested that *Euplotes aediculatus* also keeps an optimum number of base pairs between template and primer during extension (Hammond and Cech 1998).

ii. Vertebrate telomerase RNA

Vertebrate telomerase RNA can be divided into three major portions: the RNA processing domain (Box H/ACA, CR7 domain), the active site domain (template, pseudoknot, template boundary), and the trans activation domain (CR4/CR5 domains, p6 helices) (Legassie and Jarstfer 2006). The 3' end of the RNA appears to be important for proper RNA processing as it contains RNP processing box H/ACA sequences (Meier 2005). This region is essential for maturation of telomerase in vivo (Mitchell and Collins 2000; Fu and Collins 2003) but is dispensable for in vitro telomerase activity (Tesmer et al. 1999). The other two regions of hTER are essential for activity. In fact, just these two domains are sufficient to reconstitute active telomerase (Tesmer et al. 1999; Chen et al. 2002). The activation domain (CR4/CR5) likely comes into direct contact with hTERT (Mitchell and Collins 2000; Bachand and Autexier 2001; Keppler and Jarstfer 2004), and evidence that the CR4/CR5 domain directly interacts with the active site or the template in assembled telomerase also exists (Ueda and Roberts 2004). The active site domain contains the template and a highly conserved pseudoknot. Stability of the secondary and tertiary structure of the pseudoknot is important as several disorders (dyskeratosis congenita and aplastic anemia) are related to mutations in this region of the RNA (Chen and Greider 2004). Since these two portions of the RNA are so integral to telomerase function, several solution structures of these motifs have been recently solved by NMR spectroscopy.

Two NMR structures of the p6 and p6.1 helices have been solved by the Varani laboratory (Leeper et al. 2003; Leeper and Varani 2005). The p6.1 helix is phylogenetically conserved (Chen et al. 2000) and is important for both hTER-hTERT

binding and activity (Chen et al. 2002). Given its importance for activity, it is not surprising that it has been shown to interact directly with the template, though the nature

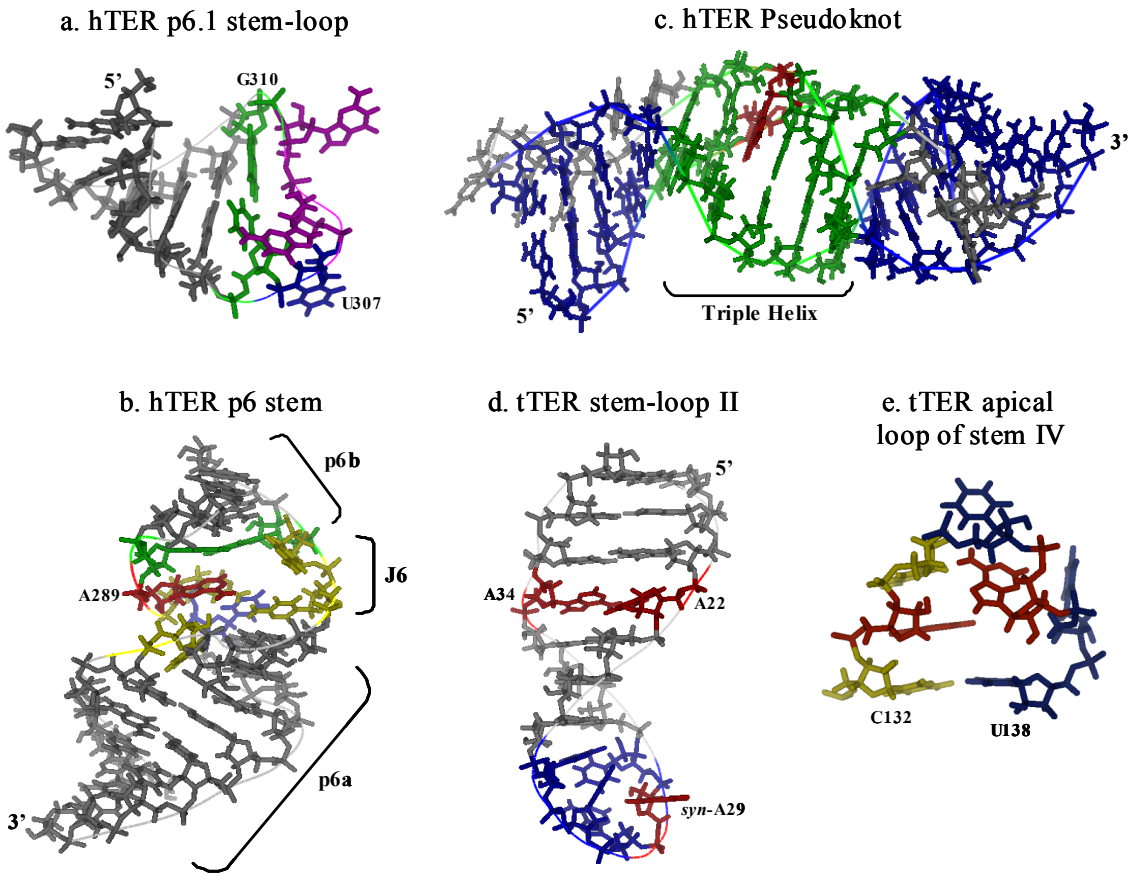

Figure 1.3 Telomerase RNA NMR structures. (a) Human telomerase RNA p6.1 stem-loop (Leeper et al., 2003). A six base pair stem capped with a non-canonical G•U base pair and a three member apical loop. Residues are colored as follows: green - non-canonical U306•G310 base pair, cyan – loop residues G309 and G308, blue – loop residue U307. (b) Human telomerase RNA p6 stem (Leeper and Varani, 2005). Stem is divided into template proximal p6a and template distal p6b by internal loop J6, as denoted. Residues are colored as follows: red – J6 loop residue A289, blue – J6 loop residue U291, yellow – J6 loop residues C266, C267, C290 and p6a bulged C262, green – G268-C288 base pair. C288-G268•C267 forms a base triple in some structures. (c) Human telomerase RNA pseudoknot (Theimer et al., 2005). The pseudoknot core is characterized by a five member triple helix (green) interrupted by an A173•U99 Hoogsteen base pair (red). A double helix (blue) extends off either side of the triple helix. Grey residues are unpaired. (d) *Tetrahymena* telomerase RNA stem-loop II (Richards et al., 2006a). A six base pair stem capped with a five-member apical loop. Residues are colored as follows: blue – apical loop residues U30, A28, U27, and G26, red – opposed, unbase paired stem residues A34 and A22, and apical loop residue *syn*-A29. (e) Tetrahymena telomerase RNA apical loop of stem IV (Richards et al., 2006b). The apical loop is closed by a non-canonical C132•U138 base pair. Residues are colored as follows: yellow – C132 and C134, red – A133 and A136, blue – U135, U137, and U138. All structures were rendered in Pymol using Protein Data Bank accession codes 1OQ0, 1Z31, 1YMO, 2FRL, and 2H2X, respectively.

of this interaction is not known (Ueda and Roberts 2004). The p6.1 NMR structure (Figure 1.3a; 1.033 Å) details a canonical 4-base pair A-form helix capped by a G•U wobble pair (green) and a rigid UGG loop (Leeper et al. 2003). All 3 loop residues expose their Watson-Crick faces to solvent. In accordance with this regions importance in telomerase activity and binding, loop residues G308-G310 are heavily modified by kethoxal (Table 1.1) in vitro but are fully protected in vivo (Antal et al. 2002), supporting direct hTERT interaction or the formation of RNA tertiary structure upon hTERT binding. The p6 stem loop is also a conserved structure (Figure 1.3b), with the NMR structure depicting an 11-base pair stem interrupted by a bulged cytosine and the J6

Table 1.1 Commonly used RNA footprinting reagents

Reagent	Modification (Cleavage) Site	Optimum pH	Other Conditions
[a] RNase T1	[b,c] ss G	7.5; 4.5	
[a] RNase T2	ss A	4.5-7.5	
[a] RNase V1	[d] ds; ss stacked regions	4.0-9.0	Mg^{2+} (>1 mM)
[a] S1 Nuclease	ss	4.5	Zn^{2+}
[a] RNase H	RNA in RNA/DNA duplex	8.0	Mg^{2+}
Dimethylsulfate (DMS)	ss (N1-A; N3-C)	7.0	
Diethylpyrocarbonate (DEPC)	ss N7-A	7.0	
β-etoxy-α-ketobutyraldehyde (kethoxal)	[e] ss N1- and N2-G	slightly acidic	
1-cyclohexyl-3-(2-morpho linoethyl)-carbodiimide metho-*p*-toluene sulfonate (CMCT)	ss (N3-U; N1-G)	8.0	

[a] Nuclease Enzyme. [b] (ss) single stranded. [c] (G) guanosine, (A) adenosine, (C) cytosine, (U) uridine. [d] (ds) double stranded. [e] Same molecule attacks both N1 and N2 position in same base.

internal loop (Leeper and Varani 2005). Phylogenetic analysis predicted U261 to be bulged (Chen et al. 2002), but the NMR structure as well as footprinting analysis (Antal et al. 2002) clearly shows C262 (yellow) is bulged instead (Figure 1.3b). The J6 loop, which is essential to telomerase function, has several intriguing aspects. First, C266

(yellow) and U291 (blue) possibly form a base pair, while both C266 (yellow) and A289 (red) stack onto the preceding helix nucleotides, giving a defined structure to the J6 bulge. Second, a possible base triple that is phylogenetically supported may form between residues C267, G268, and C288 (two green bases and proximal yellow base) (Chen et al. 2002). Additionally, the J6 loop forms a solvent accessible hole through its center that is proposed to act as an hTERT-binding motif. This is supported by DMS modification of loop residue C290 (yellow), which is eliminated upon hTERT binding (Antal et al. 2002). These two structures represent greater than 60% of the activation domain of human telomerase RNA and offer some interesting insight into this domains possible function within the active enzyme (Legassie and Jarstfer 2006; Theimer and Feigon 2006).

The Feigon laboratory has studied the pseudoknot region (pairing regions p2b and p3 and loop j2b/3) of hTER in detail (Theimer et al. 2003; Theimer et al. 2003; Theimer et al. 2005). Initially, they utilized NMR and thermal melting studies to deduce the likely cause of telomerase dysfunction in dyskeratosis congenita (Theimer et al. 2003a, b). The GC107-108 to AG mutation creates a stable YNMG-like loop that has an internal U105•G108 base pair. This stable loop shifts the equilibrium away from the pseudoknot toward a stem-loop structure that is deleterious to telomerase function. Another interesting finding from these studies is that the extended p2b stem contains a run of 3 stable U•U base pairs followed by a C•U base pair. These studies showed that there appears to be an equilibrium between pseudoknot and stem-loop structures in functional telomerase, but if bulged U177 is removed the pseudoknot is stabilized and a striking triple helical structure results (Figure 1.3c) (Theimer et al. 2005). This triple helix

(green) is five members long with one interrupting A173•U99 Hoogsteen base pair (red). Importantly, when two of these base triples were mutated so as to form possible C-G•C^+ triples, the thermal stability of the pseudoknot markedly increased upon a lowering of pH. All of the residues required to form this remarkable structure are conserved in vertebrates (Chen et al. 2000) suggesting an intimate role for this motif in both hTERT binding and telomerase catalytic function. Accordingly, mutations that likely perturb this structure render telomerase inactive, while the U177 deletion only reduces telomerase activity to 50% of wild type, suggesting that the pseudoknot is present in catalytically active telomerase (Theimer et al. 2005). Unfortunately, chemical footprinting results for this region of the RNA are difficult to interpret and likely reflect solvent accessibility issues induced by the tertiary structure of the pseudoknot or by direct hTERT interaction (Antal et al. 2002).

iii. *Tetrahymena* telomerase RNA

Tetrahymena thermophila TER has been the most studied telomerase RNA with currently three NMR structures that cover nearly 40% of the total RNA. The conserved stem-loop IV structure has been determined by two separate labs (Chen et al. 2006; Richards et al. 2006) and a portion of the template boundary element, stem-loop II, has also been determined (Richards et al. 2006). Other RNA regions have been analyzed in detail by three different enzymatic and chemical footprinting studies (Bhattacharyya and Blackburn 1994; Zaug and Cech 1995; Sperger and Cech 2001). All of these studies combine to illuminate an RNA structure that in conserved regions appears to agree with phylogenetically based structural assignments, and diverge in areas of lower

conservation. Specifically, the pseudoknot and template region appear to be different in the free RNA when compared to that in the telomerase complex. Unfortunately, the tTERT bound structures of these regions is not entirely clear since tTERT interaction blocks RNA modification by the footprinting reagents used to date (Zaug and Cech 1995; Sperger and Cech 2001).

The template boundary element is an essential region of tTER for both proper template boundary definition and tTERT binding (Licht and Collins 1999; Lai et al. 2002). The essential portions of this region are the conserved sequences A16-C19 and G37-A40 as well as the proximal portion of stem II. The NMR structure (0.78 Å) of stem II (Figure 1.3d) illustrates a tight 6-base pair A-form helix with two opposing unbase paired adenines (red) stacked into the middle of the helix (Richards et al. 2006). Interestingly, RNase V1 (Table 1.1) heavily cleaved the 5' side of the helix, but did not cleave the 3' side in the presence of tTERT (Sperger and Cech 2001) or in its absence (Bhattacharyya and Blackburn 1994; Sperger and Cech 2001). This suggests that the template side of helix II may be sterically hindered from RNase V1 attack by being either in contact with or in close proximity to another portion of the RNA. Residues G26 and U27 of the structured penta-loop stack onto the end of the helix and A28 is located at the apex of the helix with its Watson-Crick face pointing down the helix axis (blue). A29 (red) is in a rare *syn* conformation with its Watson-Crick face solvent exposed, while U30 (blue) is partially stacked onto the end of the helix. A28 and A29 were both modified by DEPC (Table 1.1) and DMS without tTERT present with A29 always modified to a decreased extent (Bhattacharyya and Blackburn 1994; Zaug and Cech 1995). With tTERT present only A28 was modified by DMS (Zaug and Cech 1995). G26 was

efficiently cleaved by RNase T1 (Table 1.1) both with (Sperger and Cech 2001) and without tTERT bound (Bhattacharyya and Blackburn 1994; Sperger and Cech 2001). The fact that *syn*-A29 was relatively reactive in complex with tTERT, and A28 and G26 were not, leads to speculation that tTERT may directly interact with the 5' side of the loop. tTERT interaction at this region is certainly possible since the template boundary element is also the highest affinity tTERT binding region of the RNA, but it is obviously not required as A29 is not conserved (Ye and Romero 2002) and the distal portion of stem II is dispensable for binding and activity (Licht and Collins 1999; Mason et al. 2003).

The structure of stem IV of tTER was solved concurrently by two labs (Chen et al. 2006; Richards et al. 2006), and our lab contributed to one of the publications (Chen et al. 2006). The distal portion of stem IV is essential for telomerase activity and processivity (Lai et al. 2003; Mason et al. 2003) and the NMR structures detail some interesting structural characteristics of this region. First, the predicted 7-residue apical loop is observed as a five-member loop (Figure 1.3e). The first two loop residues stack onto the end of the A-form helix and form a non-canonical C132•U138 base pair. Residues A131 through C134 all stack onto each other continuing the A-form helical structure into the loop. U135 (blue) is at the apex of the loop and its Watson-Crick face is solvent exposed. U135 through U138 all have a higher rmsd than the 5' loop residues with U137 the least well-defined residue. The Watson-Crick faces of all the loop residues point toward the major grove side of the loop forming a hydrophobic pocket in the center of the loop. Analysis of point mutations of these residues indicates that C132 (yellow), U137 (blue) and U138 (blue) are essential for activity, while mutation of

residues A136 (red) and U135 (blue) have an intermediate effect on activity (Figure 1.3e) (Sperger and Cech 2001; Lai et al. 2003; Mason et al. 2003). Mutational analysis of the remaining loop residues had little effect on activity (Sperger and Cech 2001; Lai et al. 2003; Mason et al. 2003). DEPC heavily modified loop residues A133 and A136 consistent with their being single stranded (Bhattacharyya and Blackburn 1994). Further characterization of these loop residues is extensively discussed in chapter III of this work.

The stem portion of stem-loop IV contains a number of interesting features. First, an absolutely conserved GA bulge flanked by two GC base pairs causes an estimated 40° kink in the helical axis (Chen et al. 2006; Richards et al. 2006). G121 of the bulge was efficiently cleaved by RNase T1 without tTERT (Bhattacharyya and Blackburn 1994), but was partially protected while in complex with tTERT (Sperger and Cech 2001). Similarly, A122 was heavily modified by DMS and DEPC without tTERT present (Bhattacharyya and Blackburn 1994; Zaug and Cech 1995), but was protected from DMS modification in vivo (Zaug and Cech 1995). This bulge-generated kink divides the stem IV structure into template proximal and distal regions. The distal region contains an eight base pair stem that is interrupted by a single bulged U127. NMR data suggest that at least a subset of the structures exhibit a bulged U126, leading to an inherent flexibility of this region (Chen et al. 2006). This is supported by RNase V1 footprinting which heavily cleaved the stable helix after the bulged U127 up to the apical loop (Bhattacharyya and Blackburn 1994). The proximal region of stem IV contains an eight base pair stem that is interrupted by a bulged U117. Two neighboring base pairs A118-U149 and U119-A148 appear to form weak pairings or no pairings at all (Chen et al. 2006), suggesting flexibility in this region of the RNA. Interestingly, deletion of either

bulged uridine does not effect telomerase activity levels (Richards et al. 2006). RNase V1 cleaves at A115, C116, and C120 without tTERT present, but most of this region is protected from chemical and enzymatic modification with tTERT bound (Zaug and Cech 1995; Sperger and Cech 2001). Recent, studies have also shown that the proximal portion of stem IV and the GA bulge are essential, high-affinity p65 binding regions (Prathapam et al. 2005; O'Connor and Collins 2006; Stone et al. 2007).

The region of tTER from the pseudoknot through the template has been investigated using various footprinting techniques both in the presence and absence of tTERT. DEPC treatment of tTER in the absence of tTERT suggested that the template recognition element, residues 52-65, is structured despite the prediction that it is single stranded. Furthermore, the pseudoknot appeared to be largely unstructured (Bhattacharyya and Blackburn 1994). Similarly, DMS analysis without tTERT showed pairing or stacking of the template cytosine residues as well as a structured template recognition element and an incompletely formed pseudoknot (Zaug and Cech 1995). This same study showed strong DMS modification of all template cytosine and adenine residues and a complete protection of all pseudoknot residues when intracellular tTER was probed. RNase T1 (Table 1.1) cleaved tTER with a similar pattern both in the absence and presence of tTERT (Bhattacharyya and Blackburn 1994; Sperger and Cech 2001), while profiles of RNase V1 (Table 1.1) reactivity showed a structured template and template recognition element and an incompletely formed pseudoknot without tTERT present (Bhattacharyya and Blackburn 1994; Sperger and Cech 2001) and a more well formed pseudoknot structure with tTERT present (Sperger and Cech 2001). RNase V1 and T1 footprinting also suggested that mutations in the stem IV apical loop affected

pseudoknot formation in the presence of tTERT (Sperger and Cech 2001). These footprinting results suggest a reorganization of the pseudoknot-template region upon tTER association with tTERT.

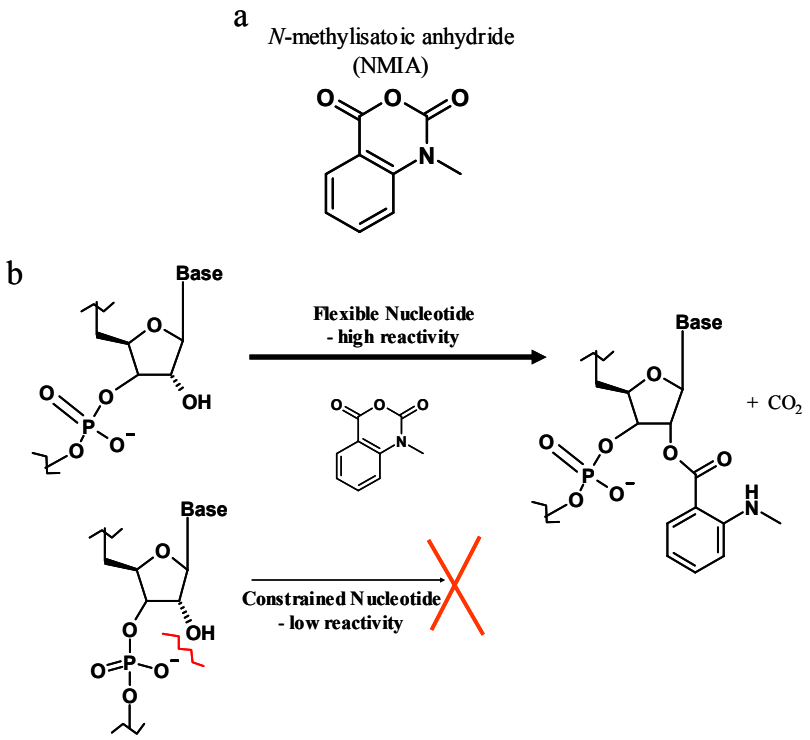

Figure 1.4 *N*-methylisatoic anhydride (NMIA) 2'-hydroxyl ribose chemistry. (a) NMIA structure. (b) NMIA preferentially reacts with conformationally unconstrained RNA nucleotide residues by forming an ester with the 2'-hydoxyl group of the ribose sugar, and eliminating CO_2. This reactivity appears to be sensitive to the proximity of the 3'-phosphodiester anion. Adapted from Merino et al., (2005).

C. SHAPE chemistry analysis

A new method of RNA chemical probing of particular utility is used in this work and involves the acylation of the 2'-hydroxyl group of RNA. This approach employs *N*-methylisatoic anhydride (NMIA; Figure 1.4a) to modify the 2'-hydroxyl group of the ribose sugar of RNA (Merino et al. 2005; Wilkinson et al. 2006). This modification is highly selective to the conformational flexibility of RNA residues (Figure 1.4b) and is easily mapped by reverse transcription followed by sequencing gel electrophoresis.

Termed SHAPE (Selective 2'-Hydroxyl Acylation analyzed by Primer Extension), the major advantage of this approach over other previously described footprinting techniques is that it is not residue specific. Table 1.1 lists other common RNA footprinting reagents, most of which are base specific or only inspect solvent accessibility. A number of recent publications that probe RNAs of unknown structure (Badorrek and Weeks 2005; Badorrek et al. 2006; Badorrek and Weeks 2006) or compare RNA crystal or NMR structures with SHAPE analysis (Wilkinson et al. 2005; Chen et al. 2006; Vicens et al. 2007) illustrate the precision and utility of this approach for high resolution RNA mapping.

D. Specific aims of this research

1. (Chapter II) Construct DNA-dependent *Tetrahymena* telomerase enzyme to characterize the ability of telomerase to utilize DNA as a template

2. (Chapter III) Utilize SHAPE technology to analyze the structure of mutants of Tetrahymena telomerase RNA (tTER) stem IV and compare with a high resolution NMR solution structure

3. (Chapter III) Compare the reaction profiles of isatoic anhydride analogues for analysis of a known RNA structure (tTER stem IV)

4. (Chapter IV) Characterize the solution structure of tTER using SHAPE chemistry technology

5. (Chapter V) Characterize the structure of tTER in the telomerase complex using SHAPE technology

Chapter II. Investigating the ability of *Tetrahymena thermophila* telomerase to utilize a DNA template

Adapted from: Legassie, J. D. and M. B. Jarstfer, *Telomerase as a DNA-dependent polymerase.* Biochemistry, 2005. 44(43): p. 14191-201.

A. Introduction

Detailed studies relating the primary and secondary structure of tTER with telomerase activity have been performed using the in vitro reconstituted *Tetrahymena* telomerase as well as the native complex (Autexier and Greider 1998; Gilley and Blackburn 1999; Sperger and Cech 2001; Lai et al. 2003). The template region, one of the most studied portions of tTER (Greider and Blackburn 1989; Wang et al. 1998; Miller et al. 2000), is defined by nine nucleotides, 3′-^{51}AACCCCAAC^{43}-5′. The first three, 3′ nucleotides within this template domain function in aligning the telomerase primer, while the following six nucleotides function as the coding residues (Figure 2.1b) (Autexier and Greider 1994; Autexier and Greider 1995; Gilley et al. 1995). Previous studies revealed that telomerase can tolerate many changes within its template region while retaining catalytic ability. Specifically, Ware et al. (2000) showed that telomerase containing a non-telomeric template composed entirely of AU repeats or only poly-U was capable of extending a primer by adding the proper complementary sequence, although the processivity of these template mutants was dramatically reduced. Furthermore, Miller and Collins (Miller and Collins 2002) demonstrated that the template could be added entirely in trans to the remainder of the RNA subunit and still yield a functional

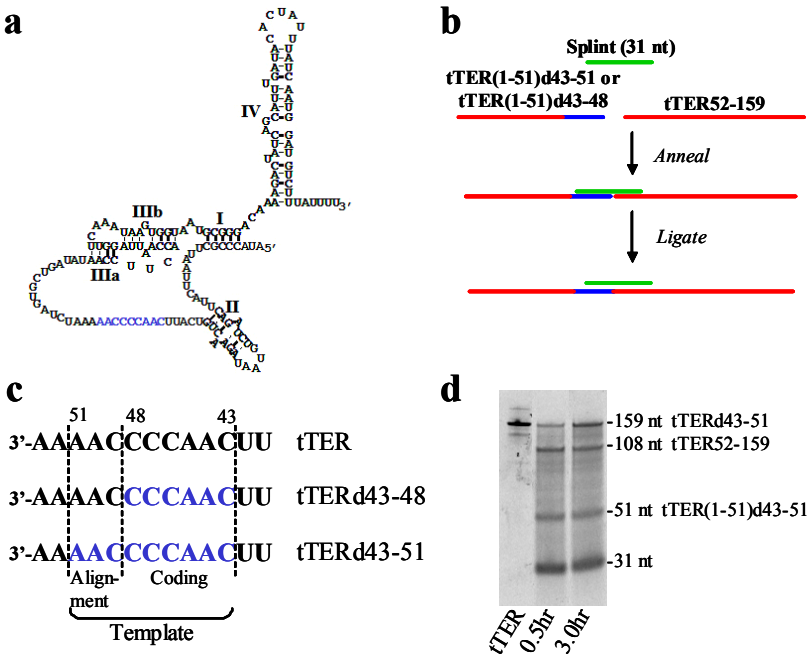

Figure 2.1 ***Tetrahymena*** **telomerase RNA and DNA containing mutants.** (a) Proposed secondary structure of tTER (Adapted from Chen and Greider (2004)). (b) The template regions of tTER and DNA template mutants tTERd43-48 and tTERd43-51 with dNMPs colored blue. (c) Schematic of splint ligation reactions used to produce chimeric tTER mutants. (d) Denaturing PAGE analysis of ligation progression. Aliquots of a small-scale ligation reaction were taken at 30 min and 3 hr time points and analyzed by denaturing PAGE and stained with SYBR Green II. Wild type tTER was included as a reference.

telomerase, though with severely reduced activity. These key studies indicate that while telomerase is functional with a variety of RNA templates, it is an obligate ribonucleoprotein complex that requires specific elements both within and away from the template to establish full activity.

To further the understanding of telomerase as a specialized reverse transcriptase, it is important to examine its template specificity compared to other RTs. A logical inquiry for a reverse transcriptase is if it can efficiently utilize DNA as a template for transcription. However, the ability of telomerase to utilize a DNA template has been more difficult to probe because the role of the RNA subunit in establishing an active telomerase is more complex than merely supplying the template for reverse transcription. To examine the backbone specificity of telomerase, we therefore synthesized two mutants

of the *Tetrahymena* telomerase RNA that contain deoxyribonucleotides only within the templating portion.

B. Results

1. Construction and validation of two DNA template-containing mutants of tTER

These telomerase RNA template mutants were constructed by splint ligation (Figure 2.1c) (Moore and Sharp 1992). In one mutant, tTERd43-48, DNA was substituted into only the coding residues of the template, positions 43 through 48, while in the other, tTERd43-51, DNA was substituted into the entire template domain, positions 43 through 51, which includes the alignment region (Figure 2.1b). To ensure that the ligation proceeded efficiently, samples from a small-scale ligation were removed at varying time points and analyzed by denaturing PAGE. The amount of full-length ligation product increased over three hours with further incubation time not affecting the overall yield (Figure 2.1d). Optimized large-scale ligations typically yielded 50-60% full-length product RNA. Ligation products (tTERd43-48 and tTERd43-51) and in vitro transcribed wild type tTER were sequenced after RT PCR amplification to ensure they were correct, and they were treated with RQ1 DNase to confirm the presence of DNA in the template (data not shown). We also found that M-MLV RT was able to reverse transcribe across the chimeric tTERs and wild type tTER with minimal pausing (data not shown).

2. *Tetrahymena* telomerase can assemble with chimeric tTER

We used a RRL expression system to transcribe and translate the *Tetrahymena* telomerase protein subunit, tTERT, with an N-terminal T7 epitope tag. Telomerase was then conveniently assembled by the addition of tTER or one of the chimeric tTERs to the RRL reaction (Bryan et al. 2000). To assess the binding of tTERT to the chimeric tTER mutants, we co-immunoprecipitated 5′-^{32}P-labeled wild type and chimeric tTERs with ^{35}S-labeled tTERT. We found that both tTERd43-48 and tTERd43-51 associated with tTERT (Figure 2.2). However, the amount of the chimeric tTER mutants that co-

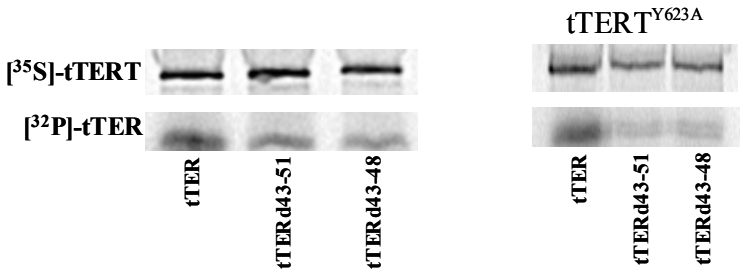

Figure 2.2 Association of chimeric tTER mutants with tTERT and tTERT^{Y623A}. ^{35}S-labeled tTERT or tTERT^{Y623A} was synthesized in RRL in the presence of 5'-^{32}P-labeled tTER, tTERd43-51, or tTERd43-48. Complexes were immunoprecipitated with anti-T7 agarose beads and were resolved on 6% SDS PAGE gels.

immunoprecipitated with tTERT was consistently lower than that of wild type tTER (48% ± 20% for tTERd43-48; 49% ± 23% for tTERd43-51; data from three independent trials). The reduced binding of tTERT to the tTER mutants was unexpected since the presence of a template does not appear to be an important contributor to the stability of the telomerase complex (Miller and Collins 2002; Mason et al. 2003). However, we did observe decreased stability of the chimeric tTERs in the RRL, when compared to tTER (data not shown), suggesting that decreased stability of the mutants could explain the diminished co-immunoprecipitation efficiency. Controls using expression of an empty vector revealed that the co-immunoprecipitation of tTER and the chimeric tTER mutants

required the presence of tTERT (data not shown). Importantly, once assembled into the holoenzyme, the mutant tTERs were stable, as long-term storage of assembled mutant telomerase did not result in a noticeable decrease of enzymatic activity.

3. A DNA-dependent telomerase reaction

Telomerase has two types of catalytic activity, deoxynucleotide addition (Greider and Blackburn 1985) and exo- or endonuclease cleavage (Collins and Greider 1993). Telomerase also demonstrates two types of processivity. Type I processivity, common to all nucleic acid polymerases, is the processive addition of single deoxynucleotides to a primer until the template boundary is reached. Type II processivity, which is also called repeat addition processivity, describes the synthesis of multiple telomeric repeats and requires primer realignment after extension to the template boundary and is unique to telomerase (Huard et al. 2003; Lue 2004). We characterized the catalytic properties of telomerase when it utilizes a DNA template by using a telomerase-dependent primer extension assay (Bryan et al. 2000). Telomerase reconstituted with either tTERd43-48 or tTERd43-51 (Figure 2.3, lane 3 or 4, respectively) demonstrated reduced overall activity (<10% of wild type activity), as measured by total lane density, when compared to telomerase reconstituted with wild type tTER (lane 1). Furthermore, telomerase reconstituted with either of the chimeric tTER mutants demonstrated no observable type II processivity. tTERd43-48 telomerase efficiently added only two dGMP residues to the primer, whereas tTERd43-51 telomerase added only one. Neither mutant complex was efficient at the addition of dTMP. Negative controls included RNase treatment (lane 2), in which RNase A was added to the reaction prior to primer addition (Greider and

Blackburn 1989), reactions using tTERT assembled with the RNA fragments used to synthesize the chimeric tTERs, tTER52-159 (lane 5), tTER(1-51)d43-48 (lane 6), or tTER(1-51)d43-51 (lane 7), and no tTERT reactions, where an empty plasmid was added to the RRL for assembly with tTERd43-48 (lane 8) or tTERd43-51 (lane 9). These controls demonstrated that the observed activity required full-length tTER or chimeric tTER as well as the catalytic protein subunit (lanes 5-9).

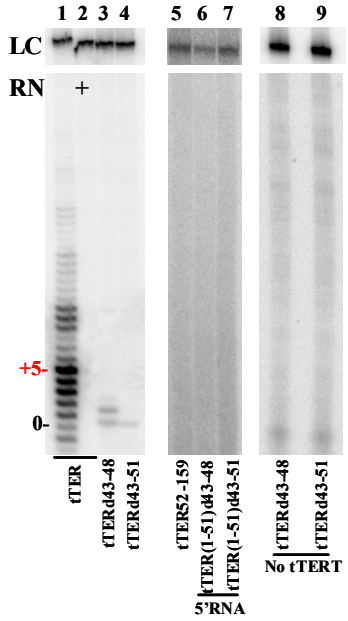

Figure 2.3 In vitro reconstitution of telomerase activity with DNA template tTERs. Telomerase was reconstituted in vitro in RRL with tTERT and tTER (lanes 1 and 2), tTERd43-48 (lane 3) or tTERd43-51 (lane 4). As a negative control for tTER fragment activity, tTERT was reconstituted in RRL with the 3' fragment tTER52-159 (lane 5) and the 5' chimeric fragments tTER(1-51)d43-48 (lane 6) and tTER(1-51)d43-51 (lane 7). As a control for tTERT activity, RRL expressing and empty vector was incubated with tTERd43-48 (lane 8) or tTERd43-51 (lane 9). Crude telomerase complexes in RRL were incubated with primer p5 ($G(T_2G_4)_2TTGG$), dTTP, and [α-^{32}P]-dGTP. The red "5" indicates the 5th nucleotide added to the end of the primer (addition of dGMP across template position 43) as well as the end of the template. The black "0" indicates the length of unextended primer p5. Note that the shift in lanes 2-4 is a gel artifact also reflected in the loading control (LC). A ^{32}P-labeled 114-nt oligonucleotide was used as a recovery and LC. Lanes labeled with RN are assays of samples pretreated with RNase A.

4. Substrate K_M is not affected by DNA template

One explanation for the decreased ability of telomerase to utilize a DNA template could be reduced affinity for its DNA primer (Sperger and Cech 2001). We therefore

examined the effect of primer concentration on wild type and chimeric tTER telomerases (Figure 2.4). Notably, the K_M for the primer was not altered significantly between the wild type telomerase and the chimeric tTER telomerases (0.5 ± 0.06 μM for tTER; 0.9 ±

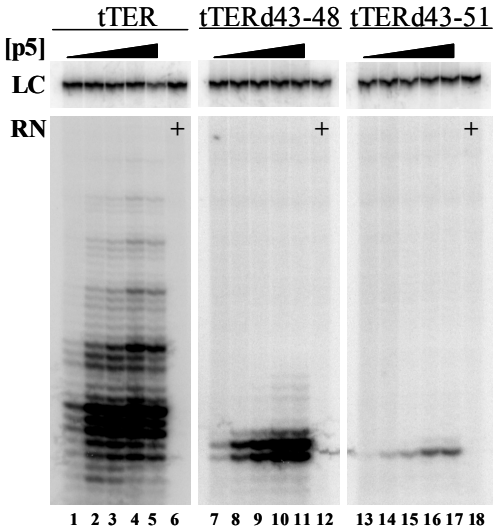

Figure 2.4 Primer concentration dependence of DNA-dependent and wild type telomerase activity. Wild type telomerase (lanes 1-6), telomerase reconstituted with tTERd43-48 (lanes 7-12), and telomerase reconstituted with tTERd43-51 (lanes 13-18) were assayed under standard assay conditions with increasing concentrations of primer p5 ($G(T_2G_4)_2TTGG$): 0.1 μM (lanes 1, 7, and 13); 0.5 μM (lanes 2, 8, and 14); 2 μM (lanes 3, 6, 9, 12, 15, and 18); 10 μM (lanes 4, 10, and 16); 20 μM (lanes 5, 11, and 17). A ^{32}P-labeled loading control (LC) is indicated. Lanes labeled with RN are assays of samples pretreated with RNase A.

0.3 μM for tTERd43-48; 0.3 ± 0.1 μM for tTERd43-51). The increase in type II processivity that was observed in this experiment for tTERd43-48 telomerase at primer concentrations of 2 μM and above was probably related to the overall increase in activity. The concentration dependence of nucleotide substrates dTTP and dGTP was also tested, and we observed a similar K_M for each dNTP with mutant and wild type telomerase complexes (data not shown). Furthermore, we observed no increase in type II processivity with increased dGTP concentrations with the chimeric tTER telomerases, probably as a result of low overall activity. By contrast, the wild type enzyme displayed an expected dGTP-dependent increase in type II processivity (Collins and Gandhi 1998;

Bryan et al. 2000; Hardy et al. 2001) (data not shown). In each case tested, the overall activity of the chimeric tTER telomerases was below that of the wild type.

5. Activity of chimeric telomerase mutants varies with primer 3′ end

Tetrahymena telomerase can initiate extension of a primer that is aligned, based on sequence complementarity, at any position from C49 to C43 (Autexier and Greider 1994; Autexier and Greider 1995). We examined if the primer alignment affects the efficiency of extension by the DNA-dependent telomerase mutants using a series of primers that align at five positions along the template (Figure 2.5a). We found, as expected, that wild type telomerase is efficient at extending a DNA primer (Figure 2.5b, lanes 1-5) with some specific primer alignments demonstrating increased activity (lanes 3-5). The activity of telomerase reconstituted with tTERd43-48 (lanes 6-10) was dramatically dependent on primer alignment. Telomerase tTERd43-48 was most active extending primers p4 and p5 (lanes 8 and 9, respectively) for which the first and second nucleotides added are dGMP, respectively (note that the orange asterisks mark the length of unextended primers on the gel). With these primers, the addition of dTMP was generally inefficient. Notably, telomerase tTERd43-48 was incapable of extension to the end of the template with some primers (lanes 7, 9, and 10), while primers p1 and p4 were extended weakly to the template boundary (note red arrow, lanes 6 and 8, respectively). tTERd43-48 telomerase exhibited reduced overall activity with primers p1 (lane 6), p2 (lane 7), and p6 (lane 10) when compared to primers p4 and p5. This can be explained in part for p2 because the majority of the products from this primer result from cleavage of two nucleotides from the primer to template position C46 before addition of ^{32}P-dGMP,

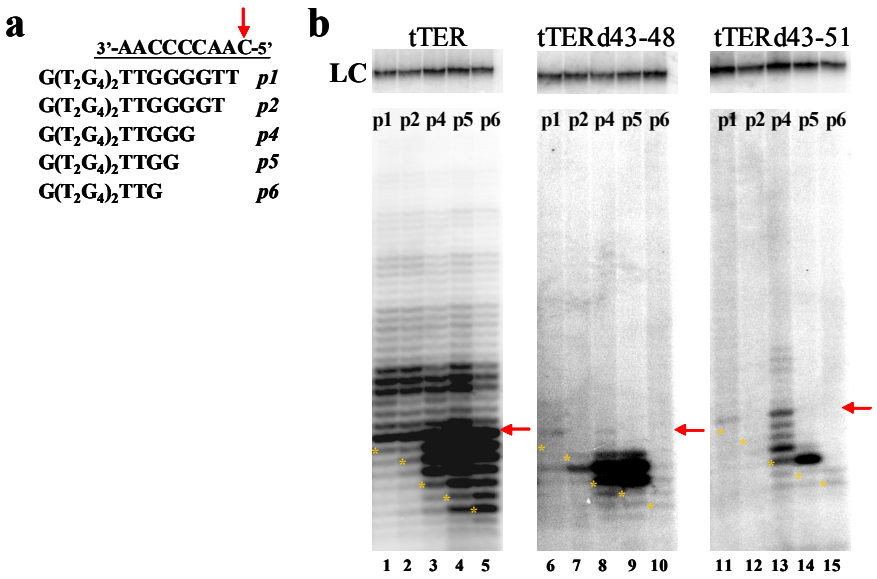

Figure 2.5 Affect of primer alignment on DNA-dependent and wild type telomerase activity. (a) Schematic of the primer and template alignment of the five primers utilized in the primer extension assays. (b) Denaturing polyacrylamide gels of telomerase-catalyzed primer extension products using standard telomerase assay conditions and telomerase reconstituted with tTER (lanes 1-5), tTERd43-48 (lanes 6-10), and tTERd43-15 (lanes 11-15). An orange asterisk "*" denotes the length of the unextended primer for each primer used. The asterisk is placed at the left of side of the denoted band to avoid obstructing the band from view. The primer extended in each lane is indicated near the top of the gel. The red arrow indicates extension to the end of the template for all primers. A ^{32}P-labeled loading control (LC) is indicated.

which is the most extensive product (lane 7, band below orange asterisk). Primer p1 was also at least partially excised by nuclease activity to template position C46 before extension (lane 6, band below orange asterisk). Primer p6 (lane 10), the poorest substrate of the six primers, can align with the template in two orientations: either fully extended to the template boundary or annealed to only the alignment domain. The inability to extend primer p6 suggests either that tTRd43-48 telomerase is incapable of adding a nucleotide across from the first template nucleotide, C48 (lane 10, light band above orange asterisk), following translocation, or that the fully extended DNA-DNA duplex is not translocated efficiently. Telomerase reconstituted with tTRd43-51 was unable to extend primer p2 (lane 12). Primers p4, p5, and p6 generated products that were shorter than the original primers, indicating that they were processed by nuclease activity to position C48 prior to

extension (note bands equal to or shorter than orange asterisk in lanes 13-15, respectively). For primer p5, the darkest band represents addition of dGMP across template position C47 (lane 14, dark band above orange asterisk), similar to the banding pattern seen for tTERd43-48 telomerase. Most important is the ability of tTERd43-51 to extend primer p4 to the end of the template (lane 13, red arrow) followed by primer realignment and a second round of extension, demonstrating the ability to perform type II processivity and therefore product translocation with a DNA template. Translocation efficiency was calculated as previously described (Hardy et al. 2001; Huard et al. 2003) for primer p4 and we found that wild type telomerase (translocation efficiency = 12%) was more efficient at primer translocation than tTERd43-48 telomerase (translocation efficiency = 5%).

6. Chain terminators reveal decreased nucleotide addition activity

To examine the effect of a DNA template on primer alignment, single nucleotide addition and nucleotide addition processivity (type I processivity) in the absence of repeat addition processivity (type II processivity), we utilized a dideoxythymidine triphosphate (ddTTP) stop assay modified from a previously described protocol (Strahl and Blackburn 1994). In the presence of ddTTP, *Tetrahymena* telomerase extends a primer to the position across from template residue A45 then adds a ddTMP residue, resulting in extension termination (Figure 2.6a, stop sign). With tTERd43-48 telomerase, primer extension did not proceed far enough to allow addition of ddTMP, suggesting that ddTMP addition is inefficient for this mutant (Figure 2.6b, lanes 3, 7, and 11). Because the banding pattern is not affected by ddTTP, we infer that primer alignment is the same

in the DNA-dependent telomerase as in the wild type, though this is a tenuous assignment given the lack of robust activity. Of interest, primer p2, which should preclude the addition of ^{32}P-dGMP because ddTMP would be the first added nucleotide, did allow

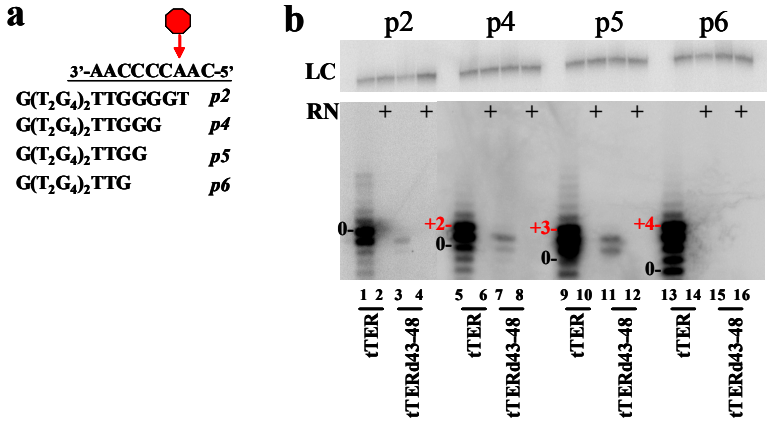

Figure 2.6 Dideoxythymidine primer extension stop assay confirms correct template-primer alignment and reduced nucleotide addition activity. (a) Template and primer sequences of the tested primers. The stop sign and arrow indicate the location of the first ddTMP (at A45), which terminates oligonucleotide primer extension. (b) tTERT assembled with tTER (lanes 1, 2, 5, 6, 9, 10, 13, and 14) or tTERd43-48 (3, 4, 7, 8, 11, 12, 15, and 16) was assayed under standard conditions except 100 μM ddTTP was substituted for dTTP. A black "0" indicates original primer length and red numbers indicate the position of ddTMP addition for each primer tested. A ^{32}P-labeled loading control (LC) is indicated. Lanes labeled with RN are assays of samples pretreated with RNase A.

dGMP incorporation for both the wild type and chimeric tTERs (lanes 1 and 3), suggesting that the primer is processed by a nuclease activity prior to extension. This previously observed nuclease activity (Collins and Greider 1993) cleaved the primer at least back to position C46 before extension for both wild type tTER and chimeric tTER telomerases (Figure 2.6b, lanes 1 and 3, respectively; Figure 2.5b, lane 7). The wild type tTER telomerase had product bands shorter than or of equal length to the unextended primer for primers p4, p5, and p6 (lanes 5, 9, and 13, respectively), while the tTERd43-48 telomerase had a band equal in length to the primer for primer p4 (lane 7), suggesting that these primers were also processed by nuclease activity before extension. Primer p5 did not have products shorter than or equal in length to the primer when extended by

tTERd43-48 telomerase (lane 11). Primer p6 was not extended by tTERd43-48 telomerase (lane 15). We did observe extension products past the A45 stop point with wild type telomerase (lanes 1, 5, 9, and 13), which presumably resulted from contaminating dTTP present in the RRL.

7. Chimeric tTER telomerases efficiently utilize an RNA primer

In the previous experiments, we tested the ability of telomerase assembled with chimeric tTER mutants to extend DNA primers. The next logical question to ask is

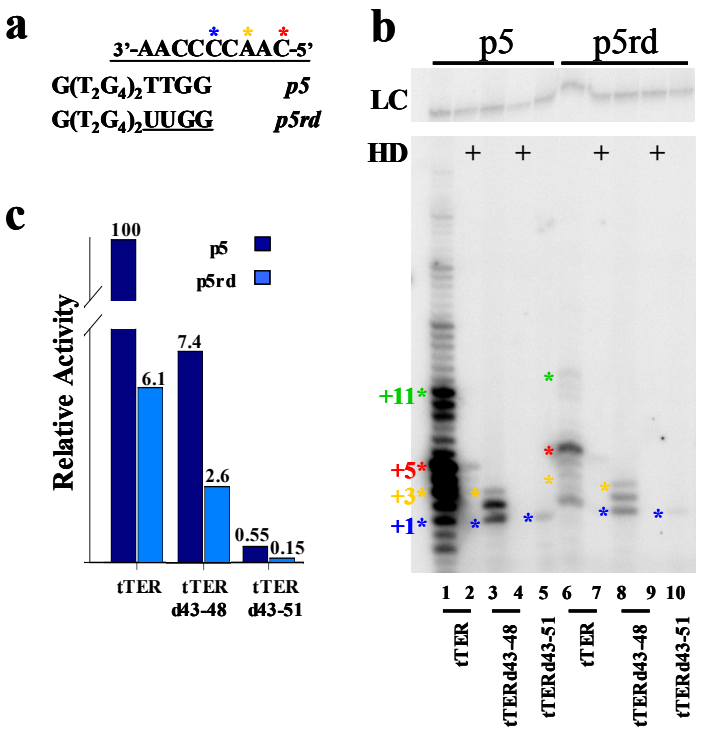

Figure 2.7 Extension of a chimeric RNA-DNA primer with telomerase assembled with chimeric tTER. (a) Alignment of template and primers tested in the assay. p5rd has rNMPs (underlined) substituted for dNMPs at the last four 3′ positions. (b) Telomerase activity was assayed using standard conditions with 2 μM p5 primer (lanes 1-5) or 2 μM p5rd primer (lanes 6-10). Blue "*", orange "*", red "*", and green "*" numbers and asterisks to the left of select lanes indicate the extension of the indicated primer by one, three, five, and eleven nucleotides, respectively. Heat denatured (HD) samples, 95 ºC for 3 min prior to assay, served as a control for background activity instead of RNase, which would degrade the p5rd primer. A ^{32}P-labeled loading control (LC) is indicated. (c) Quantification of reactions in Figure 2.7b. Product intensities were normalized to the LC and to 100% activity, which was defined as the activity of wild type telomerase with primer p5.

whether or not the DNA-dependent telomerase mutants can extend an RNA primer, in effect reversing the polarity of the template-nascent product duplex from the native RNA-DNA to DNA-RNA. In this assay, dNTPs were used because telomerase is selective for dNTP substrates, thus the product is a chimera. We tested two primers, a DNA primer, p5, and a chimeric primer containing ribonucleotides as the final four 3′ bases, p5rd (Figure 2.7a). This chimeric primer was used because an entirely RNA primer, p5r, was not extended by telomerase (data not shown), consistent with previous studies (Collins and Greider 1995). Wild type telomerase could efficiently extend p5 and p5rd (Figure 2.7b, lanes 1 and 6, respectively) and exhibit type II processivity (see green asterisks, lanes 1 and 6) but the overall activity was significantly decreased for p5rd (6.1% of p5 activity; Figure 2.7b, lane 1 vs. lane 6; Figure 2.7c). Telomerase tTERd43-48 was able to extend both primers (lanes 3 and 8) yielding an identical banding pattern (see blue and orange asterisks) but without type II processivity. The activity with p5rd was decreased to 35% of the activity with p5 (Figure 2.7b, lane 3 vs. lane 8; Figure 2.7c). Similarly, telomerase tTERd43-51 extended p5rd with the same banding pattern as p5 (see blue asterisks, lanes 5 and 10) and with decreased activity, 27% of the activity with p5 (Figure 2.7b, lane 5 vs. lane 10; Figure 2.7c), and displayed no repeat addition processivity.

8. tTERT^{Y623A} telomerase can efficiently extend an RNA or DNA primer using rGTP.

To further characterize the catalytic potential of telomerase, we examined its ability to function as an RNA polymerase. To conduct this experiment, the mutant tTERT^{Y623A}, which has decreased dNTP/rNTP discrimination (Miller et al. 2000), was employed. Following reconstitution with tTER and immunoprecipitation, tTERT^{Y623A}

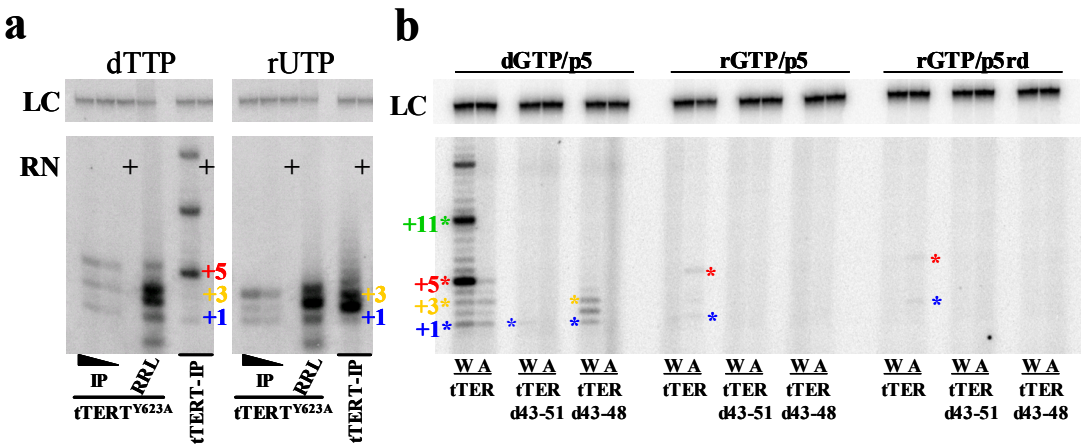

Figure 2.8 Telomerase-catalyzed extension of a chimeric primer using rGTP as the substrate. (a) Primer extension assay under standard conditions with p5 primer except 100 μM rUTP (Lanes 6-10) was substituted for dTTP (Lanes 1-5) where indicated. Assays of immunoprecipitated tTERT^{Y623A} (Lanes 1, 2, 6, and 7) and tTERT (Lanes 4, 5, 9, and 10), and crude tTERT^{Y623A} (Lanes 3 and 8) each assembled with tTER are indicated. (b) Wild type tTERT (W; Odd numbered Lanes) or tTERT^{Y623A} (A; Even numbered Lanes) were assembled with tTER (Lanes 1, 2, 7, 8, 13, and 14), tTERd43-51 (Lanes 3, 4, 9, 10, 15, and 16), or tTERd43-48 (Lanes 5, 6, 11, 12, 17, and 18) then immunoprecipitated and assayed under standard reaction conditions with 10 μM [α-^{32}P]-dGTP (Lanes 1-6) or [α-^{32}P]-rGTP (Lanes 7-18), 2 μM p5 (Lanes 1-12) or p5rd (Lanes 13-18), and 100 μM dTTP (All Lanes). Blue (*), orange (*), red (*), and green (*) asterisks and/or numbers represent the extension of the indicated primer by one, three, five, and eleven nucleotides, respectively. A ^{32}P-labeled loading control (LC) is indicated. Lanes labeled with RN are assays of samples pretreated with RNase A.

was assayed for its ability to incorporate rUTP. In assays containing rUTP and ^{32}P-dGTP, tTERT^{Y623A} was able to add two dGMPs and then a single rUMP across template position 45 but no further primer extension was observed (Figure 2.8a). When dTTP was substituted, the primer was extended to the end of the template, suggesting that dTMP was added efficiently. Type II translocation was not observed for either rUTP or dTTP. As previously reported, unpurified tTERT^{Y623A} yielded extension products, which did not run equally as control extension products in the presence of dTTP or rUTP (Miller et al. 2000). Presumably, endogenous rGTP from the RRL was added to the extended primer altering its electrophoretic mobility, and causing a shift in the product bands. Of interest is the observation that the RRL assay with rUTP did not extend the primer to the end of the template, suggesting that telomerase does not incorporate more than one rUMP onto a

primer even though the d/rNTP selectivity is reduced. To eliminate the effects of endogenous rNTPs and dNTPs present in the RRL, immunopurified telomerase complexes were employed in the following assays. Immunopurified wild-type telomerase was able to extend the primer in the presence of dTTP, while only extending to template position 46 in the presence of rUTP (Figure 2.8a). When immunopurified telomerase reconstituted with either tTERT or $tTERT^{Y623A}$ was incubated with a primer, ^{32}P-rGTP, and dTTP, wild type telomerase was unable to add rGTP whereas $tTERT^{Y623A}$ assembled with tTER was able to extend primers p5 and p5rd to the end of the template (Figure 2.8b). When $tTERT^{Y623A}$ was reconstituted with either tTERd43-48 or tTERd43-51, the resulting telomerase complex was inactive. Apparently, the combination of the tTERT mutant with reduced activity and a tTER mutant that confers reduced activity did not allow the production of an RNA polymerase. In assays containing rUTP, ^{32}P-rGTP, and immunopurified protein and template mutants, no activity was observed (data not shown).

9. Template-Primer thermal stability

The reduced activity of telomerase when utilizing a DNA template could be a result of decreased stability of the template-nascent product duplex. In general, duplex thermal stability for identical sequences decreases in the order RNA-RNA>RNA-DNA>DNA-DNA. We used UV melting curves to determine the melting temperature for the four possible 9 base pair duplexes formed by the template and primer (Table 2.1). Not surprisingly, the native duplex melting temperature of 41.0 ºC is higher than the DNA-DNA melting temperature of 39.0 ºC. This difference may contribute to the

Table 2.1. Duplex Melting Temperatures of Template-Primer Pairs[a]

Template[b]	Primer[c]	T_m [d] (ºC)
RNA	DNA	41.0 ± 0.5[e]
DNA	DNA	39.0 ± 0.5
DNA	RNA	44.5 ± 0.5
RNA	RNA	60.0 ± 0.5

[a] Melting temperatures were determined from temperature-dependent UV absorbance measurements using 4 μM of each strand. [b] Template sequence: (5'-CAACCCCAA) [c] Primer sequence: (5'-TTGGGGTTG) [d] T_m was calculated from the first derivative of the melting curve at 260 nm. [e] Standard deviation from two separate determinations.

reduced activity level of the mutants. Based on this possibility, we examined the temperature dependence of telomerase-catalyzed primer extension. We found that a reduction in assay temperature to 10 ºC resulted in an equivalent decrease in overall activity for both mutant and wild type enzymes and an increase in the type II processivity of the wild type enzyme (data not shown). A similar effect of temperature on processivity was recently reported by Aigner and Cech (Aigner and Cech 2004). Because decreasing the temperature did not rescue the activity of the mutant telomerase, it appears that decreased duplex stability does not explain the reduced ability of telomerase to function as a DNA-dependent polymerase.

C. Discussion

Telomerase is a unique RT, which uses a portion of its integral RNA subunit as a template for the extension of telomeric 3′ overhangs. In this report we described the synthesis and characterization of two mutants of *Tetrahymena* telomerase RNA that contain a deoxyribose backbone replacing the natural ribose backbone in the templating

region. These chimeric tTER mutants allowed ribonucleoprotein (RNP) assemblage, enabling us to investigate the important features of the template-primer interactions including template specificity and contributions of the structure of the template-nascent product duplex to activity. We showed, for the first time, that telomerase can utilize a DNA template. However, the activity of the DNA-dependent telomerase mutants was greatly reduced when compared to natural telomerase RT activity.

1. Telomerase requires regions of its RNA subunit other than the template even after holoenzyme assembly

Telomerase exhibits three specific enzymatic activities: single nucleotide addition (Greider and Blackburn 1985), telomere repeat addition (Greider and Blackburn 1985), and nuclease activity (Collins and Greider 1993). When telomerase functioned as a DNA-dependent DNA polymerase, we found that, while the activity levels were reduced (Figure 2.3, lane 1 vs. lanes 3 and 4), the hallmarks of wild type telomerase activities were conserved. Telomerase is a RNP complex that requires its RNA subunit for both the template of DNA synthesis as well as enzymatic activity separate from its templating role. We found that telomerase assembled with either of the chimeric RNA subunits was sensitive to RNase (Figure 2.4, lanes 12 and 18). Because the template in these chimeric molecules is DNA, the RNA sensitivity must come from degradation of non-templating portions of tTER. Since this occurred after telomerase was assembled, it offers further evidence that telomerase is a specialized and obligate RNP (Miller and Collins 2002), and it provides the first direct evidence that the RNA subunit is required for maintaining a functional active site even after the holoenzyme structure has been established.

2. Telomerase can utilize a DNA template to extend a primer

During DNA synthesis, telomerase catalyzes two types of processivity. Type I is extension of a primer to the template boundary, and type II is repeat addition processivity, which requires translocation of the nascent DNA product to allow realigning after the template terminus has been reached (Huard et al. 2003; Lue 2004). When telomerase utilized a DNA template, it was capable of limited primer extension (Figure 2.3, lanes 3 and 4). Furthermore, depending on the primer used to initiate DNA synthesis, the DNA-dependent telomerase demonstrated both type I (Figure 2.5b, lanes 6, 8, 11, and 13) and type II (Figure 2.4, lanes 10 and 11; Figure 2.5b, lane 13) processivity. These results demonstrate that the chimeric tTER-containing enzyme assembled correctly, properly aligned its template and primer in the active site, and could utilize a DNA template to extend a DNA primer. Thus telomerase, like retroviral RTs can utilize both DNA and RNA as a template. Telomerase is unique among RTs, however, in that its DNA-dependent activity is dramatically reduced compared to its RNA-dependent activity.

3. The nascent primer-template helix structure is an important factor in telomerase processivity

The low activity of the DNA-dependent telomerase mutants could be a result of several factors. The presence of a DNA template could alter the template-nascent primer helix geometry or reduce the thermal stability of the template-nascent primer duplex. We found that the thermal stability of the four possible template-primer duplexes does differ (see Table 2.1), but conducting assays at lower temperatures did not affect the activity of the DNA template mutant. However, the structure of the template-primer helix in the

active site is likely to be affected by the presence of a DNA template. Two experimental observations support the hypothesis that telomerase is sensitive to the structure of the template-nascent product duplex. First, tTERd43-48 telomerase exhibits more robust type I processivity than the tTERd43-51 telomerase (Figure 2.3, 2.4 and 2.5b), and second, both template mutants demonstrated a reduced ability to incorporate dTTP (Figures 2.3, 2.4, 2.5b and 2.6b). The difference in activity of tTERd43-48 telomerase is likely due to the presence of RNA in the alignment region of this template mutant. These three additional RNA-DNA base pairs (A51-C49) could confer H- or A-form duplex character onto the primer annealed to the coding region of the template (C48-C43) (Nakano et al. 2004). The less active mutant, tTERd43-51, contains DNA in the alignment region, which increases the possibility that the all DNA template-nascent primer duplex in the active site will tend towards a B-form structure (Nakano et al. 2004). The decreased ability of the DNA containing telomerase mutants to effectively add dTMP is consistent with the hypothesis that telomerase is sensitive to the helical structure contained in its active site, since T-A-rich DNA-DNA duplexes fail to form H- or A-form helices under normal conditions (Pilet et al. 1975; Stefl et al. 2001), whereas DNA-DNA duplexes high in G-C base pairs can easily be induced to form H- or A-form helices (McCall et al. 1985; Minchenkova et al. 1986; Sarma et al. 1986).

We made several efforts to force the template-nascent primer DNA-DNA duplex to assume a more A-form like helix in order to recapitulate the natural helix shape and rescue primer extension activity (Saenger 1984). The addition of a dehydrating agent such as methanol, which has been used successfully to rescue activity in other polymerases by forcing the template-primer duplex to adopt an A-form helix (Huang et

al. 1997), inhibited telomerase activity in general (data not shown). However, the telomerase containing a DNA template could utilize an RNA-containing primer with less reduction in activity than the wild type enzyme when activity was compared to extension of DNA primers (Figure 2.7b). There was a 16-fold decrease in total activity of the wild type telomerase when extending p5rd compared to a 2.8- and 3.7-fold decrease for tTERd43-48 and tTERd43-51 telomerase, respectively (Figure 2.7c). Perhaps the mutants are less affected by the use of an RNA primer than wild type telomerase because the DNA-RNA duplex formed more closely resembles the duplex structure preferred by wild type telomerase.

4. Telomerase prefers an A-form like template-nascent product duplex

We conclude that *Tetrahymena* telomerase prefers an H- or A-form like template-nascent product duplex. This assertion is consistent with published structural studies of RTs, polymerases, and chimeric duplexes. The crystal structure of a covalently trapped catalytic complex of HIV RT (Huang et al. 1998) shows that approximately five base pairs of the DNA-DNA duplex in the active site is forced into an A-form helix, while the rest of the duplex is B-form. This posits that HIV RT and possibly other RTs force the duplexes that reside in their active site into an A-form conformation regardless of the sugar backbone identity (Kunkel and Bebenek 2000). This is not unique to RTs, since T7 RNA polymerase also shows evidence of forcing A-form structure on its template-nascent primer helix, and RNA polymerase can be converted to a DNA polymerase by the addition of a dehydrating reagent such as methanol (Huang et al. 1997). Also, crystal structures of *Bacillus stearothermophilus* DNA polymerase show an A-form DNA duplex

in the active site while the rest of the DNA is B-form (Kiefer et al. 1998). Studies of poly(dG):poly(dC) duplexes have shown these duplexes naturally form A-form structures in both crystal structures (McCall et al. 1985) and solution NMR structures (Sarma et al. 1986). This may explain why telomerase demonstrates greater ability to utilize dGTP as a substrate when compared to dTTP when it functions with a DNA template.

5. Telomerase fidelity and nuclease activity may be dependent upon proper template-nascent product helix structure

The preference of telomerase for an H- or A- form helix in its active site may be a determinate of its fidelity and give rise to the apparent increase in the observed nuclease activity, which appears to precede nucleotide addition in many experiments (Figure 2.5b, lanes 6-10, 13-15; Figure 2.6b, lanes 3 and 7). When an incorrect dNMP is added by the native enzyme, it likely causes a change in the local duplex helix geometry resulting in a non-optimally positioned 3′ hydroxyl group, hindering nucleophilic attack on the incoming dNTP. In response, the enzyme could remove the added nucleotide as part of its proofreading mechanism. In our experimental system, the altered nucleotide is in the template and not in the primer; therefore, even correctly coded extension may be recognized as misincorporation and be removed, resulting in a futile cycle of addition-excision. DNA and RNA polymerases have proofreading domains that are separate from their active sites, whereas reverse transcriptases do not and are quite error prone with misincorporation rates of 10^{-1}-10^{-4} compared to 10^{-6}-10^{-9} for typical DNA polymerases (Kunkel and Bebenek 2000; Kunkel 2004). One study of human telomerase fidelity found error rates of 10^{-3} (Kreiter et al. 1995), which is similar to other RTs. Thus, one

interpretation of our data is that the template-primer duplex geometry within the telomerase active site plays a role in the fidelity of *Tetrahymena* telomerase.

Telomerase is a unique DNA polymerase because it utilizes its RNA subunit for both structural and enzymatic functions. The experiments described above demonstrate that telomerase can utilize a DNA template, although with decreased efficiency, to recapitulate the standard enzymatic functions of the wild type enzyme including processive primer elongation and nuclease proofreading activity under standard conditions. Our results suggest that telomerase is sensitive to the structure of the nascent product-template duplex.

D. Materials and methods

1. Oligonucleotides

DNA oligonucleotides were purchased from Integrated DNA Technologies (Coralville, IA) and were purified using denaturing PAGE followed by a modified version of the crush and soak method (Maxam and Gilbert 1977; Keppler and Jarstfer 2004). Briefly, following electrophoresis, oligonucleotides were visualized by UV shadowing, gel slices were removed, crushed by passing through the tip of a sterile plastic syringe, and the oligonucleotides were extracted from the gel into TEN buffer (10 mM Tris pH 7.5, 1 mM EDTA, 250 mM NaCl). Oligonucleotides were then concentrated by ethanol precipitation and resuspended in TE (10 mM Tris-Cl pH 8.0, 1 mM EDTA). RNA oligonucleotides and the RNA-DNA chimeras tTER(1-51)d43-51 and tTER(1-51)d43-48 were purchased from Dharmacon (Lafayette, CO) in the 2′-ACE

protected form. These synthetic RNAs were deprotected following the manufacturers instructions and were not further purified before use. All oligonucleotides were analyzed by denaturing PAGE to confirm their purity. Typically, individual sequences were >95% full-length oligonucleotides. Oligonucleotide concentrations were determined by UV absorbance at 260 nm using the molar extinction coefficient provided by the manufacturer.

2. Plasmids

A construct that contains the tTERT gene with an N-terminal T7-tag inserted into the vector pET-28a (Novagen), pET-28a-tTERT, was a gift from the laboratory of Dr. Thomas R. Cech (Bryan et al. 2000). pTET-telo, a plasmid containing the tTER gene, a promoter for T7 RNA polymerase, and a self-cleaving hammerhead ribozyme that processes the 5′ end of the RNA to generate wild type tTER was a gift from Dr. Art Zaug (Zaug and Cech 1995).

3. PCR amplification of tTER52-159 template

The template for tTER52-159, the 108-nt 3′ portion of tTER used for splint ligations, was generated by PCR. Briefly, two DNA oligonucleotides, antisense strand 5'-CGGGGATCCTCTTCAAAAATAAGACATCCATTGATAAATAGTGTATCAA ATGTCGATAGTCTTTTGTCCCGCATTACCACTTATTTGAACCTAATTGGTGAA GGTTATATCAGC and sense strand 5'-CGCGGAATTCTAATACGACTCACTATAG GGAGGAGATTTCTGATGAGGCCGAAAGGCCGAAACTCCACGAAAGTGGAGT

AAAATCTAGTGCTGATATAACCTTCACCAATTAGG, which are complementary along the solid underlined portions, were subjected to five cycles of PCR, 95 °C for 30 s/55 °C for 30 s/72 °C for 30 s, to yield full-length, double-stranded product. This product was further amplified by the addition of sense primer 5′-GCGCGGAATTCTA ATACGACTCACTATAGG and antisense primer 5′-CGGGGATCCTCTTCAAAAAT AAGA using thirty additional PCR cycles. The 204 base pair PCR product was purified using Wizard PCR Preps DNA Purification System (Promega) following the manufacturers instructions. The broken-dot, underlined portion of the sense strand codes for a self-cleaving hammerhead ribozyme that generates the appropriate 5′ end required for efficient ligation of the product RNA, tTER52-159.

4. Transcription of RNAs

Full length tTER and tTER52-159 were prepared by in vitro transcription using the T7 RNA polymerase AmpliScribe kit (Epicentre) and the corresponding linear, double stranded DNA templates. For full-length tTER, 20 μg pTET-telo was digested with the restriction enzyme *Ear*I (New England Biolabs), which cuts 3′ of the tTER gene. Digested DNA was deproteinized by phenol/chloroform/isoamyl alcohol extraction, concentrated by ethanol precipitation, and resuspended in TE. The template for the tTER52-159 was prepared by PCR as described above. Both transcription reactions followed the manufacturers protocol (Epicenter). After transcription, the reactions were diluted 4 fold into 20 mM $MgCl_2$ to activate hammerhead ribozyme cleavage. Following ribozyme cleavage the RNAs were concentrated by ethanol precipitation and reconstituted in denaturing loading buffer (89 mM Tris, 89 mM boric acid, pH 8.3, 2 mM

EDTA, 7 M urea, 10% glycerol, 0.02% bromophenol blue, 0.02% xylene cyanol FF). RNAs were purified by denaturing PAGE on 1.5 mm thick, denaturing 10% polyacrylamide gels as described above.

5. Splint ligation synthesis of tTERd43-51 and tTERd43-48

Full-length chimeric tTER mutants were synthesized by ligation reactions mediated by DNA splints (Moore and Sharp 1992). Prior to splint ligation, 750 pmoles of tTER52-159 RNA were 5′ phosphorylated with ATP (25 μM) using 150 Units of T4 polynucleotide kinase (PNK, New England Biolabs) and PNK buffer at 37 °C for 35 min. The reaction was stopped by heating at 95 °C for 5 min. Excess nucleotides were removed from the reaction using a MicroSpin G-25 column (Amersham Biosciences) per the manufacturer's instructions. The RNA was deproteinized by phenol/chloroform/isoamyl alcohol extraction, concentrated by ethanol precipitation and resuspended in a suitable volume of TE. Ligation of 5′ phosphorylated tTER52-159 to tTER(1-51)d43-51 or tTER(1-51)d43-48 was performed by combining 500 pmole of each of the two partnering RNAs along with 600 pmole of a 31-nucleotide DNA splint, 5′-TCAGCACTAGATTTTTGGGGTTGAATGACAG, which is complementary to nucleotides 35-51 of tTER(1-51)d43-48 or tTER(1-51)d43-51 and nucleotides 52-65 of tTER52-159 (See Figure 2.1c). The 5′ and 3′ tTER components and DNA splint were heated to 95 °C and cooled slowly to 0 °C over 1 h followed by the addition of 0.1 volume of 10× T4 Ligase Buffer (Promega) and 250 Units of T4 DNA Ligase (Promega) in a final volume of 500 μL. Ligation reactions were incubated at 37 °C for 3 h after which they were extracted with phenol/chloroform/isoamyl alcohol, concentrated by

ethanol precipitation, and resuspended in denaturing loading buffer. The chimeric tTER products were purified by denaturing PAGE as described above (Maxam and Gilbert 1977; Keppler and Jarstfer 2004). Small-scale ligation reactions (10 pmole total RNA) were performed prior to large-scale reactions to optimize the ligation reaction conditions. The progress of these reactions was monitored by SYBR Green II (Molecular Probes) stained denaturing polyacrylamide gels of different ligation reaction time points.

6. 5'-^{32}P-labeling of tTERs

Telomerase RNAs were 5′ end labeled by incubating 2.75 pmole of tTER, tTERd43-51, or tTERd43-48 with 10 Units of PNK, 20 pmole of [γ^{32}P]-ATP (6000 Ci/mmol; Perkin-Elmer) and 1× PNK Buffer at 37 °C for 35 min. The radiolabeled RNAs were purified using a MicroSpin G-25 column to remove unincorporated nucleotides, extracted with phenol/chloroform/isoamyl alcohol, concentrated by ethanol precipitation, and resuspended in TE. The specific activity of the RNAs was determined by liquid scintillation counting on a Packard 1900 TR Liquid Scintillation Analyzer.

7. Translation of tTERT and telomerase assembly

tTERT was translated and assembled with tTER using a TNT Coupled Reticulocyte Lysate Systems kit (Promega) based on a previously described procedure (Bryan et al. 2000). A typical 50 μL reaction contained 1 μg of pET-28a-tTERT, 75 ng of tTER, tTERd43-51, or tTERd43-48, 34 pmole of [^{35}S]-methionine (1175 Ci/mmol; Perkin-Elmer) and additional reaction kit components provided by the manufacturer. Reactions were incubated at 30 °C for 90 min and were flash frozen in an ethanol/dry ice

bath and stored at –80 °C. 5 μL of each lysate reaction was analyzed by SDS PAGE as follows. Samples were denatured by the addition of an equal volume of 2× SDS Gel-loading Buffer (100 mM Tris-HCl pH 6.8, 200 mM DTT, 20% glycerol, 4% SDS, and 0.05% bromophenol blue) and heated at 95 °C for 5 min. The denatured samples were electrophoresed on 6% acrylamide/SDS gels (Laemmli 1970). Gels were dried before exposing overnight to phosphorimager plates, which were imaged on a Molecular Dynamics Storm 860 phosphorimager.

8. Immunoprecipitation of the telomerase complex

To purify the telomerase complex for enzyme assays and to measure the relative amounts of RNA bound to tTERT, we used an immunoprecipitation assay (Bryan et al. 2000). Anti-T7 antibody agarose beads (Novagen; 50 μL) were washed 4 times in 750 μL of Wash Buffer 1 (20 mM Tris-acetate pH 7.5, 100 mM potassium glutamate, 5 mM $MgCl_2$, 1 mM EDTA, 1 mM DTT, 10% glycerol, and 0.1% IGEPAL). Between each step, beads were recovered by centrifugation at 1,500*g* for 2 min at 4 ºC. The beads were then blocked twice using 500 μL of blocking buffer (Wash Buffer containing 0.5 mg/mL lysozyme, 0.5 mg/mL BSA, 0.05 mg/mL glycogen, and 0.1 mg/mL yeast RNA) for 15 min at 4 ºC with gentle mixing on an orbital shaker. 75 μL of RRL translation reaction containing assembled telomerase was added to 75 μL of blocking buffer and centrifuged at 17,000*g* for 10 min at 4 °C to remove any precipitates. The supernatant was then added to the 50 μL of blocked T7-agarose beads and the resultant slurry was mixed on an orbital shaker for 3 h at 4 ºC. The beads were washed 4 times with 750 μL of Wash Buffer 3 (20 mM Tris-acetate pH 7.5, 300 mM potassium glutamate, 5 mM $MgCl_2$, 1 mM

EDTA, 1 mM DTT, 10% glycerol, and 0.1% IGEPAL), 2 times with 750 μL of TMG (10 mM Tris-Acetate pH 7.5, 1mM $MgCl_2$, 1 mM DTT, and 10% glycerol) and resuspended in 50 μL of TMG to afford a 1:1 slurry. Samples were either flash frozen in an ethanol/dry ice bath and stored at –80 ºC or were prepared for SDS PAGE analysis as described above.

9. Telomerase activity assay

Telomerase assays contained telomerase from crude RRL reactions (10 μL), telomerase reaction buffer (50 mM Tris-Cl pH 8.3, 1.25 mM $MgCl_2$, 5 mM DTT), 2 μM telomeric primer, 100 μM dTTP, 10 μM dGTP, and 0.33 μM [α^{32}P]-dGTP (3000 Ci/mmol) in a final reaction volume of 20 μL. In some experiments, 0.5 μg DNase-free RNase A (USB) was added to the telomerase buffer before the addition of telomerase as a control for RNA-dependent primer extension (Greider and Blackburn 1989). Variations from standard conditions, including primer sequences and variation in nucleotide substrates are described in the appropriate figures and figure legends. Reactions were incubated at 30 °C for 1 h followed by the addition of an 80 μL aliquot of TES Stop buffer (50 mM Tris-HCl pH 8.0, 20 mM EDTA, 0.2% SDS) containing a 5'-^{32}P-labeled 114-nt oligonucleotide for extraction and loading control. Extension products were purified by phenol/chloroform/isoamyl alcohol extraction and concentrated by ethanol precipitation using 2 M ammonium acetate and 100 μg/mL glycogen as counter ion and carrier, respectively. The resulting pellets were resuspended in denaturing loading buffer and heated to 95 ºC for 5 min prior to their separation using denaturing PAGE. Products were resolved on 0.4 mm thick, denaturing 8% polyacrylamide sequencing gels, which

were run at 70 W for 1.25 h. Dried gels were exposed overnight to phosphorimager plates. Plates were imaged using a Molecular Dynamics Storm 860 phosphorimager and were analyzed using ImageQuant 5.1.

10. Thermal stability of model primer•template duplex

Duplexes d(CAACCCCAA)/r(UUGGGGUUG), d(CAACCCCAA)/d(TTGGGGTTG), r(CAACCCCAA)/r(UUGGGGUUG), and r(CAACCCCAA)/d(TTGGGGTTG) were annealed at a total strand concentration of 8 μM in 50 mM Tris-HCl, pH 8.3 and 1.25 mM $MgCl_2$ in a final volume of 500 μL. UV absorbance at 260 nm (A_{260}) was monitored on a Perkin Elmer UV/Vis Spectrophotometer Lambda 20 with the temperature controlled by a PTP-6 Peltier System and Fisher Scientific Isotemp 1016S. Temperature was changed at a rate of 2 °C/min from 10-75 °C and from 75-10 °C in duplicate. Melting temperatures were determined from the first derivative of the A_{260} versus temperature curve.

Chapter III. SHAPE analysis of tTER stem IV mutants and comparison to high resolution NMR structures

Adapted from: Chen, Y., J. Fender, J. D. Legassie, M. B. Jarstfer, T. M. Bryan and G. Varani, *Structure of stem-loop IV of Tetrahymena telomerase RNA*. EMBO J., 2005. 25(13): p. 3156-66.

A. Introduction

Selective 2'-hydroxyl acylation analyzed by primer extension (SHAPE) is a quantitative RNA structure analysis technique that offers single nucleotide resolution (Merino et al. 2005; Wilkinson et al. 2006). SHAPE analysis allows the investigation of both the structure and the relative conformational flexibility of each nucleotide using the hydroxyl selective acylating reagent *N*-methyl isatoic anhydride (NMIA). When a RNA residue is base paired it usually adopts a C3'-endo sugar pucker, which places the 3'-phosphodiester anion in relatively close proximity to the 2'-hydroxyl (~4 Å). This close proximity to the anion weakens the nucleophilicity of the 2'-hydroxyl (Chamberlin et al. 2002; Merino et al. 2005). Conversely, C2'-endo sugar pucker, which is prevalent in unbase paired RNA residues, places a greater distance between the 3'-phosphodiester anion and the 2'-hydroxyl, promoting greater reactivity (Wilkinson et al. 2006). When a particular nucleotide is more conformationally flexible, it is free to rapidly sample more conformations, and the more conformations a nucleotide samples, the more likely it will be in a conformation favorable for 2'-hydroxyl acylation by NMIA. In this particular

aspect, SHAPE is a perfect accompaniment to NMR analysis, because SHAPE essentially measures nucleotide conformation in solution, similar to NMR.

The first reagent used for SHAPE experiments was NMIA (Merino et al. 2005). Recently, other isatoic anhydride derivatives have been investigated (Mortimer and Weeks 2007) in an attempt to find reagents that may impart better or different reaction profiles, such as a) faster acting, b) differential modification of nucleotides dependent on local structural environments, or c) active under a broad range of reaction conditions. SHAPE chemistry with NMIA and derivatives should prove quite useful for high resolution RNA structure analysis.

In studies described in this chapter, SHAPE analysis of stem IV from the *Tetrahymena thermophila* telomerase RNA is compared with structures generated by high resolution NMR. Using the structural data generated, five stem IV mutants were

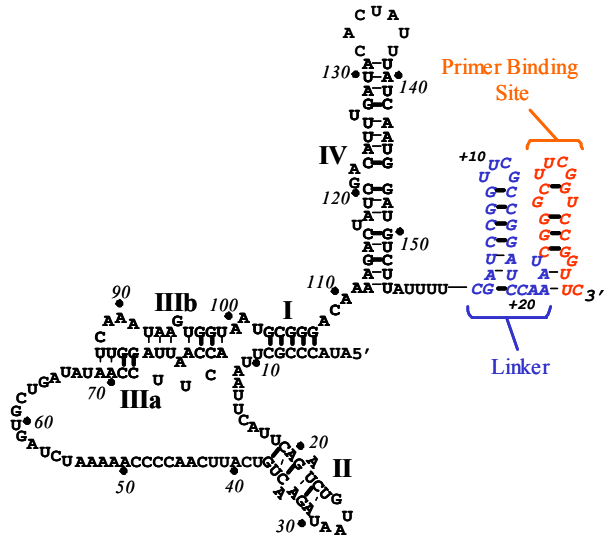

Figure 3.1 tTER secondary structure with 3' SHAPE extension. The phylogenetically determined secondary structure of tTER with 3' SHAPE analysis extension (Merino et al. 2005). Blue nucleotides represent linker and red nucleotides represent reverse transcription primer binding site.

created and analyzed for enzymatic activity and their structure was examined using SHAPE technology. With the stem IV NMR structure for comparison, two isatoic anhydride analogs were also tested on stem IV.

B. Results

1. Generation of tTER and stem IV mutants for SHAPE experiments

In order to study tTER stem IV by SHAPE analysis, a 3' extension as described by Merino et al. (2005) was added (Figure 3.1). The 3' extension contains an 18-nucleotide reverse transcriptase primer-binding site (red nucleotides) at the very 3' end followed by a 24-nucleotide linker (blue nucleotides) before the poly-U tail marking the 3' end of tTER. The combined 42-nucleotide extension forms two stable stem loops to help avoid spurious folding with the target RNA.

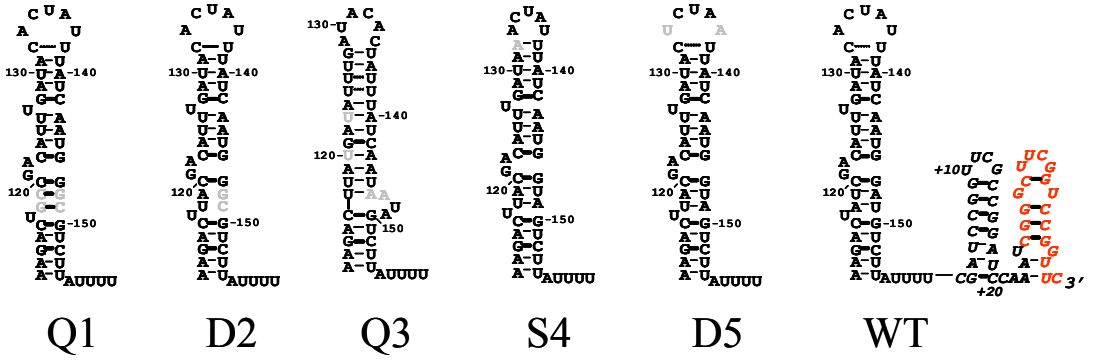

Figure 3.2 tTER stem IV mutants. Proposed secondary structures of tTER stem IV mutants. Mutated residues are colored light grey. Wild type stem IV is depicted with 3' extension, which is present in all mutants analyzed.

The Varani lab constructed five tTER stem IV mutant plasmids to study the effect of specific stem IV mutations on both telomerase structure and function (Chen et al. 2006). These plasmids were used as templates for PCR to generate each mutant with the

3' extension construct required for SHAPE analysis. Figure 3.2 denotes the proposed secondary structures of the stem IV mutants and wild type RNAs. The full-length RNAs, with 3' extensions, were transcribed and their structures were analyzed by SHAPE. The SHAPE reactivity of the full-length RNAs were compared to the NMR structures determined for the isolated stem IV constructs and provided important insight for understanding how the mutants affect telomerase activity.

2. Comparison of wild type stem IV from SHAPE analysis of tTER and the NMR structures

The structure of stem IV from tTER was determined by NMR spectroscopy by the Varani laboratory (Chen et al. 2006). The structure is characterized by a highly ordered distal stem-loop that is linked to a more flexible template-proximal region. These two structural features are separated by a previously identified GA bulge (Romero and Blackburn 1991) that creates a 40-45° kink in the structure. A major limitation of the NMR structures is that stem IV was isolated from the remainder of the RNA. The analysis of stem IV by SHAPE chemistry allows a direct comparison of the NMR structures of stem IV with the structure in the intact RNA. The structure of stem IV that was determined by NMR correlates well with the SHAPE analysis of stem IV (Figure 3.3). SHAPE data from five separate experiments were normalized and is represented as a vertical bar histogram (Figure 3.3b). This data was then color coded according to hit intensity (band intensity on gel; Figure 3.3a) as follows, 0-0.10 is black, 0.10-0.25 is blue, 0.25-0.50 is orange, and > 0.50 is red. Figure 3.3c and d depict the color-coded hit intensities mapped onto the stem IV secondary structure and NMR structure, respectively.

Several regions of the RNA were notable in their reactivity. Nucleotides U117, U127 and GA122-121 were highly reactive (all greater than 40% hit intensity) suggesting these residues are unconstrained and not engaged in base pairing. The NMR structure further supports the conformational flexibility of residues U127, U126 and U125, which

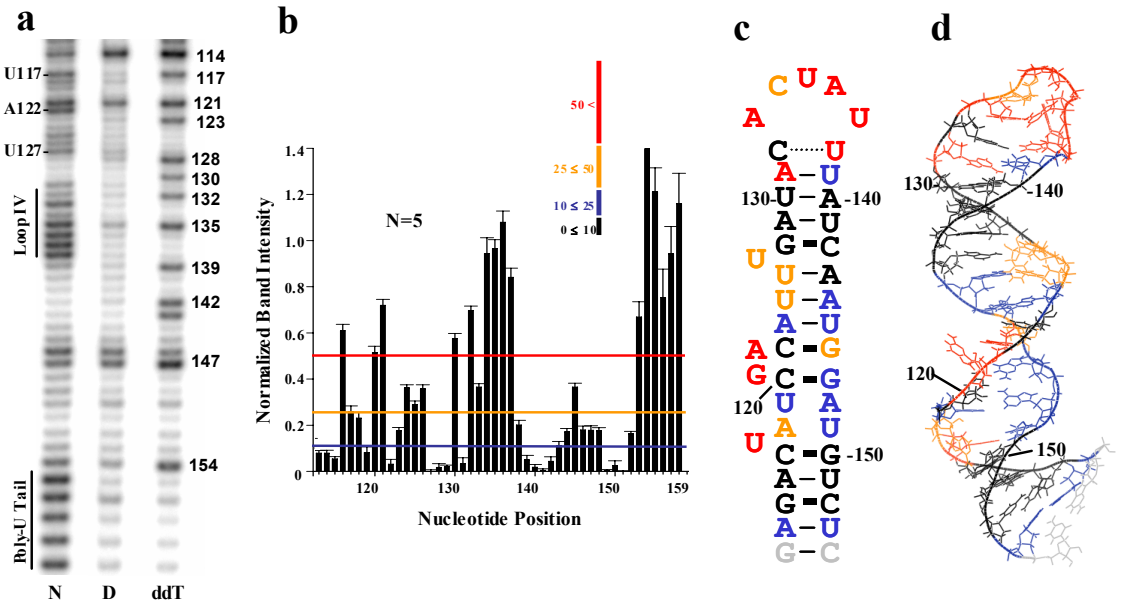

Figure 3.3 SHAPE chemistry analysis of wild type stem IV for comparison to NMR structure. (a) SHAPE chemistry denaturing sequencing gel. NMIA modifications of stem IV residues are mapped with ^{32}P-labeled DNA primer reverse transcription. Sites of acylation cause reverse transcription to stop exactly one nucleotide before the modification site, resulting in the presence of a band. The dideoxythymidine ladder (ddT) is labeled to include this shift. Lanes are labeled according to treatment with 10 mM NMIA (N) or 10% DMSO (D). (b) Histogram of average normalized NMIA hit intensities. Mean band intensities from five separate experiments were normalized and plotted against nucleotide position with standard error bars. Blue, orange, and red lines indicate divisions for color-coded hit intensity for structures in (c, d) as 0.10-0.25, 0.25-0.50, and >0.50, respectively. Any value below 0.10 is represented as black. (c) Hit intensity color-coded secondary structure of stem IV. The grey GC base pair at the terminus of helix represents construct used for NMR structure generation. (d) Hit intensity color-coded high resolution NMR structure of stem IV. Structure rendered in Pymol from Protein Data Bank coordinates with accession code 2FEY.

appear to be able to alternate in base pairing with A143 and A144. Interestingly, A143 and A144 are constrained and in the NMR structures stack into the helix structure, leaving one of these three uridine residues bulged. The most stable NMR structure results from U127 being bulged with U126 being bulged in some of the less stable structures, but SHAPE analysis indicates an approximately equal probability that U127,

U126, or U125 is bulged (~30-40% hit intensity for each). In the NMR structure, base pairing interactions could not be assigned to A118 or U119, but the residues did stack into the A-form helix structure and this is supported by SHAPE chemistry as these two bases are only moderately reactive (~25%). Their predicted base pairing partners, U149 and A148, are also moderately reactive (~18%), which is not surprising as the NMR data show the sugars of all four residues are in exchange between N- and S-type conformations. As previously predicted (Bhattacharyya and Blackburn 1994), GA121-122 bulges out and causes a large kink in the stem (~40°). The NMR structure shows this is a rigid conformation with the Watson-Crick face of G121 solvent accessible and A122 stacked onto C123. SHAPE analysis indicates high reactivity of these two residues (> 50%) consistent with the non-base paired assignment. The GA bulge flanking base pairs, C123-G146 and C120-G147, which are absolutely conserved (Romero and Blackburn 1991; McCormick-Graham and Romero 1995; Ye and Romero 2002), are well formed in the NMR structure. This is partially supported by SHAPE chemistry. G146 is relatively reactive (~40%) suggesting some conformational flexibility of this residue, which is not indicated by the NMR structure.

The apical loop of stem IV forms a well-defined structure (r.m.s.d. 0.67 Å over 20 structures). The most striking characteristic of the loop is the presence of a weak single hydrogen bond base pairing between the C132-NH and the U138-O4. The SHAPE data shows that C132 is very unreactive (< 5%), while U138 is reactive (~85%). The NMR structure shows that the 5' side of the loop, residues C132-A134, continue helical stacking into the loop and are somewhat constrained, while the 3' side of the loop, residues U135-U138 have increased $T_{1\rho}$ values indicative of increased motion on the ps-

ns timescale. Both C132 and U138 stack onto the last base of the stem, A131 and U139, respectively. SHAPE chemistry shows that residues U135-U138 all exhibit high NMIA reactivity (> 85%), while only A133 on the 5' side shows high reactivity (~70%). C134 shows intermediate reactivity (~38%). Surprisingly, A131 is highly reactive (~60%) even though it is shown to be base paired and constrained in the NMR structure.

3. Stem IV mutants

To assess the importance of the structural features revealed by the NMR structure of stem IV, a series of mutations was constructed (Figure 3.2). The first three mutations attempt to alter the flexibility of the stem of the RNA. Mutant Q1 switched the AU118-119 to UA149-148 base pairs with G-C base pairs in an attempt to make this region of the RNA more rigid. Figure 3.4, lanes 4, 5, and 6 depict NMIA hit RNA, DMSO control and dideoxythymidine ladder, respectively, and the boxed region in lane 4 shows only U117 as being reactive to NMIA. The wild type RNA shows a heavy band for U117 (Figure 3.4, lane 1), but also shows two more bands representing AU118-119. This confirms that mutation Q1 constrains these residues and a subsequent telomerase assay showed a reduction in activity to 40% of wild type levels (Chen et al. 2006). While mutant Q1 was designed to decrease flexibility in this region, mutant D2 was designed to increase it. Mutant D2 alters UA149-148 to CG, presumably removing potential base pairing in this region. In figure 3.4, lane 7, the boxed regions show this to be the case with residues AU118-119 and CG149-148 being heavily modified by NMIA. Causing more flexibility in this region of stem IV appears to have little effect on telomerase function (80% of wild type activity). Mutant Q3 was designed to weaken the conserved, rigid G-C base pairs

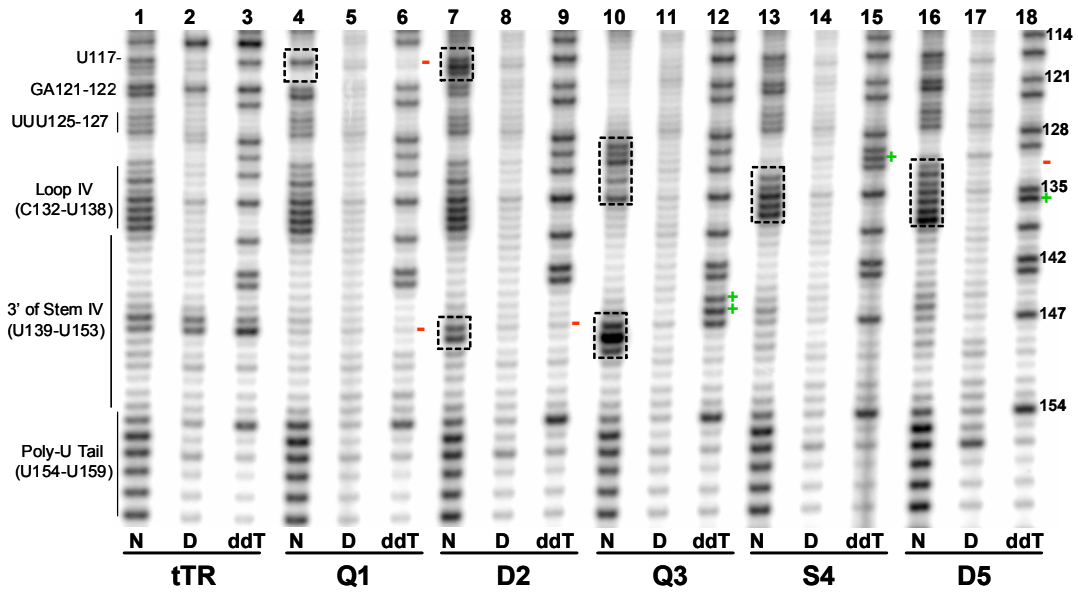

Figure 3.4 SHAPE chemistry analysis of tTER stem IV mutants. The analysis was executed on full-length tTER carrying the appropriate mutations, but only stem IV is shown for clarity. tTER and the five mutants were reacted with 10 mM NMIA, and the resulting 2'-acylated RNAs were mapped by reverse transcription. Sites of acylation cause reverse transcription to stop exactly one nucleotide before the modification site. The ladders are labeled to include this one-nucleotide shift. Each RNA was reacted with either NMIA (N) or the carrier DMSO (D) as labeled below each lane. A dideoxythymidine ladder (ddT) was generated to illustrate nucleotide position. The position of every added adenine (Q3: G146A, G147A; S4: C132A; D5: U137A) or removed adenine (Q1: A118G, A148G; D2: A148G; D5: A133U) for each mutant is notated by a green (+) or red (-), respectively. Dashed boxes highlight altered nucleotide reactivity of the mutants to NMIA compared to wild type.

flanking the GA bulge. C120-G147 and C123-G146 were both altered to U-A base pairs, respectively, in an attempt to make this region less rigid, but upon further analysis it was determined that the mutations redirected the folding of the RNA to the structure indicated in figure 3.2. This structure was suspected after mFOLD (Zuker 1989) was used to predict the folding of the sequence and was confirmed by SHAPE analysis (Figure 3.4, lane 10). The boxed regions indicate the reactive 6-member apical loop and 3-nucleotide bulge. These mutations evidently cause a stable misfolding of the stem IV structure that is predictably deleterious to telomerase activity (5% of wild type activity).

The final two stem IV mutations tested focused on the apical loop on stem IV, a region that is highly conserved and implicated in telomerase activity and processivity (Sperger and Cech 2001; Ye and Romero 2002; Lai et al. 2003; Mason et al. 2003).

Mutation S4 alters C132 to A in an attempt to force a stronger base pair between A132 and U138, as opposed to the non-canonical C•U base pair that was observed by NMR (Chen et al. 2006; Richards et al. 2006). Figure 3.4, lane 13 shows that the 7-member loop is reduced to 5 reactive residues, with neither A132 or U138 being modified. A telomerase activity assay indicated this mutation essentially abolishes telomerase activity (< 1% of wild type activity). Mutation D5 is a base transversion where A133 and U137 are switched to U and A, respectively. In figure 3.4, lane 16, the boxed region shows that all seven of the apical loop residues are reactive, but their reactivity profile has changed from wild type as all of the residues are modified equally (compare with lane 1, loop region). This change in sequence and local structure renders an inactive telomerase enzyme (< 1% of wild type activity).

4. Isatoic anhydride analogue modification of stem IV

The reaction rate of isatoic anhydrides can be modulated by chemical modification. The parent compound, isatoic anhydride (IA) (Figure 3.5a), reacts with water and the 2' hydroxyl of ribose sugars relatively slowly. Its half-life is approximately three times that for NMIA (Figure 3.5b) at any given (Gherghe, C., and Weeks, K.M., personal communication). The addition of a methyl group to the nitrogen

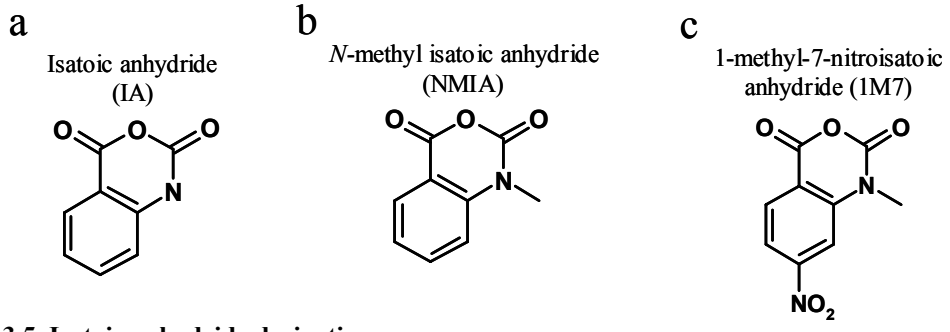

Figure 3.5 Isatoic anhydride derivatives.

in NMIA stabilizes the nitrogen leaving group (2° versus 1° nitrogen), thereby increasing the hydrolysis and reaction rate of NMIA at least three fold over IA. The reaction rate is increased again by the addition of an electron withdrawing *para* nitro group in 1-methyl-7-nitroisatoic anhydride (1M7) (Figure 3.5c). The nitro group increases reactivity by both increasing the electrophilicity of the reactive carbonyl and stabilizing the negative charge generated during the reaction transition state (Mortimer and Weeks 2007). These effects increase the reaction rate of 1M7 approximately 20-fold over NMIA and the reaction is complete in approximately a minute at 37 °C.

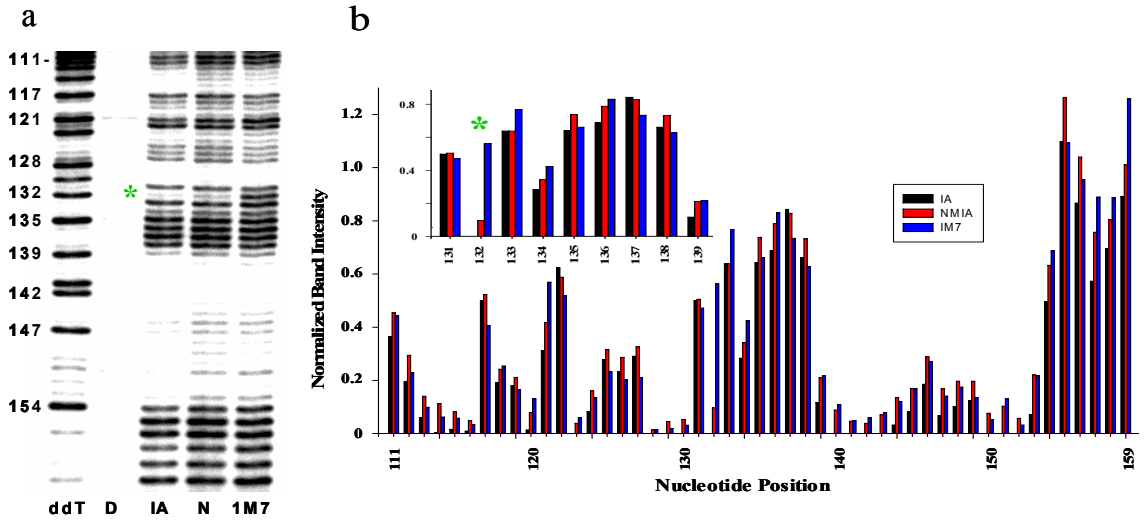

Figure 3.6 SHAPE chemistry analysis of isatoic anhydride derivatives on tTER stem IV. The analysis was executed on full-length tTER, but only stem IV is shown for clarity. (a) tTER was reacted with 10 mM isatoic anhydride (IA), 10 mM *N*-methyl isatoic anhydride (N), or 5 mM 1-methyl-7-nitroisatoic anhydride (1M7), and the resulting 2'-acylated RNAs were mapped by reverse transcription. Sites of acylation cause reverse transcription to stop exactly one nucleotide before the modification site. The dideoxythymidine ladder (ddT) is labeled to include this one nucleotide shift. 10% DMSO treatment serves as a background control (D). The green asterisk denotes C132. (b) Histogram of normalized IA, NMIA, and IM7 hit intensities. Inset histogram details hit intensities of loop residues 131-139. Green asterisk denotes differentially reactive residue cytosine 132.

Since a high resolution NMR structure of stem IV exists, isatoic anhydride analogues were tested to see if their modification profiles were the same. One anticipated result was that the varying reagents would allow more detailed structural information to

be gleaned from SHAPE reactivity profiles. In theory the reactive carbonyl should modify a 2' hydroxyl in the correct conformation regardless of the reaction rate of the molecule, but perhaps the reagents might be differently susceptible to reaction profiles dictated by conformational flexibility. Figure 3.6a shows the SHAPE reaction profile of all three analogues, and figure 3.6b plots their SAFA (Das et al. 2005) determined densities on a histogram. All of the residues react to a similar degree except for C132. The green asterisk on the gel and the inset histogram indicate that this residue is not reactive to IA and NMIA (~0 and 10%, respectively), but is highly reactive to 1M7 (56%).

C. Discussion

Tetrahymena thermophila telomerase RNA stem IV has proven to be an extraordinarily interesting RNA motif because of its complex structure and overall importance to telomerase activity. It appears through mutational data to be one of the most important regions of the RNA for enzyme function apart from the template region (Licht and Collins 1999; Sperger and Cech 2001; Lai et al. 2003; Mason et al. 2003). Its secondary structure was accurately predicted from phylogenetic analysis (Romero and Blackburn 1991) and its tertiary structure has been solved by high resolution NMR (Chen et al. 2006; Richards et al. 2006). These NMR structures illuminated several interesting and unpredicted structural elements. But despite the wealth of functional and structural data generated, it is still a mystery how stem IV is involved in telomerase catalysis.

1. Proximal stem IV binds p65 but has little effect on telomerase function

Mutational, functional, and footprinting studies of the proximal portion of stem IV reveal that its role in telomerase function is mostly structural. In fact only one base pair (G114-C152) is conserved in this region. Mutational studies performed in conjunction with NMR (Chen et al. 2006; Richards et al. 2006) studies suggest that neither the U117 bulge, nucleotide identity or flexibility in this region are essential for telomerase activity. SHAPE chemistry confirmed the conformational flexibility of this region in the full length RNA (Figure 3.3). RNase V1 heavily cleaves this region on both the 3' and 5' side (Bhattacharyya and Blackburn 1994; Sperger and Cech 2001) suggesting that even though it may be flexible it still retains stacked or base paired character. RNase T1 only appreciably cleaved G150, with G114 mostly protected (Bhattacharyya and Blackburn 1994; Sperger and Cech 2001), while this region was protected from DEPC modification. Surprisingly, DMS heavily modified C120 without tTERT present (Zaug and Cech 1995), which is suggested to be stably base paired by both NMR and SHAPE chemistry. One known function for this portion of the RNA is for the binding of p65, which also requires the conserved GA bulge (Prathapam et al. 2005; O'Connor and Collins 2006). Mutations that prevented base pairing in this region also moderately affected binding of the RNA binding domain of tTERT and p65 (O'Connor et al. 2005). Recently, a single molecule FRET investigation showed that there is likely a bend in stem IV that is promoted by p65 binding (Stone et al. 2007). The bending appears to occur somewhere between U127 and stem I. This bending appears to be further pronounced by the subsequent binding of tTERT.

2. The stem IV GA bulge is essential for telomerase function

The central portion of stem IV is characterized by an absolutely conserved GA bulge that is flanked by two G-C base pairs, which stabilize the ~45° kink in the stem (Chen et al. 2006; Richards et al. 2006). A122 stacks against G123 and G121 bulges out with its Watson-Crick face solvent accessible. The high SHAPE reactivity of these bases is consistent with their conformational flexibility, while the flanking G-C base pairs are not reactive to SHAPE chemistry. RNase T1 cleaved at G121 indicating single stranded character (Bhattacharyya and Blackburn 1994; Sperger and Cech 2001) and DEPC and DMS heavily modified A122 suggesting the same (Bhattacharyya and Blackburn 1994; Zaug and Cech 1995). It does not appear that the identity of the bulged pairs is important as UU and UC bulges yield nearly wild type activity (Autexier and Greider 1998; Sperger and Cech 2001), but these particular mutations adversely affect the binding of p65 (O'Connor and Collins 2006). This effectively relegates p65 function as a mediator of telomerase assembly. Conversely, if the GA bulge is deleted, then activity is severely effected as is p65 binding (Autexier and Greider 1998; Sperger and Cech 2001; O'Connor and Collins 2006). A single molecule FRET study suggests that stem IV bends when p65 or tTERT binds (Stone et al. 2007). The GA bulge likely serves to establish this bend and allow formation of a functional telomerase holoenzyme.

3. Distal stem IV and the apical loop are essential tTER motifs

The distal portion of stem IV and the apical loop is the most interesting region of stem IV. The NMR structures show a bulged U127 and some conformational flux of the preceding two nucleotides, U126 and U125. But their pairing partners A143 and A144

stack into the helix and are constrained. The next four base pairs are quite stable and lead up to the apical loop. SHAPE chemistry agrees with the NMR structures with the bulged U127 and its preceding nucleotides being moderately reactive, while the next three base pairs are unreactive. Surprisingly, A131 is highly reactive to NMIA. This cannot be a result of conformational flexibility as the NMR data show it to be constrained. Perhaps this nucleotide is constrained in a C2'-endo sugar pucker conformation, which is likely the favored conformation for NMIA modification (Vicens et al. 2007). From the NMR data, the sugar pucker conformation is not well assigned, but does appear to favor C2'-endo. RNase V1 strongly cleaves in this region suggesting that some stacking or base pairing occurs (Bhattacharyya and Blackburn 1994). All adenines were unreactive to DEPC and DMS further supporting stable base pairing through this region (Bhattacharyya and Blackburn 1994; Zaug and Cech 1995). Functionally, this region of stem IV is amenable to mutation. Deletion of bulged U127 renders telomerase inactive, but activity is fully rescued by the addition of p65 (Richards et al. 2006). An A131C or U139G single mutation is also deleterious, but is rescued by p65, while the double compensatory mutation has little effect on activity with or without p65 (Richards et al. 2006). In another study using circularly permutated tTERs, deletion of C123-U127 was shown to have little effect on activity, while deletion of G128-A131 or U139-G146 renders the enzyme inactive (Mason et al. 2003). All of these data suggest that regions close to the apical loop are more important for activity, while regions further away are also important but can be rescued with the addition of p65. This suggests that the apical loop is invariantly important for enzymatic activity, while other regions of stem IV are

present only to properly position the loop within the holoenzyme. p65 can rescue these structural stem mutations by helping to correctly bend the stem.

The most conserved region of stem IV is the apical loop and has been shown to be essential for telomerase-catalyzed repeat addition processivity and proper RNA folding upon tTERT binding (Sperger and Cech 2001; Lai et al. 2003; Mason et al. 2003). The only nucleotide in the loop that varies in *Tetrahymena* species is C134 (Ye and Romero 2002). The NMR structures reveal a highly structured loop that is closed by a non-canonical base pair between C132 and U138. The 5' side of the loop is more constrained as nucleotides C132-C134 continue helical like stacking into the loop (Chen et al. 2006; Richards et al. 2006). The 3' side of the loop is more flexible with U135-U138 exhibiting greater conformational freedom. The most unconstrained residues are either U135 (Chen et al. 2006) or U137 (Richards et al. 2006), depending on the study. The Watson Crick faces of A133 to U137 are all solvent exposed and the hydrophobic faces of A133 and A136-U138 face together to form a hydrophobic patch in the center of the loop. SHAPE analysis shows that C132 is unreactive, and that C134 has reduced reactivity, but the rest of the loop residues are highly reactive confirming conformational freedom. Residues A133 and A136 are reactive to DEPC and surprisingly, A135 is cleaved by RNase V1, possibly due to a tertiary interaction with another portion of the RNA (Bhattacharyya and Blackburn 1994). Mutational data indicates that only nucleotides C133, U137, and U138 are essential for telomerase activity (Sperger and Cech 2001; Mason et al. 2003; O'Connor et al. 2005). This effect of stem IV on activity appears to coincide with the ability of the pseudoknot to properly fold when tTERT binds (Sperger and Cech 2001). In this study, mutations in the loop that were deleterious to

activity also prevented proper pseudoknot folding, suggesting a structural link between these two motifs (Sperger and Cech 2001). The exact nature of this relationship remains elusive but may include RNA-RNA or RNA-protein interactions. Confirming the importance of stem-loop IV to enzymatic activity, two subsequent studies were published that showed the distal portion of stem IV (residues 128-142) can be added to tTER in trans and effectively rescue repeat addition processivity at high add back concentrations (Lai et al. 2003; Mason et al. 2003). This can be accomplished with as little as the first 107 nucleotides present, although the total activity is only 10-20% of wild type. Distal stem IV is also sufficient to rescue the activity of a full-length tTER containing a catalytically inactive UU137-138 to AA mutation (Mason et al. 2003). Current speculation suggests that stem loop IV directs correct folding of the pseudoknot upon tTERT binding and possibly changes conformation itself (Stone et al. 2007) and then, either directly or through interactions with the pseudoknot or tTERT, stimulates polymerase catalysis (Sperger and Cech 2001; Lai et al. 2003; Mason et al. 2003).

4. Stem IV mutant structures confirm the importance of the apical loop and illustrate the sensitivity of SHAPE analysis

SHAPE analysis of the five mutants of stem IV suggested flexibility is not important, but the GA bulge and loop structure are important. Mutants Q1 and D2 attempted to rigidify and unpair proximal stem IV (Figure 3.2), respectively, but neither mutant adversely affected activity. SHAPE chemistry confirmed that these mutations behaved as predicted (Figure 3.4). Mutant Q3 attempted to loosen the GA bulge by altering the flanking nucleotides. Unfortunately, this caused a global misfolding of stem IV that did not answer the question asked. What was revealed was that non-canonical

base pairs are equally constrained in this structure and are not reactive (U125•U138 and U126•U137). This serves as an effective example of the sensitivity of NMIA modification. The Feigon laboratory constructed stem IV helix mutations to test the importance of the stem bulges for telomerase activity (Richards et al. 2006). They found that deletion of U117, U127, or the GA bulge severely affected telomerase activity, but the addition of p65 completely rescued the single nucleotide uridine bulge deletions, but not the GA bulge deletion. They also mutated the A131-U139 base pair and found that this base pair was required, but the loss of the base pair could be rescued by addition of p65. Mutants S4 and D5 altered essential loop residues C132, or A133 and U137, respectively, in an attempt stably decrease the loop size (Figure 3.2). The structural effects of both mutations were precisely mapped with NMIA and both resulted in catalytically inactive telomerase. The two main points made by these series of mutations was that neither flexibility or nucleotide identity of the proximal portion of stem IV are important for telomerase function and that the structure imparted on the loop by the non-canonical base pair C•U is essential, since a similar but canonical base pair A-U resulted in an inactive telomerase.

5. Isatoic anhydride derivatives exhibit similar reaction profiles

Despite their vastly different reaction rates, the three isatoic anhydride derivatives tested yielded almost identical reaction profiles. It has already been documented that 1M7 reactivity does not vary with Mg^{2+} concentration, while NMIA does (Mortimer and Weeks 2007). This makes 1M7 an efficient reagent for Mg^{2+} related RNA studies. Figure 3.6 illustrates that all but one residue exhibits the same reactivity for the three

reagents (C132). The Weeks laboratory has documented that in some cases, residues that are more conformationally constrained and sometimes even base paired will be modified more by the slower reacting reagents (Gherghe, C., and Weeks, K.M., personal communication). Their hypothesis is that either these residues are constrained in a conformation favorable for modification, or that the longer half-lives of NMIA and IA afford them more opportunity to react with these residues when they do attain the correct reactive conformation. Neither possibility is mutually exclusive. For C132, we observe the exact opposite phenomenon. The faster reacting reagents modify C132 to a greater extent (0, 10, and 56% for IA, NMIA and 1M7, respectively; Figure 3.6, histogram inset). One possibility is that the hydrophobic pocket formed in the center of the loop described by the Varani lab (Chen et al. 2006) forms a high affinity binding pocket for 1M7 that promotes modification of C132. This is mere speculation and if this were the case, we might expect the other loop residues to be more heavily modified by 1M7, which we do not observe. Ultimately, our data combined with discussions of the data generated by the Weeks laboratory shows that the highest correlation with reactivity does not correspond with one specific conformation, but with a residues ability to sample many different conformations. In order to fully characterize the difference between these reagents reactivity profiles more studies will need to be performed on RNA motifs of known structure, including non-canonical base pairings.

D. Materials and methods

See chapter IV, section D for methods on SAFA data analysis and band density normalization.

1. PCR construction of tTER-C DNA construct

A 5' and 3' extension was PCR generated from the plasmid pTet-telo, which contains the wild-type RNA with a 5' hammerhead ribozyme, using primers with sequences listed in Table 3.1. The 3'-linker and primer binding site was generated by

Table 3.1 tTER-C PCR Primers

	Primer	Sequence
A	5'-tTER + HH	TCTAATACGACTCACTATAGGG
B	3'-tTER + 3'-Linker	GAACCGGACCGAAGCCCGATTTGGATCCGGC GAACCGGATCGAAAAATAAGACATCCATTG
C	3'-tTER (Q1D2) + 3'-Linker	GAACCGGACCGAAGCCCGATTTGGATCCGGC GAACCGGATCGAAAAATAAGACGCCCATTG
D	3'-tTER (Q3) + 3'-Linker	GAACCGGACCGAAGCCCGATTTGGATCCGGC GAACCGGATCGAAAAATAAGACATTTATTG

using primer C (Table 3.1) and the native 5' end by using a hammerhead ribozyme, primer A (Table 3.1). PCR generated constructs were agarose gel purified using wizard PCR prep kits and RNAs were transcribed and gel purified from these templates as previously described (Chapter II).

2. PCR construction of tTER stem IV mutant templates

Five stem IV mutants with 3' linkers and reverse transcription primer binding sites were generated by PCR from their corresponding plasmids in a similar fashion as described above all using the same 5' primer A and the following 3' primers: mutants Q1 and Q2 used primer C, mutant Q3 used primer D, and mutants S4 and D5 used primer B (Table 3.1). PCR generated constructs were agarose gel purified using wizard PCR prep kits and RNAs were transcribed and gel purified from these templates as previously described (Chapter II).

3. NMIA hit reaction

RNA (1 pmol) was snap annealed in deionized water, total volume 7 μL by heating at 95 °C for 2 min and cooling on ice for 5 min before 2 μL of 5x tTER Hit Buffer (250 mM Hepes pH 8.0 (Mediatech, Inc), 10 mM RNase-free $MgCl_2$ (Ambion)) was added. The solution was then incubated at 35 °C for 5 min. The RNA was immediately treated with 1 μL of 100 mM *N*-methylisatoic anhydride (Molecular Probes) or 1 μL of anhydrous DMSO (Sigma) as a control, incubated at 30 °C for 90 min (five NMIA half-lives), precipitated with ethanol in the presence of 0.2 M RNase-free NaCl (Ambion) and 200 μg/mL RNase-free glycogen (Ambion) as counter ion and carrier, respectively, washed once with 70% ethanol, speed vacuumed till dry, and reconstituted in 5 μL of RNase-free TE buffer pH 8.0 (Ambion).

4. 1M7 and IA hit reactions

The same procedure was followed for 1-methyl-7-nitroisatoic anhydride (1M7) and isatoic anhydride (IA; Acros Organics) hit reactions with the following changes. Final concentrations used for 1M7 and IA were 5 mM and 10 mM, respectively. Incubation times for 1M7 and IA were 5 min and 90 min, respectively.

5. Superscript III reverse transcription reaction

NMIA modified RNA (5 µl; 1 pmole) was mapped by the addition of 1 μL of 5'-[^{32}P]-labeled DNA primer (1 pmol; 5'-GAACCGGACCGAAGCCCG) in a standard 0.6 mL tube. The reverse transcription primer was annealed to the RNA by heating the mixture to 95 °C for 1 min, 65 °C for 6 min, 35 °C for 10 min, and on ice for 5 min followed by the addition of 2 μL of 5x First-Strand Buffer (Invitrogen) reverse transcription buffer (250 mM Tris-Cl pH 8.3, 375 mM KCl, 15 mM $MgCl_2$), 0.5 μL 10 mM dNTPs (Invitrogen), and 0.5 μL 100 mM DTT. The solution was heated to 52 °C for 1 min on a Perkin Elmer Gene Amp 2400 thermocycler, 1 μL of Superscript III reverse transcriptase (100 units; Invitrogen) was immediately added to the reaction, mixed by gentle tapping, and allowed to extend for exactly 3 min at 52 °C. The reaction was quenched by the addition of 10 μL of 400 mM NaOH and heated at 95 °C for 5 min, neutralized by the addition of 10 μL of 400 mM HCl, ethanol precipitated with 2 M ammonium acetate (Ambion) and 200 μg/mL glycogen (Ambion) and resuspended in 5 μL denaturing formamide loading buffer (75% formamide (FisherBiotech), 45 mM Tris/borate, 5 mM EDTA, 0.01% bromophenol blue and 0.01% xylene cyanol FF).

Dideoxythymidine sequencing ladders were generated by the addition of 0.5 mM ddTTP (Invitrogen) to the reverse transcription reaction of unmodified RNAs.

6. Sequencing gel electrophoresis

The radiolabeled extension products generated by reverse transcription of NMIA hit RNA were separated by electrophoresis on 40 cm x 0.4 cm 8% denaturing sequencing gels (29:1 acrylamide: bisacrylamide/7M urea, 90 mM Tris/borate, 2 mM EDTA) run at 65 W for 1.5 h and visualized by phosphorimaging using ImageQuant 5.1.

Chapter IV. SHAPE analysis of the solution structure of tTER

A. Introduction

The structure of *Tetrahymena thermophila* telomerase RNA (tTER) has been studied by chemical, enzymatic and spectroscopic approaches. Initially, the secondary structure of tTER was determined by comparative phylogenetic analysis (Romero and Blackburn 1991; McCormick-Graham and Romero 1995; Ye and Romero 2002) and the proposed structure has held up well in the face of biochemical investigations with several chemical and enzymatic RNA footprinting reagents (Bhattacharyya and Blackburn 1994; Zaug and Cech 1995; Sperger and Cech 2001). More recently, NMR spectroscopy has offered three highly defined models of tTER structures that indicate that previous techniques were quite accurate. Two separate labs reported the structure of stem IV (Chen et al. 2006; Richards et al. 2006), and one structure of stem II has been reported by the Feigon lab (Richards et al. 2006). These structures were consistent with predicted secondary structure with a few surprise conformations in each structure that could not have been biochemically revealed. The stem IV structure was observed as a long A-form helix with a GA121-122 bulge, which induced an approximately 40° kink at its midway point as previously predicted (Bhattacharyya and Blackburn 1994). The GA bulge is flanked by two C-G base pairs giving the kink little flexibility at the bulge. Two additional bulges, U117 and U127 on the template proximal and distal side of the GA bulge, respectively, are in regions of weak base pairing with A118-U149 and U119-A148

being quite flexible, and U126-A143 and U125-A144 being in conformational flux. A non-canonical and therefore unpredicted C132•U138 base pair closes a five member apical loop that was predicted to be a seven member loop. The stem II structure is as predicted except one nucleotide, A29, in the apical loop adopts a presumably rare *syn* conformation.

How any of these structures contributes to telomerase function is not know in detail. The loop of helix II is dispensable for activity despite the fact that the flanking sequences around helix II are absolutely required for tTERT binding and telomerase function. Mutations of stem IV indicate that much of this structure is required for activity and single nucleotide mutations of loop residues C132, U137, and U138 in the loop all completely abolish enzyme activity (Sperger and Cech 2001; Lai et al. 2003; Mason et al. 2003). Stem IV mutations do not affect tTERT binding as strongly as stem II mutations, but do seem to affect global tTER folding and holoenzyme stability (Sperger and Cech 2001; Stone et al. 2007). This collection of mutational analyses paint a picture of stem IV being more involved with enzyme activity, while stem II is more involved in tTERT binding. This is interesting since stem II is closer to the template and presumably the active site, but only appears important for tTERT binding, while stem IV is farther from the template but is more involved with enzymatic activity. However, the three dimensional folding topology of the RNA is not known, so stem IV may in fact be in close proximity to the template region once the RNA is natively folded and assembled with tTERT.

To more intimately characterize the structure of tTER we have employed an RNA analysis technique termed SHAPE for Selective 2'-Hydroxyl Acylation analyzed by

Primer Extension (Merino et al. 2005; Wilkinson et al. 2006). This technique, which utilizes *N*-methyl isatoic anhydride (NMIA) to selectively acylate the 2'-hydroxyl of conformationally flexible nucleotides, allows for the analysis of every nucleotide in a RNA in one experiment. The acylation or hit profile is then mapped by radiolabeled primer reverse transcription and indicates nucleotides that are likely involved in base paired or tertiary interactions.

B. Results

1. Construction and evaluation of SHAPE analysis extensions to tTER

In order to study the *Tetrahymena thermophila* telomerase RNA, we PCR generated 3' and 5' extensions of the RNA as previously described (Merino et al. 2005). Two tTERs were generated for analysis. One contained only the 3' extension, tTER-C

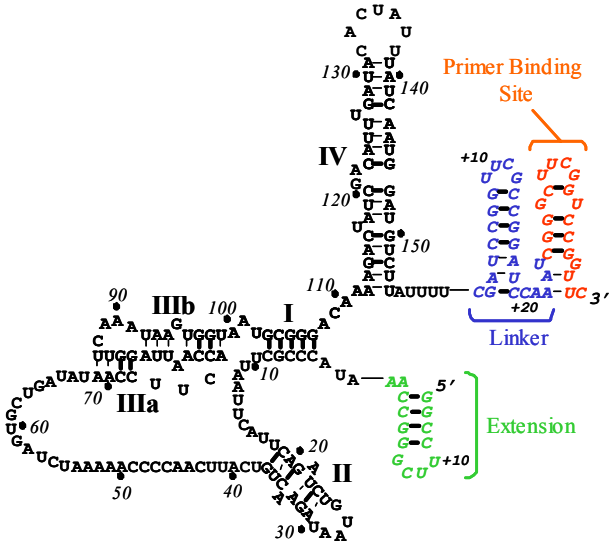

Figure 4.1. tTER secondary structure with 3' and 5' SHAPE extensions. The phylogenetically determined secondary structure of tTER with SHAPE analysis extensions (Merino et al. 2005). 3' extension: blue nucleotides represent linker and red nucleotides represent reverse transcription primer binding site. 5' extension: green nucleotides.

(Figure 4.1, red and blue nucleotides only), and the other contained the 3' extension and the 5' extension, C-tTER-C (Figure 4.1). The 3' extension provides an 18-nucleotide reverse transcriptase primer-binding site (red nucleotides) at the 3' end followed by a 24-nucleotide linker (blue nucleotides) before the poly-U tail, marking the 3' end of tTER. The combined 42-nucleotide extension forms two stable stem loops to help avoid spurious folding with the target RNA. The 14-nucleotide, 5'-extension (green nucleotides) facilitates analysis of the very 5' end of the target RNA and also forms a stable stem loop structure to avoid spurious folding. To determine which construct to use for further study, a telomerase reconstitution and radiolabeled nucleotide primer extension activity assay was performed (Legassie and Jarstfer 2005). The tTER containing both the 5' and 3' extensions, C-tTER-C, was deleterious to telomerase activity (12.8%; Figure 4.2), while the 3'-extension modified tTER, tTER-C, was at wild-

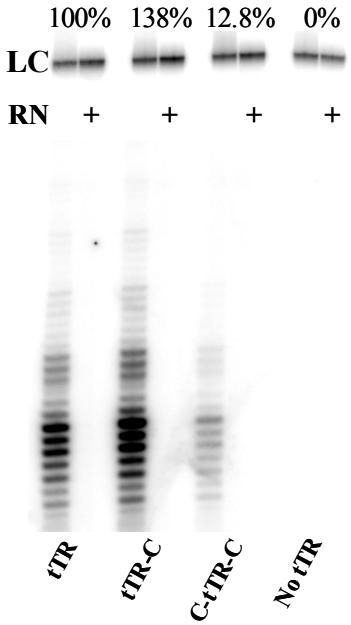

Figure 4.2. Telomerase activity assay of tTERs containing 3' and 5' extensions. Telomerase activity was assessed by direct ^{32}P-radiolabeled nucleotide primer extension assay. Sample treated with RNase A are denoted. A 114-nt 5'-^{32}P-labeled DNA oligonucleotide served as a loading control (LC).

type activity level (138%; Figure 4.2). RNase A treated samples served as negative controls as well as a no tTER control.

2. Optimization of NMIA concentration for tTER study

A number of recent publications by the Weeks laboratory (Merino et al. 2005; Wilkinson et al. 2005; Wilkinson et al. 2006) indicate that an effective concentration range to attain single hit kinetics using NMIA with a 159-nucleotide RNA is around 5-12 mM. To determine which concentration to use, NMIA was titrated in at final concentrations ranging from 0.5 mM to 12.5 mM (Figure 4.3). Hit intensities from 0.5-5 mM NMIA (lanes 4-7) were relatively weak as compared to other published data (Barrodek and Weeks 2005; Wilkinson et al. 2005; Vicens et al. 2007). Hit intensities

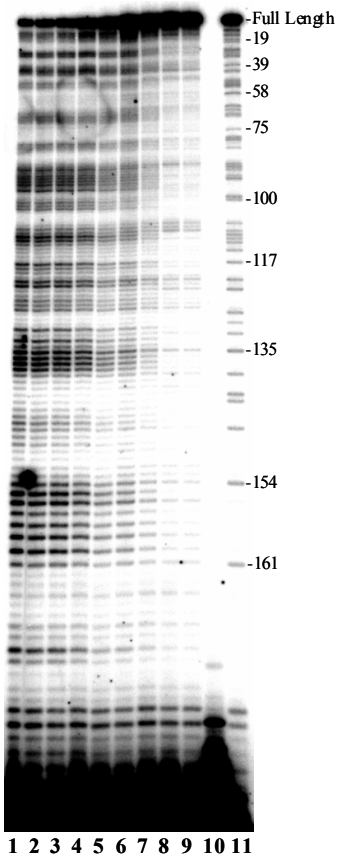

Figure 4.3. SHAPE chemistry analysis at varied NMIA concentrations. tTER-C was treated with NMIA at 12.5 mM (lane 1), 10 mM (lane 2), 7.5 mM (lane 3), 5 mM (lane 4), 2.5 mM (lane 5), 1 mM (lane 6), and 0.5 mM (lane 7) or 10% DMSO (lanes 8 and 9), and the resulting 2'-acylated RNAs were mapped by reverse transcription. Sites of acylation cause reverse transcription to stop exactly one nucleotide before the modification site. The dideoxythymidine ladder (ddT) is labeled to include this one-nucleotide shift (lane 11). As a control for unannealed primer extension, no tTER was added to one RT reaction (lane 10).

from 7.5-12.5 mM (Lanes 1-3) appeared almost identical upon density analysis with SAFA (Das et al. 2005). We finally settled on 10 mM to insure good hit intensities under a variety of conditions. 12.5 mM was deemed too high a concentration as a noticeable precipitate occasionally formed upon addition, presumably due to concentrations being at the solubility limit for the standard temperature employed (30 °C). 10% DMSO was added as negative control in lanes 8 and 9, while lane 10 is a no-RNA reverse transcription control, and lane 11 is an adenine sequencing ladder.

3. SHAPE reactivity profile of tTER

Using 10 mM NMIA as the working concentration, tTER-C was analyzed with SHAPE chemistry. To fully map all nucleotides, we employed two primers. One primer anneals to the 3' extension, and the second primer, whose 3' end was complementary to residue G103, anneals internally. This internal primer allowed mapping of the 5' end of the RNA, which was lower in resolution using the primer that annealed to the 3' extension due to gel electrophoresis limitations. Figure 4.4 depicts representative gels of SHAPE assays, along with average normalized densities from five separate experiments. A figure representing the predicted tTER secondary structure with color-coded nucleotides indicating normalized hit intensity levels is also provided (Figure 4.4e).

a. Stem IV

The SHAPE reactivity of stem IV is consistent with a secondary structure that is in strong agreement with the predicted structure (Romero and Blackburn 1991). Starting from the 3' end, the poly-U tail (nts 159-154) is highly reactive to SHAPE chemistry

suggesting that it is conformationally unconstrained (Figure 4.4a, c) and is likely single stranded. The 3' side of stem IV is represented by a long stretch (nts 153-140) that is unreactive to SHAPE chemistry, consistent with a double-stranded structure. A 7-nucleotide apical loop (nts 139-132) is modified in a position dependent manner, indicating possible local structure (Chen et al. 2006; Richards et al. 2006). The 5' side of

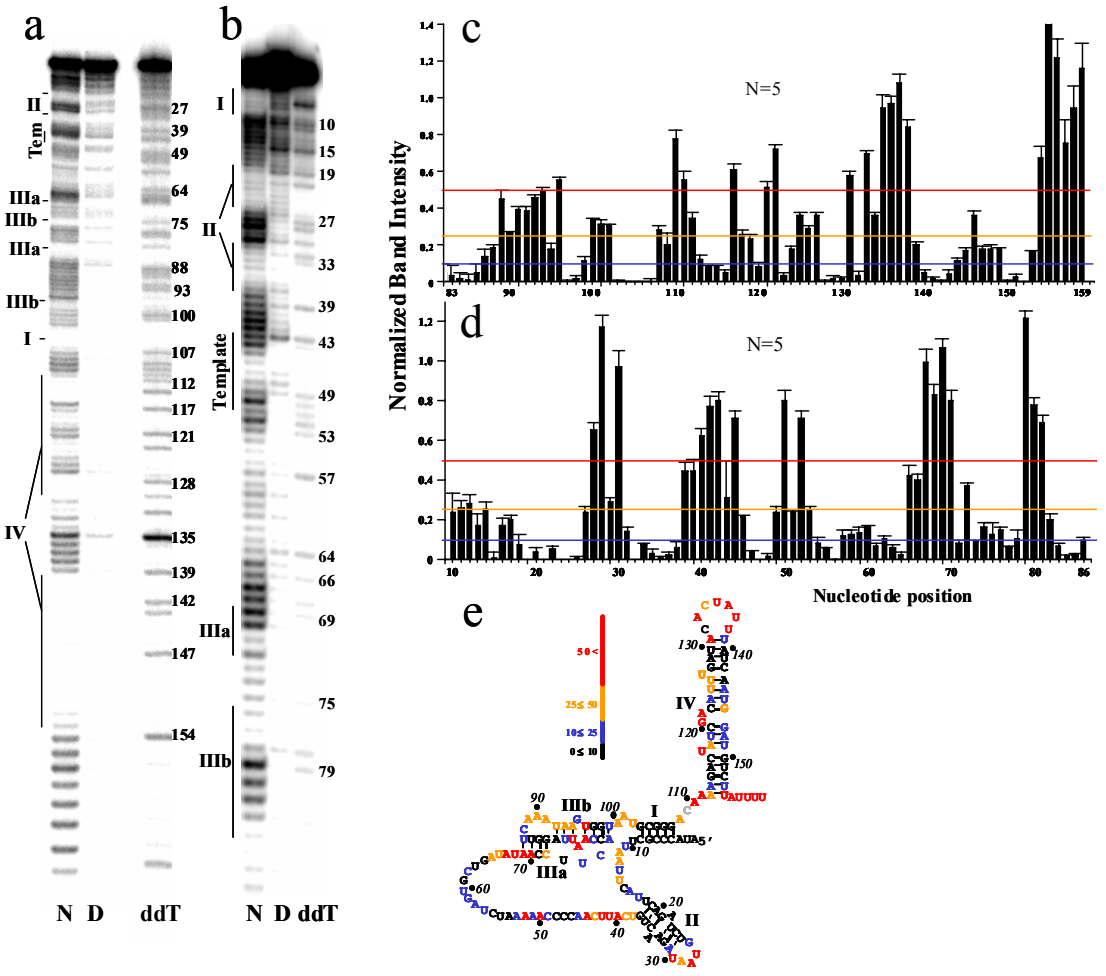

Figure 4.4. SHAPE chemistry analysis of tTER. (a, b) tTER-C was treated with 10 mM NMIA (N) or 10% DMSO (D), and the resulting 2'-acylated RNAs were mapped by reverse transcription with a 3' primer (a) and an internal primer (b). Sites of acylation cause reverse transcription to stop exactly one nucleotide before the modification site. Dideoxythymidine ladders (ddT) are labeled to include this one nucleotide shift. (c, d) Histograms of average normalized NMIA hit intensities. Normalized band intensities from five separate experiments were averaged and plotted against nucleotide position with standard error bars for both primers. Blue, orange, and red lines indicated divisions for color-coded hit intensity for structure in (e) as 0.10-0.25, 0.25-0.50, and >0.50, respectively. Any value below 0.10 is represented as black. (e) Secondary structure of tTER with color-coding of residues to match data from (c) and (d). Grey residues represent positions where accurate values could not be assigned.

stem IV contains three bulges, all of which are reactive to NMIA. The U127 bulge is modified as well as U126 and U125, though to a slightly lesser extent. These are predicted to be weak base pairing partners with A144 and A145, respectively (Chen et al. 2006). GA121-122 is heavily modified as is expected for these bulged, unbase paired nucleotides. U117, A118 and U119 are also reactive, with U117 being the more reactive of the three, indicating some conformational flexibility of A118 and U119, which are presumed to be base paired nucleotides.

b. Stem I and III

The second major motif of tTER is stem I and stem III (or the putative pseudoknot). The region between stem IV and stem I is single stranded and predictably is highly reactive to NMIA (nts 111-108), while the highly conserved GC rich stem I (nts 107-103) forms a stable, unreactive structure as evidenced by no modifications in this region. Nucleotides 102-100, linking stem I and stem IIIb, are heavily modified as would be expected for a single stranded region. The predicted pseudoknot begins with stem IIIb, nucleotides 99-97, which are protected, but U96, predicted to be base paired is highly reactive (55%; Figure 4.4c, e). Conversely, G95, which is predicted to be a bulged nucleotide, is not modified by NMIA (~18%). The next seven-nucleotides (nts 94-89) are all highly reactive (orange or red in Figure 4.4e) in opposition to the predicted base pairing of nucleotides 94-92. Nucleotides 86-82 are unreactive in partial agreement with the placement of stem IIIa (predicted to be nts 87-84) (Figure 4.4b, d). Nucleotides 81-79 are heavily modified (>75%), counter to the predicted involvement of both U81 and A79 in base pairing association with stem IIIb (Figure 4.4e). The next six nucleotides, 78-73,

are protected, with 78-76 representing part of stem IIIb, and 75-73 representing a connecting loop. Surprisingly, three of the four nucleotides predicted to form the 5' side of stem IIIa, 72-69, are heavily modified. This is unexpected since the 3' side of stem IIIa is unreactive.

c. Template region

The template region is defined as nucleotides 68-38 and is predicted to be single stranded. There is absolute conservation of sequence of the template and regions closely flanking, while nucleotides 68-55 appear quite variable in *Tetrahymena* species (Romero and Blackburn 1991; McCormick-Graham and Romero 1995; Ye and Romero 2002). Nucleotides 68-65 are highly reactive to SHAPE chemistry and are therefore predicted to be single stranded. Surprisingly, nucleotides G64 through A54 are unreactive to SHAPE chemistry with reactivity values less than 20% of the normalized maximum reactivity (Figure 4.4d, e). Within the conserved template region, an interesting reactivity profile shows residues A52 and A50 are reactive (~80%), but A51 is not (~25%). Then, the presumed single stranded series of cytosines in the template is unreactive (nts 48-46; <5%) with the flanking nucleotides, C49 and A45, partially reactive (~20%). The last two nucleotides of the template are highly modified along with the template boundary up to the beginning of the stem II structure (nts 44-38).

d. Stem II

SHAPE chemistry reveals a well-formed stem II structure. The stem region, nucleotides 37-29 and 25-19 are unmodified, including both bulged adenines, A26 and

A22 (<10%; Figure 4.4b, d). The apical loop (nts 30-26) is heavily modified, though A29 is relatively unreactive (~30%) compared with U30 and A28 (>95%). The predicted single stranded region between stem II and stem I was unreactive from nucleotides 18-15, and modified from nucleotides 14-10. The final nine nucleotides were not able to be reproducibly mapped due to the strong band incurred from the prevalent full-length reverse transcription product.

4. Proposal of an alternate solution structure for the tTER pseudoknot-template region

After careful analysis of our SHAPE data, it was apparent that that the pseudoknot and template region do not appear to form as phylogenetically predicted (Romero and Blackburn 1991; McCormick-Graham and Romero 1995; Ye and Romero 2002). To help guide the proposal of alternate structures, the SHAPE data constraints were added to the tTER sequence and folded with the program RNAstructure (Mathews et al. 2004). One disadvantage of this program is that it does not predict pseudoknots effectively, but this function was not required as there is already a pseudoknot model. Instead, our interest was in identifying other structural alternatives. The lower case nucleotides represent residues that were highly reactive to SHAPE chemistry (orange or red; Figure 4.4e) and were selectively forced to be single stranded by the program (Figure 4.5a). The program precisely predicted stems I, II and IV, and also predicted a 9-base pair internally bulged stem loop in the combined pseudoknot-template region (Figure 4.5a). Nucleotides 99-97 were surprisingly base paired to nucleotides 45-47 of the template in one of the lowest energy structures. While this pairing seems unlikely in the telomerase complex, it fits the data generated as is reasonable in the free RNA.

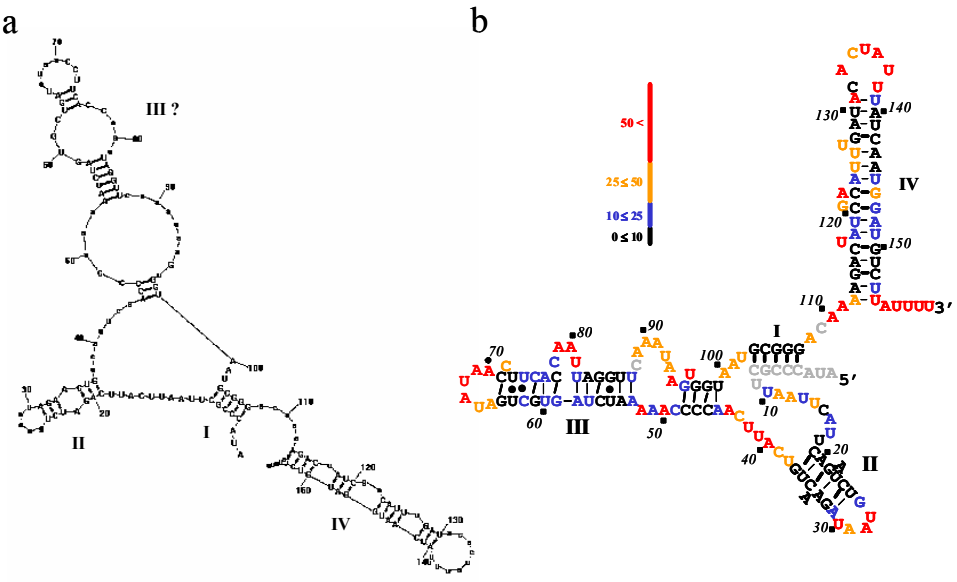

Figure 4.5. An extended stem III in the solution structure of tTER. (a) Secondary structure predicted by the RNA folding program RNAstructure. Lower case nucleotides had a normalized reactivity of 0.40 or higher and were forced to be single stranded in the structure prediction. (b) Revised tTER structure derived from SHAPE chemistry hit data (Figure 4.4 c, d) and RNAstructure predicted folds. The residues are color-coded to illustrate the agreement with the assigned structure.

The RNAstructure generated secondary structure was modified to accurately reflect all of the high-resolution SHAPE data, resulting in the color-coded structure depicted in figure 4.5b. Since nucleotides 64-53 were well protected these nucleotides were all base paired resulting in a 12-base pair stem with a 4-nucleotide bulge midway through the structure, nucleotides 81-78, and a 6-nucleotide apical loop. C72 is depicted as being a single nucleotide bulge in an attempt to match SHAPE modification data, but may very well be base paired to G64 at the stem terminus instead of C71. This, of course, would form a 7-nucleotide apical loop, but would result in two nucleotides having modification data that does not match their base pairing environments. Additionally, there are three non-canonical base pairings in the long stem (G85•U55, U74•C62, and U73•U63). The template base pairing was also modified from figure 4.5a to more accurately reflect the SHAPE data. An additional base pairing interaction between G95

and C48 was added to further stabilize the stem. This creates a single nucleotide bulge of U96, which is heavily modified by NMIA, and would constrain more of the template as is suggested by SHAPE analysis.

C. Discussion

Phylogenetic analysis of telomerase RNA from *Tetrahymenine* ciliates indicates that the most conserved regions are the apical loop and GA bulge of stem IV, stem I, and the template region including the defined template boundary element (Romero and Blackburn 1991; McCormick-Graham and Romero 1995; Ye and Romero 2002). Comparatively, the putative pseudoknot and large single stranded region, nucleotides 68-54, is not conserved save a few nucleotides. Considering the low sequence conservation of this region, it is not surprising that the RNA appears to fold differently than predicted in the absence of tTERT. In fact, phylogenetically predicted secondary structures are often revised in the face of modern, high-resolution structural determination methods (Leeper and Varani 2005; Theimer et al. 2005). Considering the phylogenetic data, it is not surprising that SHAPE data strongly supports the predicted structure of tTER in regions that are highly conserved, but appears to deviate from the predicted structure in areas of low conservation at least in the defined solution structures. However, much of the mutational data (Licht and Collins 1999; Lai et al. 2003; Mason et al. 2003) and one footprinting study (Sperger and Cech 2001) suggest that the pseudoknot is the correct structure in the context of the holoenzyme.

1. Stem I and II form stable, phylogenetically predicted structures

Stem I is a well conserved element also found in *Euplotes* and *Paramecium* (Lingner et al. 1994) and is essential for p65 binding in *Tetrahymena* (O'Connor and Collins 2006). It is essential for the overall architecture of ciliate telomerase RNAs as it closes off the large loop and template, bringing the template and stem II back in close proximity to stem IV and the pseudoknot. Our SHAPE analysis reveals nothing remarkable about stem I other than its presence and stability.

Stem II is an important structure in the template boundary element (Lai et al. 2002; Richards et al. 2006). While the distal portion of the stem does not appear to be essential for telomerase function, the proximal region and the immediately flanking sequences in the 5' and 3' direction are essential for tTERT binding and accurate template boundary definition (Lai et al. 2002). The recent NMR structure of stem II (Richards et al. 2006) correlates well with SHAPE chemistry data. The NMR structure details a tight 7-member A-form helix with a 5-member apical loop. There are two opposing, unpaired adenines (A34 and A22) that stack into the helix without interrupting the overall helical structure. SHAPE chemistry shows these adenines are unreactive indicating the NMR structure is accurate and these nucleotides are constrained through base stacking. The solution structure includes a *syn*-conformation of adenine at position 29. A *syn*-adenine is when the base is rotated around to be *syn* to the sugar, whereas the normal conformation of oligonucleotide bases is *anti* to the sugar. The *syn*-conformation is predicted to be stable and possibly the conformation of free nucleotides, so its not surprising that A29 is relatively unreactive (>95% for G30 and A28 versus ~30% for A29) to NMIA. RNase V1 footprinting confirms the presence of stem II

Table 4.1 Summary of footprinting data from past studies of tTER in solution

nt residue	DMS[a]	DEPC[b]	RN T1[b,c]	RN V1[b]	NMIA	nt residue	DMS[a]	DEPC[b]	RN T1[b,c]	RN V1[b]	NMIA
U10				++	+	G85			+/ -	++	-
A11	++	++			++	U86					-
A12	++	++			++	U87					+
U13					+	C88	-				+
U14					++	A89	++	++			++
C15	++				-	A90	++	++			++
A16	++	+			+	A91	+	++			++
U17					+	U92					++
U18					-	A93	++	++			++
C19	-				-	A94	+	++			++
A20	-	-			-	G95			+/ +		+
G21			- / -	+++	-	U96					+++
A22	+	+		+	-	G97			+/ -	+	-
U23				+	-	G98			+/ -	+	-
C24	-			+	-	U99				+	+
U25					-	A100	++	+			++
G26			+++ / +++		+	A101	+	+			++
U27					+++	U102					++
A28	++	+++			+++	G103			- / -		-
A29	+	++			++	C104	-			++	-
U30					+++	G105			- / -	++	-
A31	-	+			+	G106			+/ -		-
G32			- / -		+	G107			++ / +		-
A33	-	-			-	A108	++	+			++
A34	+	+			-	C109	++				+
C35	-			++	-	A110	++	+			+++
U36					-	A111	++	+			+++
G37			+/ +		-	A112	+	+			++
U38					++	A113	-	-			+
C39	++				++	G114			- / ++		-
A40	+	+			+++	A115	-	-		+	-
U41				+	+++	C116	-			++	-
U42					+++	U117					+++
C43	++				ND	A118	+	-			++
A44	++	+			+++	U119					+
A45	+	+			+	C120	++			++	-
C46	-				-	G121			+++ / +++		+++
C47	-			+	-	A122	++	++			+++
C48	-				-	C123	+				-
C49	+				+	A124	+	-			+
A50	++	+		+	+++	U125					++
A51	++	+			+	U126					++
A52	++	+			+++	U127				+	++
A53	-	+			+	G128			- / -	+++	-
A54	-	+			-	A129	ND	-		++	-
U55				++	-	U130				+	-
C56	-			+	-	A131	ND	-			+++
U57				+	+	C132	ND				-
A58	-	-			+	A133	ND	+++			+++
G59			+/ ++		+	C134	ND			+	++
U60					+	U135				++	+++
G61			++ / +		-	A136	ND	+++		+	+++
C62	++			++	+	U137					+++
U63				++	-	U138					+++
G64			+++ / +	++	-	U139					+
A65	-	+			++	A140	ND	-			-
U66					++	U141					-
A67	+	+			+++	C142	ND			+	-
U68					+++	A143	ND	-		++	-
A69	++	++			+++	A144	ND	-		+	+
A70	++	+			+++	U145				+	+
C71	++				-	G146			+/ ND		++
C72	++			++	++	G147			+/ ND		+
U73				++	-	A148	ND	+			+
U74					+	U149				++	+
C75	-				+	G150			++ / ND	++	-
A76	-	-		+	+	U151				+++	-
C77	-				-	C152	ND			++	-
C78	-				+	U153				+++	+
A79	++	++		+	+++	U154				++	+++
A80	-	++			+++	A155	ND	++			+++
U81				+	+++	U156					+++
U82					+	U157					+++
A83	-	-		++	-	U158					+++
G84			- / -	++	-	U159					+++

Hit intensities were scored according to their publications as follows: - none, + light, ++ intermediate, +++ heavy, ND residue not determined. RN T1 was scored from two studies (b, c) and the hits are divided by a slash, respectively. RN – RNase. a Zaug and Cech (1995), purified endogenous tTER; b Bhattacharyya and Blackburn (1994), in vitro transcripts; c Sperger and Cech (2001), in vitro

(Bhattacharyya and Blackburn 1994; Sperger and Cech 2001) and A28 and A29 are both modified by DEPC (Bhattacharyya and Blackburn 1994) and DMS (Zaug and Cech 1995), although A29 to a lesser extent in both cases (Table 4.1). These results illuminate the sensitivity of SHAPE chemistry to such a fine structural detail and further substantiates that the structure of the stem II fragment is indeed comparable to its conformation in the context of the full length RNA. It is tempting to assign significance to this presumably rare *syn*-adenine conformation that lays in close proximity to the enzyme active site, but all biochemical data suggest this region of tTER is not essential for telomerase function since the distal portion of stem II can be removed with little effect (Miller and Collins 2002; Mason et al. 2003). The single stranded loop, nucleotides 18-9, makes up the other half of the template boundary element (Lai et al. 2002) and is part of a high affinity tTERT binding motif (Miller and Collins 2002; Mason et al. 2003). Nucleotides U18-C15, which are conserved and required for proper function, were unreactive to NMIA, but residues C15 and A16 were heavily modified by DMS (Table 4.1). No current or past model predicts base pairing within this region. The lack of SHAPE reactivity is likely due to unpredicted local or tertiary structure, or unexpected base pairing. Nucleotides 14-10 show no conservation and are intermediate in reactivity (~25%) suggesting single stranded or transient base pairing nature.

2. An extended stem III appears to form in solution instead of the pseudoknot

The pseudoknot and template regions are shown in detail in figure 4.6. The putative pseudoknot (Figure 4.4e) spans 31-nucleotides from U99 to A69. The first 8-nucleotides are predicted to make up the 3' side of stem IIIb with G95 bulged out.

SHAPE analysis and folding analysis using the RNAstructure program suggest a different structure. While nucleotides 99-97 are unmodified, nucleotides 96-88 are heavily modified (Figure 4.6a) suggesting the second part of stem IIIb (94-92) may not form properly in solution. In fact, the new structure proposed has nucleotides 99-97 base pairing with template positions 47-45 (Figure 4.5b and 4.6c) and nucleotides 96-88 as a single stranded loop. In this model, U96 is not base paired, and G95 may or may not pair with C48 or C49. G95 is currently represented as being base paired in this way since it is unreactive (~18%) in comparison with positions 96-89, which average 40% reactivity. DEPC and DMS footprinting of tTER supports this model as A94-93 and A91-89 were heavily modified (Bhattacharyya and Blackburn 1994; Zaug and Cech 1995). The interpretation offered here is also consistent with a lack of RNase V1 cleavage in this region reported by both the Blackburn and Cech laboratories (Bhattacharyya and Blackburn 1994; Sperger and Cech 2001). The lack of RNase V1 cleavage is also consistent with a single stranded conformation (Table 1.1). RNase T1 did not efficiently cleave G95-G98 in either study. Interestingly, in the Sperger and Cech (2001) study the cleavage profile for G98, G97, and G95 was markedly different for tTER in solution versus in reticulocyte lysate without tTERT present, as all three Gs are heavily cleaved in the lysate. This suggests a tTER structural shift in the lysate not due to tTERT but perhaps due to some other accessory proteins or non-specific RNA binding proteins. On the template side, RNase V1 reproducibly cleaved the alignment region (51-49) (Sperger and Cech 2001) and template residue C47 (Bhattacharyya and Blackburn 1994). In a manner very similar to the SHAPE reactivity for this region, DMS methylation was blocked for residues C46-C48, while the surrounding residues were readily

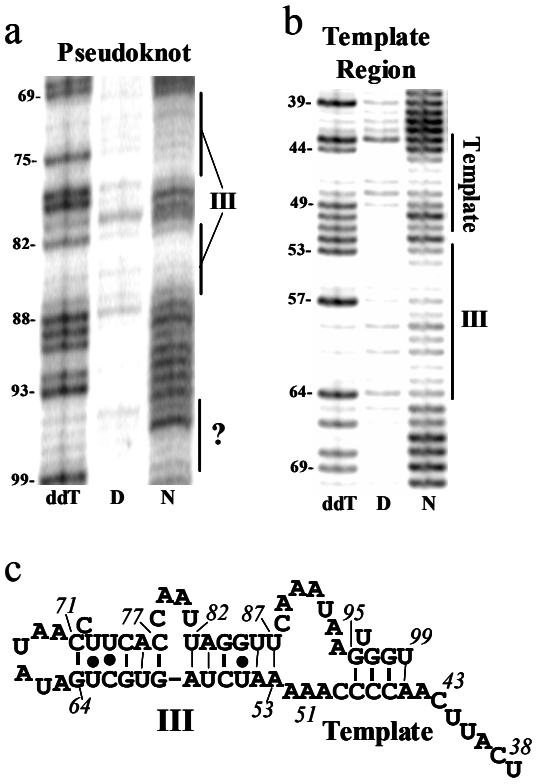

Figure 4.6. tTER (solution) stem III SHAPE chemistry. Close up of representative SHAPE chemistry analysis gel of the phylogenetically predicted pseudoknot region of tTER, residues 69-99 (a), and of the template region of tTER, residues 38-69 (b). (c) Newly proposed tTER (solution) stem III secondary structure including template pairing.

modified (Zaug and Cech 1995). Surprisingly, the human template cytosine residues (C52-C50) were also blocked from modification by DMS both with and without hTERT present (Antal et al. 2002), suggesting that the template may be involved in a base pairing, stacking, or tertiary interaction in these telomerases.

The proximal portion of the newly predicted stem III, nucleotides U87-U82 (Figure 4.6a, c), are unreactive to NMIA and are paired with A53-A58, which are also unreactive (Figure 4.6b, c). This portion of stem III contains one non-canonical wobble pair, G85•U55, and is supported by past footprinting data (Table 4.1). RNase T1 does not cleave G85-84 suggesting this region is not single stranded (Bhattacharyya and Blackburn 1994; Sperger and Cech 2001) and DEPC does not modify A83 or A58 and only partially modifies A54 and A53 supporting the structure that we predict in this region (Bhattacharyya and Blackburn 1994). Additionally, RNase VI shows moderate

cleavage between U86-A82 and A58-U55 in support of the proposed structure (Bhattacharyya and Blackburn 1994).

One of the more interesting proposals of the new stem III solution structure is the presence of a 4-nucleotide bulge formed by residues CAAU78-81. Residues AAU79-81 are heavily modified by NMIA, while the fourth proposed loop residue, C78, is unreactive (11%). This residue may be involved in an unknown tertiary or stacking interaction. DEPC heavily modified AA80-79 (Bhattacharyya and Blackburn 1994), but DMS only modified A79, with C78 and A80 being protected (Zaug and Cech 1995). In the pseudoknot model, only A80 is not predicted to be base paired (Figure 4.4e). Presumably, this bulge would impart a large kink in the stem. The structure of an adenine rich tetra-bulge has been solved in the *Tetrahymena* group I intron, P4-P6 domain (Cate et al. 1996; Cate et al. 1997). This structure is involved in magnesium ion coordination. Our own studies describe a well-formed three-nucleotide bulge in the misfolded Q3 stem IV mutant (Chapter III, Figures 3.2 and 3.4). Often, RNA bulges serve as metal ion chelators or recognition motifs for proteins and other RNAs (Hermann and Patel 2000).

The distal portion of stem III, C77-G59, is capped with a 6-member apical loop and possibly a bulged cytosine residue (Figure 4.6c). The stem contains three G-C pairs and two non-canonical pairs in U74•C62 and U73•U63. Non-canonical U•U and U•C pairs are sufficiently constrained to be scored as base pairs by SHAPE chemistry as was seen for the misfolded stem IV mutant Q3 in chapter III of this work, which contained two U•U base pairs in succession (Figures 3.2 and 3.4, lanes 10, 11, and 12). The fact that three out of six base pairs are G-C pairs likely makes this stem a stable structure.

The apical loop is likely a 6-member loop with C71 base paired to G64 and C72 bulged out. The SHAPE reactivity of this region shows low reactivity to NMIA of nucleotides C77-C71 (~12%), while C72 is moderately reactive (~40%; Figure 4.4d and 4.6a) similar to the reactivity level of bulged U127 in stem IV. The predicted loop residues, A70-A65, are heavily modified by NMIA. Other footprinting analyses of this region report mixed results. A70, A69, A67 and A65 are susceptible to DEPC modification, while A76 is not (Table 4.1), which is in agreement with our data. However, DMS moderately modifies C72, C71, and C64, but does not hit loop residue A65 (Table 4.1). The rest of the adenine and cytosine residues in this region were modified by DMS in accordance with our structural model. One major difference between that study (Zaug and Cech 1995) and all the other footprinting studies was that the RNA was in vivo purified and was modified with DMS in the presence of all the other RNAs that copurified with it. So it is possible that there was spurious pairing with other RNAs that would alter the tTER solution structure, especially in regions of low stability. RNase T1 showed strong cleavage of G64 and G61, but not G59 in one study (Bhattacharyya and Blackburn 1994) and relative protection of these residues in another study (Sperger and Cech 2001). RNase V1 showed strong cleavage around positions 73-72 and 64-62 (Table 4.1) indicating stacked or base pairing interactions. Taken together these studies support our structure, and in retrospect it is somewhat surprising that no one has at least suggested a similar structure previously. As mentioned earlier, the template is constrained from C48-A45 and is predicted by us to be base paired with U99-G95. This putative paired region is flanked by highly reactive regions on either side. Nucleotides A52 and A50 are highly reactive (~75%) while nucleotides A51 and C49 are not (~25%). The 5' side of the

template and the entire template boundary element up to stem II, A44-U38, are heavily modified by NMIA (Figure 4.4b, d) and is likely single stranded. In contrast to SHAPE analysis, DEPC analysis shows that A52-A50, A45, A44, and A40 all were lightly reactive, suggesting either limited solvent accessibility or base pairing in this region (Table 4.1). DMS modification of this region closely mirrored the NMIA reactivity with C49-A45 unreactive, and the rest of the residues heavily modified.

3. Stem III solution structure is likely a stable kinetic folding trap

Based on numerous mutational analysis studies, the stem III structure is likely not the final active structure the RNA adopts once in complex with tTERT. Sperger and Cech (2001) described a definite shift in tTER conformation that involved the pseudoknot and template that was mediated by stem IV. We have attempted without success to assign a similar stem III structure from other closely related ciliate RNAs using the folding program RNAstructure. Since this region is not highly conserved (Ye and Romero 2002), the solution structure of tTER may be a kinetic folding trap that exists in solution, which shifts to the functional structure when bound to tTERT. Incorrect folding becomes a more common problem the larger an RNA becomes (Weeks 1997). A similar argument has been effectively made for yeast telomerase RNA (Zappulla et al. 2005; Zappulla and Cech 2006), which when shortened to contain just the essential regions can easily be in vitro reconstituted with wild type activity. This shorter RNA was postulated to have fewer misfolding options because of its reduced size (Zappulla et al. 2005). The key questions that emerge from our study are whether this folding topology is required for the RNA to assemble with telomerase, or is it merely tolerated since tTERT likely

binds initially to other, more stable regions of the RNA (stem II). Overall the great divergence in size and structure of telomerase RNAs suggests that only a few small regions are essential for function, and random mutations and misfolding in other regions of the RNA may be tolerated as long as they do not adversely affect important functional regions of the RNA.

D. Materials and methods

See chapter III, section D for methods on NMIA hit reactions and sequencing gel electrophoresis.

1. PCR construction of tTER SHAPE extension DNA constructs

Two new DNA constructs were PCR generated from the plasmid pTet-telo, which contains the wild-type RNA with a 5' hammerhead ribozyme, using primers with sequences listed in Table 3.1. One DNA coded for an RNA that contained only a 3' extension, tTER-C, and the other coded for an RNA that contains a 3' and 5' extension, C-tTER-C. tTER-C DNA was generated by using primer C (Table 3.1) and the native 5' end by using a hammerhead ribozyme, primer A (Table 3.1). C-tTER-C DNA was generated using primer C (Table 3.1) and a primer coding for a 5' extension (GCGCTAA TACGACTCACTATAGGGAGAGGCCTTCGGGCCAAATACCCGCTTAATTCATT) depicted in figure 4.1. PCR generated constructs were agarose gel purified using wizard PCR prep kits and RNAs were transcribed and gel purified from these templates as previously described (Chapter II).

2. Superscript III reverse transcription reaction

NMIA modified RNA (5 μL; 1 pmole) was mapped by the addition of either 1 μL (0.5 pmol) of 5'-[^{32}P]-labeled 3' end primer (5'-GAACCGGACCGAAGCCCG) or internal primer (5'-GATAGTCTTTTGTCCCGC) in a standard 0.6 mL tube. The reverse transcription primer was annealed to the RNA by heating the mixture to 95 °C for 1 min, 65 °C for 6 min, 35 ° C for 10 min, and on ice for 5 min followed by the addition of 2 μL of 5x First-Strand Buffer (Invitrogen) reverse transcription buffer (250 mM Tris-Cl pH 8.3, 375 mM KCl, 15 mM $MgCl_2$), 0.5 μL 10 mM dNTPs (Invitrogen), and 0.5 μL 100 mM DTT. The solution was heated to 52 °C for 1 min on a Perkin Elmer Gene Amp 2400 thermocycler, 1 μL of Superscript III reverse transcriptase (100 units; Invitrogen) was immediately added to the reaction, mixed by gentle tapping, and allowed to extend for exactly 4 min at 52 °C. The reaction was quenched by the addition of 10 μL of 400 mM NaOH and heated at 95 °C for 5 min, neutralized by the addition of 10 μL of 400 mM HCl, ethanol precipitated with 2 M RNase-free ammonium acetate (Ambion) and 200 μg/mL RNase-free glycogen (Ambion) and resuspended in 5 µl denaturing formamide loading buffer (75% formamide (FisherBiotech), 45 mM Tris/borate, 5 mM RNase-free EDTA (Ambion), 0.01% bromophenol blue and 0.01% xylene cyanol FF). Dideoxythymidine sequencing ladders were generated by the addition of 0.5 mM ddTTP (Invitrogen) to the reverse transcription reaction of unmodified RNAs.

3. SAFA data analysis and band density normalization

Individual band intensities of NMIA and DMSO lanes were integrated using the program SAFA (3). SAFA allows the straightening of curved gels (gel rectification) and utilizes Lorentzian curve integration to determine band densities with a high degree of accuracy. Hit intensities were normalized in the following way. Band intensity was corrected for background by subtracting away the density of the corresponding band in the DMSO control lane. After this subtraction, any negative values were altered to zero (average of ~15% of nucleotides scored), since negative densities only indicate there is no modification at that position. All of the density values were summed, and then divided by the number of bands that did not have negative values. This value represented the mean band density for all modified positions, and was subsequently multiplied by three to become the normalization factor. All corrected densities were then divided by this normalization factor to give the normalized values. A good experiment typical had 2-3 normalized values exceeding 1.0 for every 85 densities scored. When independent experiments were normalized in this way and then compared, the values across all positions had little variance (~7% error for normalized hits above a threshold value of 0.20). Values lower than 0.20 typically had much higher error rates as the signal to noise is too low. Average normalized values were plotted with standard error bars in figure 4.4. A few positions, usually near RNA degradation hot spots, had widely varied normalized values. These residues with unreliable data were thrown out and are colored grey in the vertical bar histograms and RNA structures.

Chapter V. SHAPE analysis of tTER while in complex with the catalytic subunit tTERT

A. Introduction

The structure of tTER in solution has been studied in detail, and the efforts have been fruitful. These structures provide important insight into the function of the RNA and its ability to bind tTERT, but ultimately the most important structure of tTER is the one adopted while bound to tTERT and in an enzymatically active conformation. Several past studies investigated the structure of tTER in the telomerase complex. When Zaug and Cech (1995) used dimethylsulfate (DMS) to footprint *Tetrahymena* telomerase in vivo they saw that the template was reactive and therefore both single stranded and solvent accessible. This contrasted with their in vitro footprinting, which showed part of the template protected from DMS. Later, Sperger and Cech (2001) footprinted recombinant tTER in complex with tTERT assembled in vitro using rabbit reticulocyte lysate. Using a series of RNases they were able to document a change in pseudoknot structure when tTERT bound tTER, as well as some double stranded or stacked character in the template. Both of these studies suggested that there is a change in the RNA upon tTERT binding, and specifically in the pseudoknot and template regions.

In chapter IV of this work it was suggested that in solution tTER adopts an unpredicted conformation that involves a twelve base pair stem with 3 non-canonical base pairs (Figure 4.4). This stem contains a 6-nucleotide terminal loop and a 4-

nucleotide bulge on the 3' side at the halfway point of the helix. The investigation of tTER in solution presented high-resolution chemical footprinting analysis that correlated well with previous footprinting and mutagenesis studies of tTER to formulate the proposed solution structure (Bhattacharyya and Blackburn 1994; Zaug and Cech 1995; Licht and Collins 1999; Sperger and Cech 2001; Miller and Collins 2002; Lai et al. 2003; Mason et al. 2003). While the solution structure of the RNA is important, the structure of tTER in the telomerase complex and specifically in an active conformation is more germane to understanding the structural basis for telomerase function (Figure 5.1).

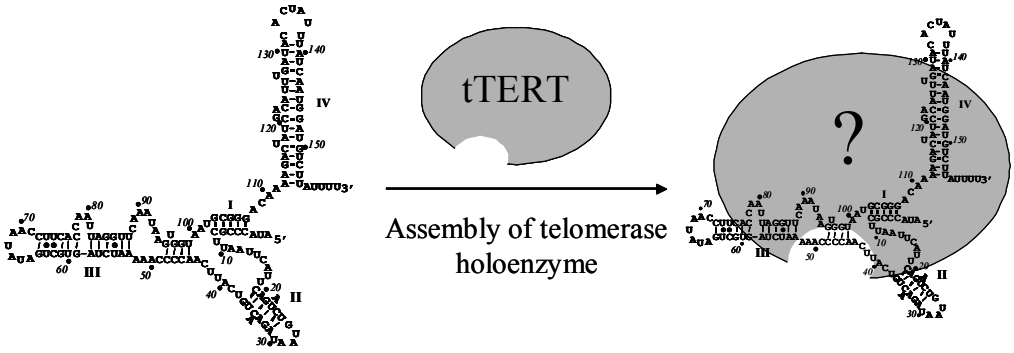

Figure 5.1 What is the structure of tTER after assembly of the telomerase holoenzyme?

In the current study, a FLAG-tag (Knappik and Pluckthun 1994) was engineered onto the N-terminus of tTERT allowing efficient purification of recombinant telomerase. This purified, soluble telomerase was then analyzed by SHAPE chemistry to determine the most detailed picture to date of tTER within the telomerase complex.

B. Results

1. Reconstitution of recombinant telomerase

Since SHAPE analysis is so sensitive, it was critical to the success of these experiments to ensure that all of the tTER examined was contained in the telomerase complex. To achieve this goal, we utilized a recombinant tTERT construct that contained a FLAG epitope to allow affinity purification. It has been shown that an N-terminally FLAG-tagged tTERT is efficiently immunopurified and eluted from agarose gel resin by the FLAG peptide (Bryan et al. 2003). A 1x FLAG sequence was cloned onto the N-terminus of the tTERT expression plasmid as described in materials and methods. The N-terminal His- and T7-tags present in the original tTERT construct were removed during the cloning procedure. The FLAG-tagged tTERT was efficiently expressed in reticulocyte lysate and was efficiently immunopurified (~40-50% total yield) and eluted (~20-25% total yield; Figure 5.2a) with FLAG peptide. The eluted telomerase was active

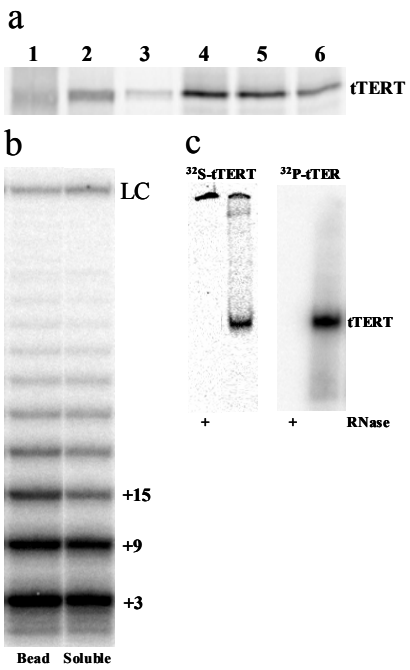

Figure 5.2 Telomerase production and activity. (a) SDS-PAGE of ^{35}S-Met-labeled tTERT following a FLAG epitope affinity purification scheme. Lane contents represent reticulocyte lysate input (1), bead unbound tTERT flow-through (2), pooled antibody bead washes (3), antibody bead bound telomerase (4), 3xFLAG peptide displaced soluble telomerase (5), and undisplaced bead bound telomerase (6). (b) Telomeric primer extension assay on antibody bead purified telomerase and purified soluble telomerase. Numbers indicate the number of nucleotides added and LC indicates a 100-nt ^{32}P-labeled loading control. (c) Native gel analysis of telomerase either ^{35}S-Met-tTERT labeled or ^{32}P-tTER-C labeled as indicated above the gels. Samples treated with RNase A are indicated.

(Figure 5.2b) and ran as one discrete band on a native gel using both ^{35}S-Met-labeled tTERT and ^{32}P-5'-labeled tTER-C to visualize the telomerase complex (Figure 5.2c). A small portion of the tTERT did not run into the native gel, staying in the well, and presumably represents misfolded, insoluble tTERT or RNA unbound tTERT that should not run into the gel at pH 8.3 due to its basic isoelectric point. No such band existed for the labeled tTER-C samples suggesting that all of the RNA is in complex with correctly folded, soluble tTERT. Samples treated with RNase A demonstrated that tTERT requires tTER-C to be negatively charged and run into the gel at pH 8.3 (Figure 5.2c).

2. Analysis of telomerase holoenzyme stability in the presence of NMIA

Before using SHAPE chemistry to analyze the structure of tTER in the telomerase holoenzyme, we determined if NMIA affected telomerase stability. Since the soluble telomerase complex ran as a discrete band on a native gel, this technique was used to investigate the stability of the holoenzyme upon NMIA addition. Our SHAPE analysis of tTER-C uses 10 mM final concentration of NMIA or 10% DMSO as vehicle control. We were concerned that NMIA might in some way cause the complex to become unstable and dissociate after a tTER-C modification event or if the NMIA reacts with a crucial tTERT amino acid residue. To assess stability, we determined the rate of telomerase dissociation in the presence or absence of NMIA using EMSA (Figure 5.3). Either NMIA or DMSO was added to purified telomerase, the samples were incubated at 30 °C, and at various times were loaded onto native gels and immediately electrophoresed. We found that NMIA caused an increased rate of telomerase dissociation on a time scale that is similar to the half-life of NMIA in water at 30 °C (Figure 5.3b) (Wilkinson et al.

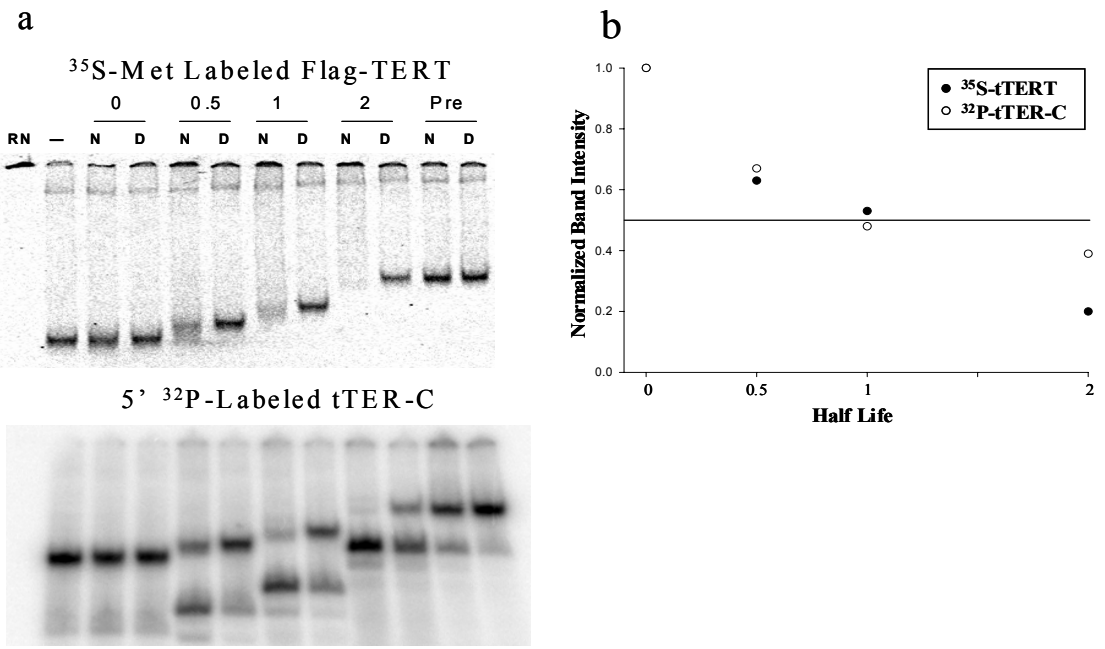

Figure 5.3 EMSA of telomerase stability after treatment with NMIA. (a) Native gels assess the stability of telomerase holoenzyme after treatment with 10 mM NMIA (N) or 10% DMSO (D), as notated above each gel. The number of half-lives incubated at 30 ºC is indicated at the top with one half-life equal to 17.5 minutes. RNase A treated telomerase (RN) and no treatment (-) served as negative and positive controls, respectively. As a control for NMIA reactivity dependent telomerase stability, NMIA was prequenched for 5 half-lives before telomerase was added (Pre). (b) Normalized band densities from two separate ^{35}S-Met-labeled tTERT (●) or 5'-^{32}P-labeled tTER-C (○) gels were plotted versus half-life increments to determine telomerase stability decay.

2006). Upon NMIA addition tTER-C dissociates from tTERT, which remains in the well, with half of the protein total remaining in the well at one half-life of NMIA decay time (Figure 5.3a, top gel). The same is seen for tTER-C, which shifts to a faster moving band that indicates a smaller size, likely free tTER-C (Figure 5.3a, bottom gel). RNase A treated controls show a shift of tTERT into the well and elimination of the tTER-C band (Figure 5.3a). Prequenching the NMIA or DMSO for 5 half-lives before adding telomerase for a 5-minute incubation, resulted in little to no increase in the telomerase complex decomposition rate (Figure 5.3a).

3. Analysis of hit profile of tTER at various NMIA reaction half-lives

The fact that the telomerase complex becomes unstable upon treatment with NMIA prompted us to investigate the NMIA hit profile at various half lives in order to maximize signal while minimizing telomerase dissociation. The concern was that if the complex dissociates after two half-lives then 25 percent of the hits on the RNA may be of free RNA. So if the hit profile looks similar at shorter half-lives, we should be able to increase the signal to noise for tTERT associated versus tTERT unassociated tTER. Figure 5.4a depicts a half-life NMIA hit profile and figure 5.4b plots band density traces for 0.5, 1, 3 and 5 half-lives as well as DMSO control and dideoxythymidine ladder.

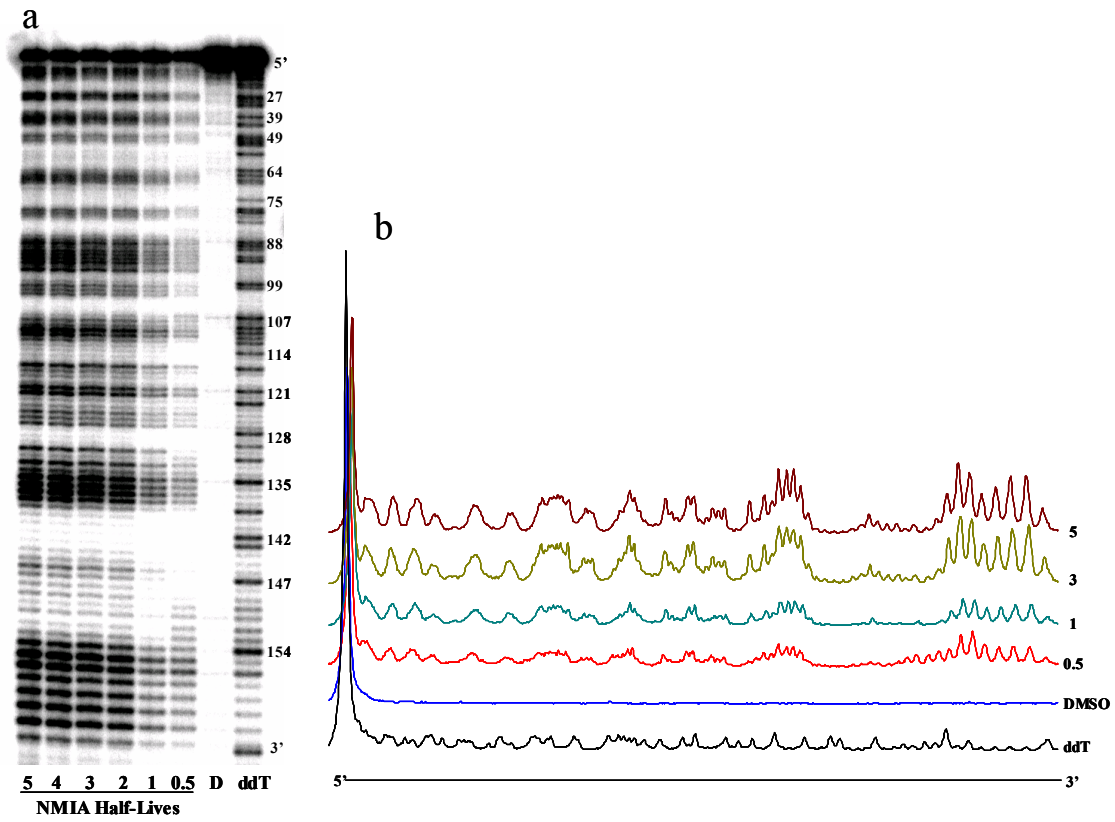

Figure 5.4 NMIA half-life hit profile of tTER-C. (a) SHAPE assay sequencing gel detailing the hit profile of NMIA when allowed to react with tTER-C at 30 °C for 0.5-5 half-lives as notated on gel. One sample was treated with 10% DMSO for 5 half-lives as a background control (D). A dideoxythymidine ladder (ddT) is included to establish RNA modification position. (b) Traces of band intensity versus nucleotide position for ddT, DMSO, 0.5 half-life, 1 half-life, 3 half-lives, and 5 half-lives respective lanes are included for comparison. The 5' and 3' end of the traces are indicated.

NMIA reactions were quenched at the desired time point by the addition of 10 mM dithiothreitol. At 0.5 half-lives the hit profile looks similar to that of longer incubations but the signal to noise ratio was not high enough to achieve robust data. At 1 half-life the gel and trace looked good and were determined to generate consistent data. Half-lives 2-5 look identical as the majority of the hits (> 75%) have occurred by these time points.

4. SHAPE assay optimization

SHAPE analysis of the telomerase complex adds increasing complexity to the work up of the hit RNA. The reaction is quenched with dithiothreitol, SDS containing buffer is added to solubilize the protein, tTERT is digested with proteinase K, then the RNA is extracted with pH 8.0 phenol/chloroform, and precipitated with ethanol. Each of these steps was optimized and the details of the optimized procedure are presented in depth in the material and methods section below. It was determined that treatment with 10 mM NMIA for 1 half-life was sufficient to generate reproducible tTER-C footprints.

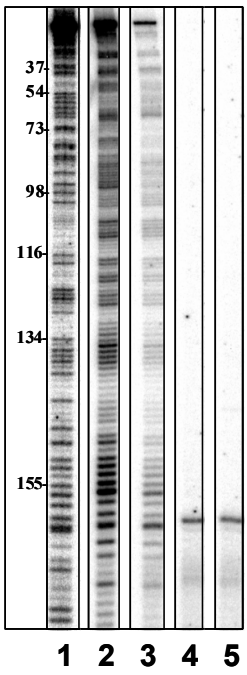

Figure 5.5 SHAPE chemistry analysis of soluble telomerase and purification controls. 10 mM NMIA was reacted with affinity purified telomerase samples containing tTERT and tTER-C (3), only tTER-C (4), or only tTERT (5). SHAPE chemistry analysis of free tTER-C in buffer was also performed for comparison (2). A dideoxythymidine ladder (ddT) is included to establish RNA modification position (1).

Figure 5.5 depicts SHAPE analysis of tTER-C (lane 2), tTER-C in complex with tTERT (lane 3) and control experiments where either just tTER-C (lane 4) or just tTERT (lane 5) were added to the reconstitution and affinity-purification reactions and then analyzed by SHAPE. These controls show that RNA isolated by non-specific binding during the purification procedure is not detected by this assay. The single band in each control is likely a self-priming artifact. The reduced intensity of the tTERT containing tTER lane is due to limiting amounts of RNA in the telomerase sample. Subsequent gels have the pixel intensity increased on the tTERT containing samples for easy comparison to the tTER-C only samples. For comparison to the affinity-purified telomerase, SHAPE analysis was attempted on unpurified recombinant telomerase in reticulocyte lysate. This was unsuccessful as a white precipitate immediately formed when NMIA was added to the lysate (presumably NMIA or an NMIA complex) and the reverse transcription mapping of the hits was inefficient in the presence of the high concentrations of tRNA and rRNA endogenous to the lysate (data not shown).

5. Comparison of SHAPE analysis of tTER-C with or without tTERT

The structure of tTER in the telomerase complex was examined by SHAPE chemistry using two separate primers, one that annealed to the RT-primer extension on the 3' end of tTER-C and an internal primer that allowed accurate analysis of the 5’ end of the RNA. The 5’ end SHAPE analysis of tTER covered stem I, stem II, the template and a portion of the putative pseudoknot. The template region and the pseudoknot were shown to be present in a drastically different conformation in free tTER (Figure 4.5b) than that predicted by phylogenetic sequence analysis (Figure 4.4e). The majority of this

region is analyzed by the internal tTER-C primer and is depicted in figure 5.6. Importantly, the changes in reactivity profile of specific residues and regions of the RNA are considered both in relation to tTER-C in the tTERT bound and unbound states, but also in relation to adjacent residues within the same SHAPE experiment. Upon general inspection of the gel (Figure 5.6a), it can be seen that the largest area of change is in the template recognition element. This region of tTER appears to be much more reactive

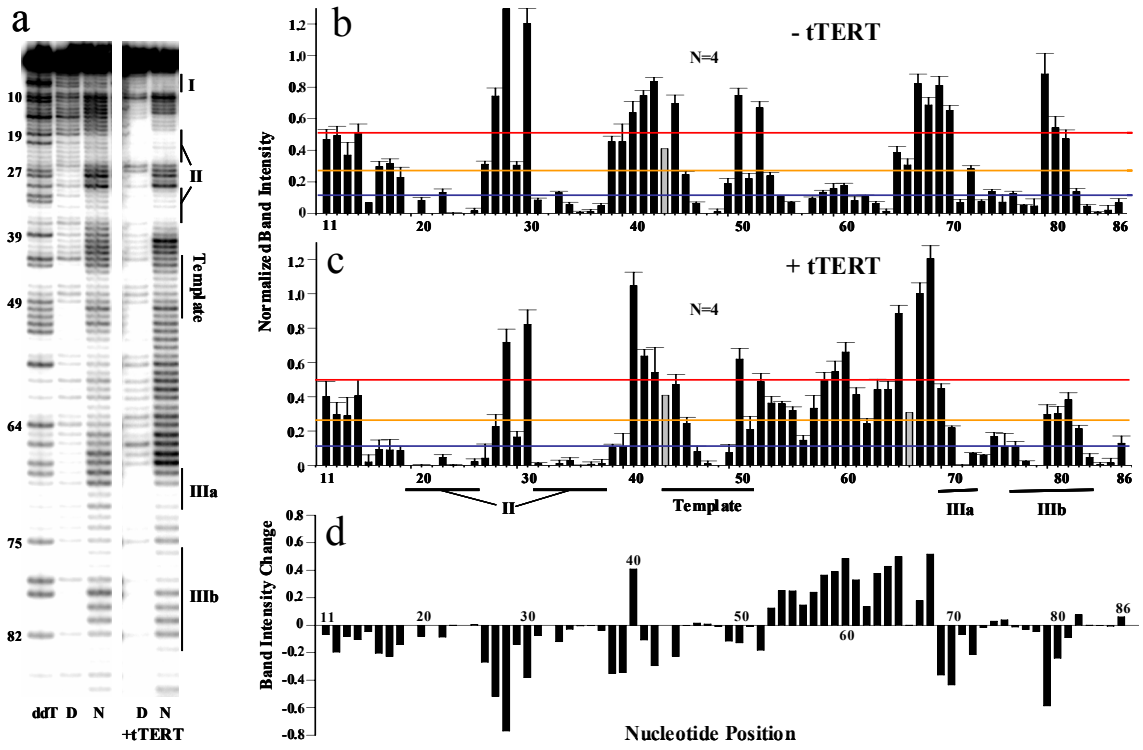

Figure 5.6 SHAPE chemistry analysis of the 5' end of tTER in complex with tTERT. (a) tTER-C was treated with 10 mM NMIA (N) or 10% DMSO (D) either free in solution or in complex with tTERT as indicated, and the resulting 2'-acylated RNAs were mapped by reverse transcription with an internal primer. Sites of acylation cause reverse transcription to stop exactly one nucleotide before the modification site. Dideoxythymidine ladders (ddT) are labeled to include this one nucleotide shift. (b, c) Histograms of average normalized NMIA hit intensities for free tTER-C (b) or in complex with tTERT (c). Normalized band intensities from five separate experiments were averaged and plotted against nucleotide position with standard error bars. Blue, orange, and red lines indicated divisions for color-coded hit intensity for structures in figure 5.8 as 0.10-0.25, 0.25-0.50, and >0.50, respectively. Any value below 0.10 is represented as black. Grey residues represent positions where accurate values could not be assigned. (d) Hit intensity difference histogram. Average normalized hit intensities from free tTER-C and tTER-C in complex with tTERT were subtracted from each other and the values were plotted versus nucleotide position. Positive bars represent tTER-C residues that increased in NMIA reactivity while in complex with tTERT and negative bars represent residues that decreased in reactivity.

relative to the other positions while bound to tTERT (see figure 5.6b-d, residues 53-64). Much of this region is above the orange or red line (averaging 40% reactivity), while in the absence of tTERT this region is quite unreactive (averaging 10% reactivity) consistent with the predicted base pairing of this region in the solution tTER stem III (Figure 4.5b).

Smaller local changes dominate the reactivity profile for regions of tTER aside from the template recognition element. The template reactivity appears similar to free tTER, except template position C49, which was less reactive (19% decreased to 7.4%; Figure 5.6b-d). Template boundary element residues U38 and C39 decreased in reactivity from 45% to 10%, while A40 increased from 64% to 100% (Figure 5.6b-d). G26 and U27 on the 5' side of stem-loop II decrease significantly in reactivity from 30% and 75% to 4% and 23%, respectively, while the remaining loop residues retain a similar reactivity profile. An essential template boundary sequence UUA18-16 is also reduced in reactivity from an average of 28% reactivity to 9% (Figure 5.6b-d). In the region 3' of the template recognition element, residues A69 and A70 decrease in reactivity from 80% and 65% to 45% and 20%, respectively, while A65 and U68 increased in reactivity from 39% and 69% to 89% and >100%, respectively. Also, residues A79 and A80 decreased in reactivity from 88% and 54% to 30%, respectively.

The SHAPE analysis of the 3' end of tTER covers stem IV, stem I, and part of stem III up to residue 87. Comparison of the tTERT bound tTER-C with the free tTER-C in this region does not reveal many significant differences (Figure 5.7). Stem IV appears essentially the same with the terminal loop slightly less reactive in the presence of tTERT. Since the relative hit profile does not change (loop IV) other than a reduction in

reactivity relative to other regions of the RNA in the same SHAPE experiment, we deduce that the structure of this region is not changed but instead may be protected by the protein. The poly-U tail exhibits increased reactivity, while the 3' side of stem IV is less reactive. On the 5' side of stem IV, the reactivity of U127-U125 and GA121-122 remain similar. Conversely, the U117 bulge decreases in reactivity from 71% to 40 % and

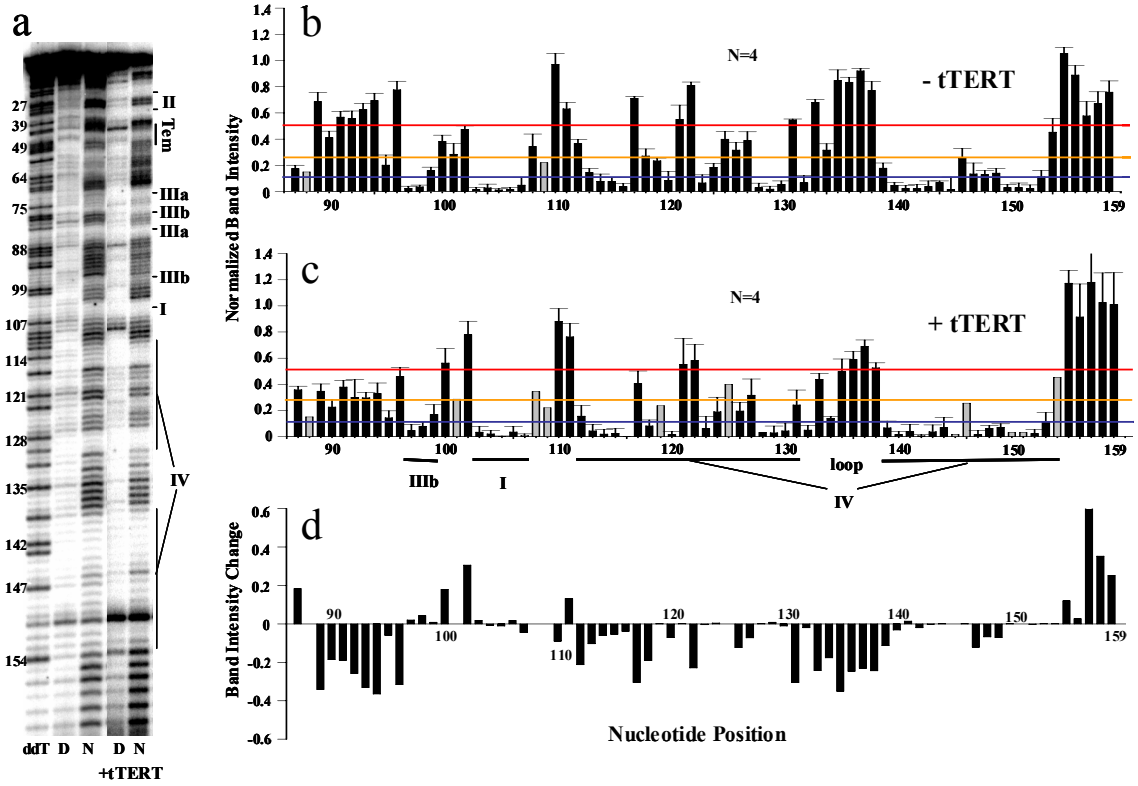

Figure 5.7 SHAPE chemistry analysis of the 3' end of tTER in complex with tTERT. (a) tTER-C was treated with 10 mM NMIA (N) or 10% DMSO (D) either free in solution or in complex with tTERT as indicated, and the resulting 2'-acylated RNAs were mapped by reverse transcription with a 3' end primer. Sites of acylation cause reverse transcription to stop exactly one nucleotide before the modification site. Dideoxythymidine ladders (ddT) are labeled to include this one nucleotide shift. (b, c) Histograms of average normalized NMIA hit intensities for free tTER-C (b) or in complex with tTERT (c). Normalized band intensities from five separate experiments were averaged and plotted against nucleotide position with standard error bars. Blue, orange, and red lines indicated divisions for color-coded hit intensity for structures in figure 5.8 as 0.10-0.25, 0.25-0.50, and >0.50, respectively. Any value below 0.10 is represented as black. Grey residues represent positions where accurate values could not be assigned. (d) Hit intensity difference histogram. Average normalized hit intensities from free tTER-C and tTER-C in complex with tTERT were subtracted from each other and the values were plotted versus nucleotide position. Positive bars represent tTER-C residues that increased in NMIA reactivity while in complex with tTERT and negative bars represent residues that decreased in reactivity.

residue A118 from 27% to 8% (Figure 5.7b, c). The end of stem IV is predicted to be the A112-U154 base pair. A112 is reactive in free tTER-C (37%), but is not in tTERT bound tTER-C (15%). Stem I and its linker to stem IV, residues A111-A108, exhibit little change in reactivity upon tTER-C association with tTERT. The 3-nucleotide linker between stem I and stem III (U102-A100) actually increased in reactivity with tTERT bound with an increase in average reactivity from 38% to 67% (Figure 5.7b, c). The proposed stem IIIb was protected from residues U99 to G97, but similar to the solution structure of tTER, U96 was reactive (46%) and G95 was protected (14%). Residues A94-A89 were less reactive (average of 31%) than in free tTER-C (average of 59%), but still retained a similar overall profile (Figure 5.7b, c). Interestingly, the last residue mapped reliably, U87, actually increases in reactivity with tTERT bound from 18% to 36%.

6. Binding of tTERT induces a conformational change in the pseudoknot domain

The SHAPE reactivity of tTER-C while bound to tTERT is measurably different than the solution structure of tTER-C. Figure 5.8a depicts the free tTER-C solution structure with color-coded residue reactivities derived from parallel control experiments detailed in figures 5.6b and 5.7b. The major difference in the hit profile for the tTERT bound tTER-C is the region 3' of the template, residues 64-53, which becomes substantially more reactive. Since this region was heavily hit and was likely single stranded, we attempted to match the hit data to the existing pseudoknot model (Figure 5.8b). As can be seen, much of what is predicted to be base paired within this pseudoknot model is colored orange (>25% reactivity), which is inconsistent with

canonical base pairing (Figure 5.8b). To more accurately match the SHAPE reactivities, a new pseudoknot model is suggested (Figure 5.8c). Stem IIIa is defined from A70-U73 and A83-U86, which is still a 4-base pair duplex just shifted one nucleotide in the 3' direction (previously U69-C72 and G84-U87; Figure 5.8b compared to 5.8c). The major difference in our proposed model of the pseudoknot is that the previously proposed paired residues U81-A83 to U92-A94 are now modeled to be single stranded. The formation of this portion of stem IIIb is not supported by SHAPE chemistry analysis.

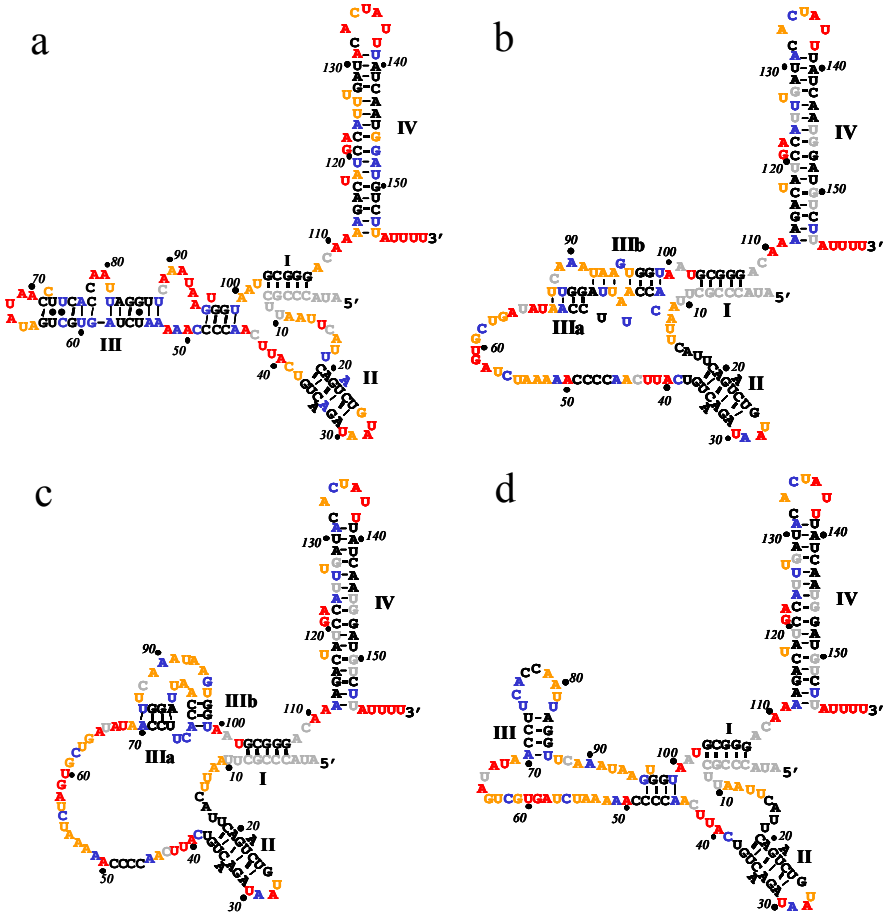

Figure 5.8 SHAPE hit intensity color-coded tTER secondary structures. (a) Secondary structure of free tTER with color-coded hit intensities derived from figures 5.6a, b and 5.7a, b. (b) Phylogenetically predicted secondary structure (Romero and Blackburn 1991; ten Dam et al. 1991) with color-coded hit intensities derived from tTER in complex with tTERT (Figure 5.6a, c and 5.7a, c). (c) Color-coded secondary structure of tTER with pseudoknot modified to reflect NMIA modification data derived from the RNA in complex with tTERT (Figure 5.6a, c and 5.7a, c). (d) Color-coded secondary structure of tTER with template pairing and half formed pseudoknot to reflect template protection data derived from the RNA in complex with tTERT (Figure 5.6a, c and 5.7a, c).

The pairing that is consistent with the SHAPE data is between residues A76-C78 and G97-U99 (Figure 5.8c), which represents half of the originally proposed stem IIIb. The two loops formed by this pseudoknot model are reactive (>30%) versus the predicted base paired residues in the pseudoknot (<15%).

C. Discussion

The SHAPE analysis described here reveals the highest resolution structural information on tTER within the telomerase complex to date. Additionally, it is the first report of a RNA that is in association with a protein component to be analyzed by SHAPE. It appears that as tTER assembles into the telomerase complex, the RNA undergoes a drastic reorganization of both the template and pseudoknot domains. This presumably starts by breaking a 12-base pair stem and forming a pseudoknot, which we predict to be similar to the previously predicted structure. However, the moderate reactivity levels of the unbase paired regions of our pseudoknot model do not rule out that there may in fact be a mixture of structures that would be difficult to detect with SHAPE chemistry, which effectively measures average nucleotide conformational freedom (Barrodek and Weeks 2005). The template remains constrained in the cytosine-rich region and this may be due to the direct binding of tTERT to the RNA backbone here, or to an unpredicted base pairing or tertiary interaction. A possible transition structure is suggested in figure 5.8d, where the solution stem III has been broken and half of the pseudoknot pairing is present, but the second pseudoknot pairing is still paired with the template. The template boundary region, which has been identified as a high affinity tTERT binding site, changes its reactivity at three residues, U38 and C39 decrease in

reactivity, and A40 increases in reactivity. This is consistent with direct tTERT interaction with U38 and C39 forming a steric block to NMIA reaction. While the structure of stem IV does not change upon telomerase assemblage, it does appear to become more ordered in agreement with a recent FRET analysis study (Stone et al. 2007). RNA structure reorganization upon protein binding is a well-documented phenomenon for ribonucleoproteins, as large and small RNAs alike do not always fold correctly until in complex with their requisite protein or proteins (Weeks 1997; Bokinsky and Zhuang 2005).

There have been two previous footprinting studies of the *Tetrahymena thermophila* telomerase RNA in complex with the protein subunit tTERT. One utilized dimethylsulfate (DMS) to modify telomerase RNA in vivo (Zaug and Cech 1995), and another employed RNases T1 and V1 to cleave tTER within telomerase reconstituted in rabbit reticulocyte lysate (Sperger and Cech 2001). The data from both studies combined with NMIA modification results is summarized in Table 5.1. DMS modification is highly subject to solvent accessibility, which does not appear to be a limiting factor for NMIA due to its modification of the ubiquitously solvated, negatively charged phosphate-sugar backbone (Merino et al. 2005; Wilkinson et al. 2006). RNase cleavage is severely limited by steric access (Ehresmann et al. 1987), which may also affect NMIA but to a lesser extent owing to the small size of the reagent (0.2 kDa) compared to the large RNases (>30 kDa). Despite the highly varied reagent properties and conditions of RNA probing: in vivo (Zaug and Cech 1995), in vitro unpurified (Sperger and Cech 2001), and in vitro soluble, purified (current study), the results correlate well. The previous studies also suggest that the pseudoknot is not properly formed in solution and

Table 5.1 Summary of footprinting data from past studies of tTER in the telomerase complex

nt residue	DMS[a]	RN T1[b]	RN V1[b]	NMIA	nt residue	DMS[a]	RN T1[b]	RN V1[b]	NMIA
U10				ND	G85		-		-
A11	+			++	U86				+
A12	+			++	U87				++
U13				++	C88	-			ND
U14				++	A89	-			++
C15	-			-	A90	-			+
A16	-			-	A91	-			++
U17				-	U92				++
U18				-	A93	-			++
C19	-			-	A94	-			++
A20	-		++	-	G95		+	+	+
G21		-	+++	-	U96				++
A22	+		++	-	G97		+		-
U23			++	-	G98		+		-
C24	-		++	-	U99				+
U25			++	-	A100	++			+++
G26		++		-	A101	++			ND
U27				+	U102				+++
A28	+			+++	G103		-		-
A29	-			+	C104	-		+++	-
U30				+++	G105		-	+++	-
A31	-		+	-	G106		-	++	-
G32		-		-	G107		-		-
A33	-			-	A108	++			ND
A34	-			-	C109	++			ND
C35	-		+	-	A110	++		+	+++
U36				-	A111	++			+++
G37		-	+	-	A112	+			+
U38				-	A113	-		+	-
C39	-			+	G114		+	+	-
A40	+			+++	A115	-		+	-
U41				+++	C116	-		+	-
U42				+++	U117			+	++
C43	++			ND	A118	-		+	-
A44	++			++	U119			+	ND
A45	++			+	C120	-		+	-
C46	++			-	G121		+		+++
C47	++			-	A122	-			+++
C48	++		+	-	C123	-			-
C49	++		++	-	A124	-			+
A50	++		++	+++	U125				ND
A51	++		++	+	U126				+
A52	++		+	++	U127			+	++
A53	++			++	G128		-	+	ND
A54	+			++	A129	-			-
U55			+	++	U130				-
C56	+		++	+	A131	-			+
U57			++	++	C132	ND			-
A58	+		+	++	A133	ND			++
G59		+++		++	C134	ND			+
U60				++	U135				+++
G61		++		++	A136	ND			+++
C62	-			+	U137				+++
U63			++	++	U138				+++
G64		++	++	++	U139				-
A65	+			+++	A140	ND			-
U66				ND	U141				-
A67	+		+	+++	C142	ND			-
U68			+	+++	A143	ND			-
A69	-		++	++	A144	ND			-
A70	-		++	+	U145				ND
C71	-		++	-	G146		ND		ND
C72	-		++	-	G147		ND		-
U73			++	-	A148	ND			-
U74			+	+	U149				-
C75	-			+	G150		ND		ND
A76	-			+	U151				ND
C77	-		++	-	C152	ND			-
C78	-		++	-	U153				+
A79	-		++	++	U154				ND
A80	-			++	A155	ND			+++
U81				++	U156				+++
U82				+	U157				+++
A83	-		++	-	U158				+++
G84		-	+++	-	U159				+++

Hit intensities were scored according to their publications as follows: - none, + light, ++ intermediate, +++ heavy, ND residue not determined. RN – RNase. a Zaug and Cech (1995), in vivo telomerase ; b Sperger and Cech (2001), in vitro unpurified telomerase.

appears either properly formed (Sperger and Cech 2001) or protected (Zaug and Cech 1995) while in the telomerase complex. When DMS was used to probe tTER in vivo it was found that 52 of 66 total analyzable adenine and cytosine residues were correctly modified according to their phylogenetically predicted base pairing state (79%; Table 5.1), while only 40 were correctly scored for the free RNA (61%; Table 4.1). Almost half of these incorrect modifications (6) occurred in the pseudoknot region, which appeared mostly solvent inaccessible and was likely bound by tTERT, another telomerase component, or folded into a tertiary structure (Zaug and Cech 1995). Each of these are possibilities as there is precedence for triple helices in the pseudoknot regions of both human (Theimer et al. 2005) and *K. lactis* TERs (Shefer et al. 2007). Using RNase T1, 16 of 19 tTER guanines were cleaved according to their predicted pairing state (84%) while in complex with tTERT in one study, and 13 of 22 guanines were cleaved correctly (59%) in the free RNA in another study. The results from these studies combined with our analysis shows that tTER adopts a different conformation while in complex with tTERT than it does free in solution.

1. NMIA treatment causes instability of the telomerase holoenzyme

The instability of the telomerase holoenzyme as observed by native gel electrophoresis could be the result of three separate phenomena. The first possibility is that the modification of the RNA causes the RNA to misfold resulting in enzyme instability. This possibility is supported by the half-life for telomerase stability, which matches the reagents half-life for RNA and water hydrolysis (Figure 5.3b). Another plausible explanation is that one of the amino acid side groups in sufficiently reactive to

be acylated by the hydroxyl-selective NMIA and causes either protein denaturation leading to subunit dissociation or inhibits a critical RNA-protein contact. Amino acid residues serine, threonine, and tyrosine contain hydroxyl groups in their side chains that may be reactive to NMIA. If just one critical modification occurred in a region of tTERT that is essential to RNA binding then the complex could be induced to dissociate. One other possibility is that unreacted NMIA may intercalate into the RNA and induce structural changes causing complex dissociation. The unreacted NMIA structure may intercalate better than the quenched product, since the quenched product does not appear to induce complex dissociation (Figure 5.3a, prequench lanes). Whatever the cause for dissociation, we subsequently determined that the hit profile at 1 half-life was comparable to 5 half-lives (Figure 5.4). Since the complex did show a time dependent dissociation and the hit profile of 1 half life was equivalent to 5 half lives, we performed all subsequent SHAPE experiments with a reaction limit of 1 half-life to increase the probability that tTER was modified while still associated with tTERT. The observation that NMIA can affect RNP stability will be critical for others conducting similar experiments.

2. The structure of stem IV in the telomerase complex

Stone et al. (2005) recently used single molecule FRET to study the effect of p65 and tTERT on the structure of tTER. They reported that the binding of p65 and tTERT induced a kink in stem IV. They were able to narrow the location of the kink to the proximal portion of stem IV including the GA bulge. We see by SHAPE analysis that the GA bulge does not appear to change in its NMIA reactivity profile, suggesting that the

induced bending may not occur at this exact point in the stem or that increased bending does not affect NMIA reactivity. In vivo DMS footprinting failed to modify A122 suggesting that p65 or tTERT is tightly associated to stem IV in this region (Zaug and Cech 1995). In contrast the reactivity profile near the U117 bulge does change. The U117 bulge decreases from 71% reactivity to 40%, and A118 decreases from 27% reactivity to 8% (Figure 5.7). The opposing base pairing partners also undergo a slight reduction in reactivity, although their reactivity is low even in the free RNA. These changes suggest that tTERT binding increases the order of the helix at this region, which was shown by NMR analysis to be flexible and with little evidence of base pairing. If the binding of p65 and/or tTERT causes tightening of this region, it may induce the bending that was evident by FRET analysis. It would be interesting to investigate the structure of this region in the presence of p65, which was shown to induce a more experimentally stable bend in the stem than just tTERT alone (Stone et al. 2007).

3. Effect of tTERT on the template boundary element

A number of studies have shown that a high affinity tTERT binding site resides near the template boundary element within tTER (Lai et al. 2002; Mason et al. 2003). SHAPE chemistry analysis shows that in free tTER-C in solution, stem II forms a well-ordered structure. When tTER-C is analyzed in the telomerase complex, stem II appears well formed with A29 being reduced in reactivity relative to its surrounding loop residues suggesting the conservation of its *syn* conformation while in complex with tTERT. This data suggests that the solution NMR structure of stem II is an accurate approximation of the structure of this element in the telomerase enzyme (Richards et al. 2006). In free

tTER-C the nucleotides just 3' of stem II are heavily modified (>45%), consistent with a single stranded or unconstrained environment. One of the most notable changes in this region with tTERT bound is in the first three nucleotides 3' of stem II. U38 and C39 both decrease in reactivity from 45% in free tTER-C to 10% in the telomerase complex, while the reactivity of A40 increases dramatically from an already reactive 65% to over 100%. Similarly, DMS lightly modified A40, but not C39 with tTERT present (Table 5.1), and modified both A40 and C39 without tTERT present (Zaug and Cech 1995). By comparison, the next twelve nucleotides (U41-A52) have almost the exact same reaction profile and intensities with or without tTERT bound. Furthermore, in the loop connecting stem II and stem I, nucleotides U18-A16 appear to decrease in overall reactivity, as do stem II loop residues G26 and U27. Other footprinting studies support these findings with A16 heavily modified by DMS without tTERT bound, but protected with tTERT bound (Zaug and Cech 1995). G26 was partially protected from cleavage by RNase T1 with tTERT bound compared to without tTERT bound (Sperger and Cech 2001). Since this region has been implicated as a direct binding site for tTERT, it is likely the change seen in hit intensity of these residues is due to direct tTERT interaction. tTERT may also be 'holding' onto tTER by the proximal portion of stem II, but the inherent lack of reactivity of this stable structure does not allow us to investigate this directly.

4. Effect of tTERT on the tTER pseudoknot structure

It was postulated in chapter IV of this work that free tTER in solution does not form a pseudoknot, but rather forms a long 12-base pair stem with a 4-nucleotide bulge

and 6-nucleotide apical loop (Figure 5.8a). There may also be pairing of the template, which is supported by previous footprinting studies with DMS and RNase V1 (Bhattacharyya and Blackburn 1994; Zaug and Cech 1995; Sperger and Cech 2001). When we analyzed tTER-C in the telomerase complex using SHAPE chemistry, we observed a drastic change in reactivity in the region from the template to the pseudoknot. These changes are consistent with formation of a pseudoknot structure in the telomerase complex (Figure 5.8c). Our model of the pseudoknot structure is similar to the previously assigned pseudoknot structure based on phylogenetic conservation (ten Dam et al. 1991), but does exhibit several notable differences. It is quite obvious that the SHAPE analysis is not consistent with base pairing interactions involving residues U96 through U92. This agrees with RNase V1 footprinting analysis, which did not detect cleavage in this predicted pairing region (Table 5.1). Additionally, Sperger and Cech (2001) saw an increase in RNase V1 cleavage of pseudoknot residues A70-U73, C77-A79, and A83-G84 upon binding of tTERT. In further support of the pseudoknot structure in the context of assembled telomerase, unpairing and subsequent compensatory mutations of two putative pseudoknot pairing regions (A70-U86, C71-G85 and C77-G98, C78-G97), show that these pairings are essential for telomerase activity since both compensatory mutations fully rescued activity (Lai et al. 2003). Interestingly, the entire pseudoknot was protected from DMS modification when telomerase was probed in vivo (Table 5.1), suggesting direct tTERT binding in this region, which may help direct refolding of the RNA.

5. The template recognition element appears unpaired while in complex with tTERT

The entire template recognition element increases dramatically in reactivity (average of 10% to 40%) when tTERT binds, suggesting an overall shift from a paired to an unpaired state. An alternative explanation is that this region is ordered by stacking in the free RNA. However, the length of the presumably single stranded region in the absence of base pairing makes it unlikely that such a large extent of order could be obtained. Treatment of endogenous telomerase with DMS also showed this increase in single stranded character as A53, A54, C56, A58, and A65 all became susceptible to modification while in complex with tTERT (Table 5.1). Surprisingly, the conserved residue C62 becomes less reactive to DMS in the telomerase complex (Figure 4.1 and 5.1) (McCormick-Graham and Romero 1995; Zaug and Cech 1995). Furthermore, the single nucleotide mutation C62G severely affects both tTERT binding and telomerase activity (Lai et al. 2001). RNase T1 cleavage of G59, G61, and G64 increases slightly with tTERT binding, but so does RNase V1 cleavage in this area. RNase V1 cleavage occurs around the conserved residues C56 and C62 (Table 5.1), suggesting structure in these regions. SHAPE analysis of these residues shows an increase in reactivity upon tTERT binding (0 to 14% for C56; 10% to 24% for C62), but they are still the two least reactive residues in this region (Figure 5.6). Combined, all of this data suggests that this region goes from being paired without tTERT bound to being unpaired in the telomerase complex, with residues C56 and C62 possibly involved in tertiary interactions or direct tTERT binding.

6. Structure of the template region

There appears to be structure in the cytosine-rich region of the template. Zaug and Cech (1995) saw a fully accessible template in their DMS in vivo study of the telomerase holoenzyme, while our study and Sperger and Cech (2001) saw evidence of substantial structure in the template (Table 5.1). Additionally, all three studies generated evidence for structure in the template of free tTER (Table 4.1). This structure may represent base pairing (such as that suggested in figure 5.8d), base stacking, tertiary structure, or direct protein contact. The major difference between the DMS study was that is was performed on telomerase in vivo, while our study and the Sperger and Cech (2001) study utilized in vitro reconstituted telomerase. There are suggested to be at least three more proteins associated in vivo with the *Tetrahymena* telomerase holoenzyme (p75, p65 and p45) that may further alter tTER structure (Witkin and Collins 2004). p65 specifically has been shown to directly bind to tTER and to promote telomerase assembly, stability, and processivity (Prathapam et al. 2005; O'Connor and Collins 2006), perhaps by freeing the template. Of note, the template cytosine residues in human TER are also protected from DMS modification both in free RNA and in complex with hTERT (Antal et al. 2002).

7. tTER likely undergoes two structural changes during telomerase holoenzyme assembly

There are three published studies aside from this work that describe the changes in conformation of tTER upon the binding of a protein subunit (Zaug and Cech 1995; Sperger and Cech 2001; Stone et al. 2007). Stem IV undergoes a bending process that accompanies p65 and tTERT binding that was directly observed in real time using single

molecule FRET analysis (Stone et al. 2007). Our SHAPE analysis also details an increased order within stem IV evidenced by a change in reactivity around the flexible U117 bulge (Figure 5.7). Two footprinting studies detail a shift in conformation of the pseudoknot region when tTER is bound to tTERT (Zaug and Cech 1995; Sperger and Cech 2001). While these studies were limited by low resolution because of the properties of their reagents (Table 1.1) these limitations are absent in our studies due to the inherent reactivity of NMIA (Merino et al. 2005; Wilkinson et al. 2006). Accordingly, we are able to examine tTER at single nucleotide resolution. This high-resolution mapping shows the formation of a pseudoknot structure upon tTERT binding. Figure 5.9 details the structural changes that have been alluded to in other publications (Sperger and Cech 2001; Lai et al. 2003; Mason et al. 2003; Stone et al. 2007). First, p65 binds tTER, stabilizes stem IV and promotes additional bending of the stem. This increased order in

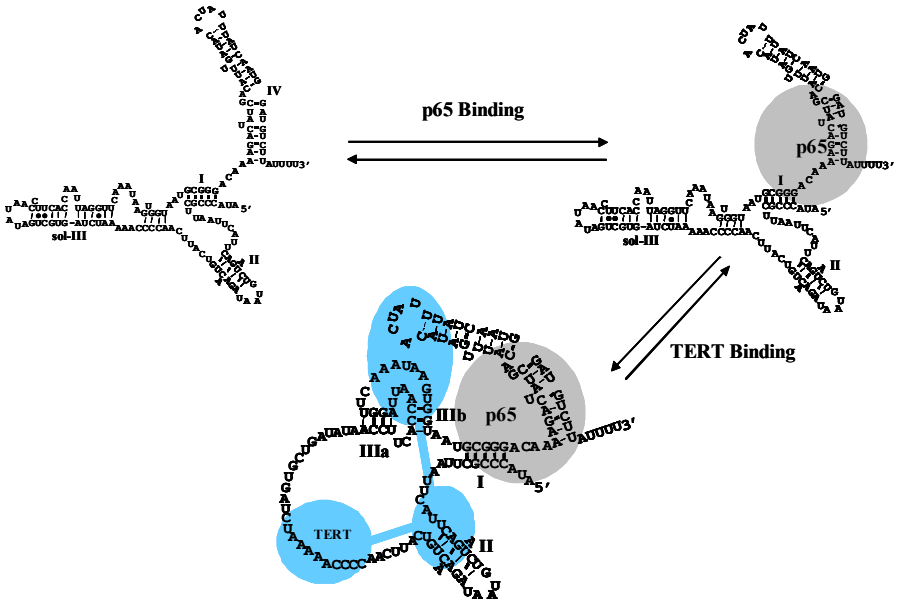

Figure 5.9 Telomerase assembly pathway. Natural biogenesis of tTER may navigate the following pathway. p65 binds the RNA, and the stabilization of the proximal portion of stem IV causes further bending of the stem. It is also possible that p65 binding loosens or breaks the solution stem III structure and/or the template pairing. When tTERT binds it likely causes further bending of stem IV as well as a reorganization of tTER to form a pseudoknot structure.

the RNA structure may help to loosen the structure of stem III in the free tTER. When tTERT binds, it presumably recognizes the template boundary element and binds tightly, causing the final reorganization of the structure to the pseudoknot, freeing the template recognition element and the template for primer recognition and binding. The structure depicted in figure 5.8d may represent a transition structure that forms after p65 binding or during the early stages of tTERT binding. This structure could easily transition to the pseudoknot structure by a simple shift in the base pairing. The ability of p65 to promote telomerase assembly and increase tTERT-tTER affinity may involve its ability to shift tTER conformation to a structure similar to figure 5.8d. Such structural reorganization of RNAs involved in RNPs has precedence (Weeks 1997; Bokinsky and Zhuang 2005).

D. Materials and methods

See chapter III, section D for methods on sequencing gel electrophoresis and chapter IV, section D for methods on Superscript III reverse transcription reaction and SAFA data analysis and band density normalization.

1. Construction of FLAG-tag tTERT plasmid construct

Tetrahymena thermophila TERT is cloned into the BamH1 and Xho1 sites in pET-28a plasmid. The oligonucleotide sequences used to insert the sequence for FLAG peptide were purchased from IDT DNA with appropriate 5' overhangs and 5' phosphates. The sequences are 5'-P-CATGGACTACAAAGACGATGACGACAAGG for tTERT FLAG sense and 5'-P-GATCCCTTGTCGTCATCGTCTTTGTAGTC for tTERT FLAG antisense. These DNA oligonucleotides were gel purified and combined in equimolar

concentration and annealed before use in cloning ligation reactions. The FLAG peptide sequence was added to the N-terminus of tTERT by cloning into the Nco1 and BamH1 sites, which both removed the Nco1 site and an Nde1 site, allowing for easy screening of positive clones. The addition of the FLAG-tag also removed the N-terminal His- and T7-tags.

2. FLAG-tag immunopurification of telomerase

The telomerase complex was purified by affinity chromatography (Bryan et al. 2003). Anti-FLAG M2 Agarose from mouse antibody beads (Sigma; 100 μL) were washed 4 times in 1400 μL of Wash Buffer 1 (20 mM Tris-acetate pH 7.5, 100 mM potassium glutamate, 5 mM RNase-free $MgCl_2$ (Ambion), 1 mM RNase-free EDTA (Ambion), 0.1 mM DTT, and 10% glycerol). Between each step, beads were recovered by centrifugation at 1,500*g* for 2 min at 4 ºC. The beads were then blocked twice using 1000 μL of blocking buffer (Wash Buffer 1 containing 0.5 mg/mL lysozyme, 0.5 mg/mL BSA, 0.05 mg/mL RNase-free glycogen, and 0.1 mg/mL yeast RNA) for 15 min at 4 ºC with gentle mixing on an orbital shaker. 400 μL of RRL translation reaction containing assembled FLAG-tagged telomerase was added to 400 μL of blocking buffer and centrifuged at 17,000*g* for 10 min at 4 °C to remove any precipitates. The supernatant was then added to the 100 μL of blocked Anti-FLAG M2 Agarose and the resultant slurry was mixed on an orbital shaker for 2 h at 4 ºC. The beads were washed 4 times with 1400 μL of Wash Buffer 3 (Wash Buffer 1 with 300 mM potassium glutamate), 2 times with 1400 μL of TMG (10 mM Tris-Acetate pH 8.0, 1 mM RNase-free $MgCl_2$, 0.1 mM DTT, and 10% glycerol) and resuspended in 100 μL of TMG to afford a 1:1 slurry.

Samples were either flash frozen in an ethanol/dry ice bath and stored at –80 ºC or were prepared for elution from the agarose.

3. Elution of soluble telomerase from Anti-FLAG Agarose with 3xFLAG peptide

200 μL of 1:1 slurry of FLAG-purified telomerase was added to a 1.5 mL Protein LoBind Tube (Eppendorf), and washed 2 times with 1200 μL of sterile filtered Wash Buffer 0 (20 mM Tris-acetate pH 7.5, 5 mM RNase-free $MgCl_2$, 1 mM RNase-free EDTA, 0.1 mM DTT, and 10% glycerol). Between each step, beads were recovered by centrifugation at 1,500*g* for 2 min at 4 ºC. 12 μL of 10 mg/mL BSA was added directly to the beads, followed by 200 μL of 3xFLAG peptide solution (Wash Buffer 0 with 0.75 mg/mL of 3xFLAG peptide (Sigma)). This slurry was nutated gently on an orbital shaker for 1 h at 4 °C. The slurry was centrifuged at 1,500*g* for 2 min at 4 °C, and the supernatant containing soluble telomerase was gently removed, leaving the agarose, and transferred to a fresh LoBind tube (Eppendorf) Samples were flash frozen in a dry ice/ethanol bath and stored at –80 °C until ready for use.

4. EMSA of soluble telomerase holoenzyme after NMIA treatment

NMIA hit reactions of soluble telomerase contained 2 μL of eluted telomerase, 1x Hit Buffer, 40 U of RNasin (Promega), and 10 mM NMIA or DMSO and was incubated at 30 °C. NMIA or DMSO was added to the reactions after preincubation at 30 °C for 2 min. After a specified time (Figure 5.3) xylene cyanol dyed 50% glycerol was added to a final glycerol concentration of 5% and the entire reaction was loaded onto a 10x10 cm

native acrylamide gel (5% acrylamide/bisacrylamide (29:1), 45 mM Tris base pH 8.3, 45 mM boric acid, 1 mM EDTA, and 4% glycerol) and ran immediately at 150 V. The gel was continuously ran during the experiment, only being stopped for quick sample loading, leading to the staggered band pattern in Figure 5.3. The gel was run for an additional 45 min after the last sample was loaded. For each experiment, control samples contained untreated telomerase, telomerase treated with 4.5 μg of ribonuclease A (USB), and telomerase added to hit reactions after NMIA or DMSO was quenched for 90 minutes (5 half-lives). Gels were dried under vacuum and exposed to phosphorimager plates to detect ^{35}S-Met labeled tTERT and/or ^{32}P-5'-labeled tTER-C.

5. NMIA hit reaction and work up of tTER-C in complex with tTERT

Eluted telomerase (25 μL; ~0.2 pmole) in 1x tTER Hit Buffer (50 mM Hepes pH 8.0 (Mediatech, Inc.), 2 mM RNase-free $MgCl_2$ (Ambion)) with total reaction volume double the volume of telomerase added (50 μL) was incubated at 30 °C for 2 min. NMIA or DMSO was added to each sample at a final concentration of 10 mM or 10% DMSO and incubated for 17 min 30 sec (1 half-life). The reaction was immediately quenched by the addition of 5 mM final concentration dithiothreitol. The solution was proteolyzed for 10 min at 37 °C with 160 μg/mL of proteinase K (USB) in 1x TE_4S (40 mM Tris pH 8.0, 4 mM RNase-free EDTA and 0.15% SDS), phenol/chloroform/isoamyl alcohol (buffered to pH 8.0) extracted, precipitated with ethanol in the presence of 200 mM RNase-free NaCl (Ambion) and 200 μg/mL of RNase-free glycogen (Ambion) as counter ion and carrier, respectively, washed once with 70% ethanol, speed vacuumed till dry, and reconstituted in 5 μL of RNase-free TE pH 8.0 (Ambion).

6. Telomerase activity assay

Telomerase activity assays were performed as described in chapter II, section D with the buffer changed to 1x tTER Hit Buffer.

Representative Works

Refereed publications:

Legassie, J.D. and Jarstfer, M.B. (2005) Telomerase as a DNA-Dependent DNA polymerase, *Biochemistry,* 44 (43): 14191-201.

Chen, Y., Fender, J., Legassie, J.D., Jarstfer, M.B., Bryan, T.M., Varani, G. (2006) Structure of Stem-loop IV of *Tetrahymena* telomerase RNA, *EMBO J.,* 25: 3156-3166.

Legassie, J.D. and Jarstfer, M.B. (2006) The Unmasking of Telomerase, *Structure,* 14 (11): 1603-9.

Legassie, J.D. and Jarstfer, M.B. (2007) *Tetrahymena* telomerase RNA undergoes a large structural shift in the pseudoknot region upon assembly with tTERT, manuscript in preparation.

Conference Presentations:

Legassie, J.D. and Jarstfer, M.J. (2003) "The Template-Active Site Interaction in the *Tetrahymena thermophila* Telomerase Enzyme," presented at the 117th North Carolina ACS Sectional Conference at Kenan Hall, UNC and at the Inaugural Pharmaceutical Sciences Research Conference at Kerr Hall, UNC both on April 26th.

Legassie, J.D. and Jarstfer, M.J. (2003) "The Template-Active Site Interaction in the *Tetrahymena thermophila* Telomerase Enzyme," presented at the RNA Society of North Carolina's Symposium on RNA Biology V: RNA, Tool and Target in Research Triangle Park, NC on October 18th.

Legassie, J.D. and Jarstfer, M.J. (2005) "A DNA-Dependent *Tetrahymena* Telomerase," presented at the Cold Spring Harbor Laboratory meeting on Telomeres & Telomerase in Cold Spring Harbor, NY on May 6th.

Legassie, J.D. and Jarstfer, M.J. (2006) "The SHAPE of *Tetrahymena* Telomerase RNA," presented at the 2nd European meeting on Telomeres and Genome Stability in Villars-sur-Ollon, Switzerland on August 31st.

Literature cited

Aigner, S. and T. R. Cech (2004). "The Euplotes telomerase subunit p43 stimulates enzymatic activity and processivity in vitro." RNA **10**(7): 1108-18.

Aigner, S., J. Postberg, H. J. Lipps and T. R. Cech (2003). "The Euplotes La motif protein p43 has properties of a telomerase-specific subunit." Biochemistry **42**(19): 5736-47.

Antal, M., E. Boros, F. Solymosy and T. Kiss (2002). "Analysis of the structure of human telomerase RNA in vivo." Nucleic Acids Res. **30**(4): 912-20.

Autexier, C. and C. W. Greider (1994). "Functional reconstitution of wild-type and mutant Tetrahymena telomerase." Genes Dev. **8**(5): 563-75.

Autexier, C. and C. W. Greider (1995). "Boundary elements of the Tetrahymena telomerase RNA template and alignment domains." Genes Dev. **9**(18): 2227-39.

Autexier, C. and C. W. Greider (1998). "Mutational analysis of the Tetrahymena telomerase RNA: identification of residues affecting telomerase activity in vitro." Nucleic Acids Res. **26**(3): 787-95.

Autexier, C. and N. F. Lue (2006). "The Structure and Function of Telomerase Reverse Transcriptase." Annu. Rev. Biochem.

Bachand, F. and C. Autexier (2001). "Functional regions of human telomerase reverse transcriptase and human telomerase RNA required for telomerase activity and RNA-protein interactions." Mol. Cell. Biol. **21**(5): 1888-97.

Badorrek, C. S., C. M. Gherghe and K. M. Weeks (2006). "Structure of an RNA switch that enforces stringent retroviral genomic RNA dimerization." Proc. Natl. Acad. Sci. U. S. A. **103**(37): 13640-5.

Badorrek, C. S. and K. M. Weeks (2006). "Architecture of a gamma retroviral genomic RNA dimer." Biochemistry **45**(42): 12664-72.

Badorrek, C. S. and K. M. Weeks (2005). "RNA flexibility in the dimerization domain of a gamma retrovirus." Nat. Chem. Biol. **1**(2): 104-111.

Baumann, P. and T. R. Cech (2001). "Pot1, the putative telomere end-binding protein in fission yeast and humans." Science **292**(5519): 1171-5.

Bhattacharyya, A. and E. H. Blackburn (1994). "Architecture of telomerase RNA." EMBO J. **13**(23): 5721-31.

Blackburn, E. H. and J. G. Gall (1978). "A tandemly repeated sequence at the termini of the extrachromosomal ribosomal RNA genes in Tetrahymena." J. Mol. Biol. **120**(1): 33-53.

Blasco, M. A. (2005). "Telomeres and human disease: ageing, cancer and beyond." Nat. Rev. Genet. **6**(8): 611-22.

Blasco, M. A. (2007). "The epigenetic regulation of mammalian telomeres." Nat. Rev. Genet. **8**(4): 299-309.

Bodnar, A. G., M. Ouellette, M. Frolkis, S. E. Holt, C. P. Chiu, G. B. Morin, C. B. Harley, J. W. Shay, S. Lichtsteiner and W. E. Wright (1998). "Extension of life-span by introduction of telomerase into normal human cells." Science **279**(5349): 349-52.

Bokinsky, G. and X. Zhuang (2005). "Single-molecule RNA folding." Acc. Chem. Res. **38**(7): 566-73.

Bosoy, D. and N. F. Lue (2004). "Yeast telomerase is capable of limited repeat addition processivity." Nucleic Acids Res. **32**(1): 93-101.

Bryan, T. M., K. J. Goodrich and T. R. Cech (2000). "A mutant of Tetrahymena telomerase reverse transcriptase with increased processivity." J. Biol. Chem. **275**(31): 24199-207.

Bryan, T. M., K. J. Goodrich and T. R. Cech (2000). "Telomerase RNA bound by protein motifs specific to telomerase reverse transcriptase." Mol. Cell **6**(2): 493-9.

Bryan, T. M., K. J. Goodrich and T. R. Cech (2003). "Tetrahymena telomerase is active as a monomer." Mol. Biol. Cell **14**(12): 4794-804.

Bryan, T. M., J. M. Sperger, K. B. Chapman and T. R. Cech (1998). "Telomerase reverse transcriptase genes identified in Tetrahymena thermophila and Oxytricha trifallax." Proc. Natl. Acad. Sci. U. S. A. **95**(15): 8479-84.

Cate, J. H., R. L. Hanna and J. A. Doudna (1997). "A magnesium ion core at the heart of a ribozyme domain." Nat. Struct. Biol. **4**(7): 553-8.

Cech, T. R. (2004). "Beginning to understand the end of the chromosome." Cell **116**(2): 273-9.

Cech, T. R., T. M. Nakamura and J. Lingner (1997). "Telomerase is a true reverse transcriptase. A review." Biochemistry (Mosc.) **62**(11): 1202-5.

Chamberlin, S. I., E. J. Merino and K. M. Weeks (2002). "Catalysis of amide synthesis by RNA phosphodiester and hydroxyl groups." Proc. Natl. Acad. Sci. U. S. A. **99**(23): 14688-93.

Chappell, A. S. and V. Lundblad (2004). "Structural elements required for association of the Saccharomyces cerevisiae telomerase RNA with the Est2 reverse transcriptase." Mol. Cell. Biol. **24**(17): 7720-36.

Chen, J. L., M. A. Blasco and C. W. Greider (2000). "Secondary structure of vertebrate telomerase RNA." Cell **100**(5): 503-14.

Chen, J. L. and C. W. Greider (2004). "An emerging consensus for telomerase RNA structure." Proc. Natl. Acad. Sci. U. S. A. **101**(41): 14683-4.

Chen, J. L. and C. W. Greider (2004). "Telomerase RNA structure and function: implications for dyskeratosis congenita." Trends Biochem. Sci. **29**(4): 183-92.

Chen, J. L., K. K. Opperman and C. W. Greider (2002). "A critical stem-loop structure in the CR4-CR5 domain of mammalian telomerase RNA." Nucleic Acids Res. **30**(2): 592-7.

Chen, Y., J. Fender, J. D. Legassie, M. B. Jarstfer, T. M. Bryan and G. Varani (2006). "Structure of stem-loop IV of Tetrahymena telomerase RNA." EMBO J. **25**(13): 3156-66.

Cohen, S. B., M. E. Graham, G. O. Lovrecz, N. Bache, P. J. Robinson and R. R. Reddel (2007). "Protein composition of catalytically active human telomerase from immortal cells." Science **315**(5820): 1850-3.

Collins, K. (1999). "Ciliate telomerase biochemistry." Annu. Rev. Biochem. **68**: 187-218.

Collins, K. (2006). "The biogenesis and regulation of telomerase holoenzymes." Nat. Rev. Mol. Cell Biol. **7**(7): 484-94.

Collins, K. and L. Gandhi (1998). "The reverse transcriptase component of the Tetrahymena telomerase ribonucleoprotein complex." Proc. Natl. Acad. Sci. U. S. A. **95**(15): 8485-90.

Collins, K. and C. W. Greider (1993). "Tetrahymena telomerase catalyzes nucleolytic cleavage and nonprocessive elongation." Genes Dev. **7**(7B): 1364-76.

Collins, K. and C. W. Greider (1995). "Utilization of ribonucleotides and RNA primers by Tetrahymena telomerase." EMBO J. **14**(21): 5422-32.

Cong, Y. S., W. E. Wright and J. W. Shay (2002). "Human telomerase and its regulation." Microbiol. Mol. Biol. Rev. **66**(3): 407-25, table of contents.

Cooper, J. P., E. R. Nimmo, R. C. Allshire and T. R. Cech (1997). "Regulation of telomere length and function by a Myb-domain protein in fission yeast." Nature **385**(6618): 744-7.

Crabbe, L. and J. Karlseder (2005). "In the end, it's all structure." Curr. Mol. Med. **5**(2): 135-43.

Cristofari, G., K. Sikora and J. Lingner (2007). "Telomerase unplugged." ACS Chem. Biol. **2**(3): 155-8.

Dandjinou, A. T., N. Levesque, S. Larose, J. F. Lucier, S. Abou Elela and R. J. Wellinger (2004). "A phylogenetically based secondary structure for the yeast telomerase RNA." Curr. Biol. **14**(13): 1148-58.

Das, R., A. Laederach, S. M. Pearlman, D. Herschlag and R. B. Altman (2005). "SAFA: semi-automated footprinting analysis software for high-throughput quantification of nucleic acid footprinting experiments." RNA **11**(3): 344-54.

de Lange, T. (2005). "Shelterin: the protein complex that shapes and safeguards human telomeres." Genes Dev. **19**(18): 2100-10.

Ehresmann, C., F. Baudin, M. Mougel, P. Romby, J. P. Ebel and B. Ehresmann (1987). "Probing the structure of RNAs in solution." Nucleic Acids Res. **15**(22): 9109-28.

Featherstone, C. and S. P. Jackson (1999). "Ku, a DNA repair protein with multiple cellular functions?" Mutat. Res. **434**(1): 3-15.

Forstemann, K. and J. Lingner (2005). "Telomerase limits the extent of base pairing between template RNA and telomeric DNA." EMBO Rep. **6**(4): 361-6.

Fouche, N., I. K. Moon, B. R. Keppler, J. D. Griffith and M. B. Jarstfer (2006). "Electron microscopic visualization of telomerase from Euplotes aediculatus bound to a model telomere DNA." Biochemistry **45**(31): 9624-31.

Friedman, K. L., J. J. Heit, D. M. Long and T. R. Cech (2003). "N-terminal domain of yeast telomerase reverse transcriptase: recruitment of Est3p to the telomerase complex." Mol. Biol. Cell **14**(1): 1-13.

Fu, D. and K. Collins (2003). "Distinct biogenesis pathways for human telomerase RNA and H/ACA small nucleolar RNAs." Mol. Cell **11**(5): 1361-72.

Gilley, D. and E. H. Blackburn (1999). "The telomerase RNA pseudoknot is critical for the stable assembly of a catalytically active ribonucleoprotein." Proc. Natl. Acad. Sci. U. S. A. **96**(12): 6621-5.

Gilley, D., M. S. Lee and E. H. Blackburn (1995). "Altering specific telomerase RNA template residues affects active site function." Genes Dev. **9**(18): 2214-26.

Gottschling, D. E. and T. R. Cech (1984). "Chromatin structure of the molecular ends of Oxytricha macronuclear DNA: phased nucleosomes and a telomeric complex." Cell **38**(2): 501-10.

Greider, C. W. and E. H. Blackburn (1985). "Identification of a specific telomere terminal transferase activity in Tetrahymena extracts." Cell **43**(2 Pt 1): 405-13.

Greider, C. W. and E. H. Blackburn (1989). "A telomeric sequence in the RNA of Tetrahymena telomerase required for telomere repeat synthesis." Nature **337**(6205): 331-7.

Griffith, J. D., L. Comeau, S. Rosenfield, R. M. Stansel, A. Bianchi, H. Moss and T. de Lange (1999). "Mammalian telomeres end in a large duplex loop." Cell **97**(4): 503-14.

Hahn, W. C., S. A. Stewart, M. W. Brooks, S. G. York, E. Eaton, A. Kurachi, R. L. Beijersbergen, J. H. Knoll, M. Meyerson and R. A. Weinberg (1999). "Inhibition of telomerase limits the growth of human cancer cells." Nat. Med. **5**(10): 1164-70.

Hammond, P. W. and T. R. Cech (1998). "Euplotes telomerase: evidence for limited base-pairing during primer elongation and dGTP as an effector of translocation." Biochemistry **37**(15): 5162-72.

Hardy, C. D., C. S. Schultz and K. Collins (2001). "Requirements for the dGTP-dependent repeat addition processivity of recombinant Tetrahymena telomerase." J. Biol. Chem. **276**(7): 4863-71.

Harrington, L. (2003). "Biochemical aspects of telomerase function." Cancer Lett. **194**(2): 139-54.

Hayflick, L. (1965). "The Limited in Vitro Lifetime of Human Diploid Cell Strains." Exp. Cell Res. **37**: 614-36.

Hermann, T. and D. J. Patel (2000). "RNA bulges as architectural and recognition motifs." Structure **8**(3): R47-54.

Huang, H., R. Chopra, G. L. Verdine and S. C. Harrison (1998). "Structure of a covalently trapped catalytic complex of HIV-1 reverse transcriptase: implications for drug resistance." Science **282**(5394): 1669-75.

Huang, Y., A. Beaudry, J. McSwiggen and R. Sousa (1997). "Determinants of ribose specificity in RNA polymerization: effects of Mn2+ and deoxynucleoside monophosphate incorporation into transcripts." Biochemistry **36**(44): 13718-28.

Huard, S., T. J. Moriarty and C. Autexier (2003). "The C terminus of the human telomerase reverse transcriptase is a determinant of enzyme processivity." Nucleic Acids Res. **31**(14): 4059-70.

Jacob, N. K., R. Lescasse, B. R. Linger and C. M. Price (2007). "Tetrahymena POT1a regulates telomere length and prevents activation of a cell cycle checkpoint." Mol. Cell. Biol. **27**(5): 1592-601.

Jacobs, S. A., E. R. Podell and T. R. Cech (2006). "Crystal structure of the essential N-terminal domain of telomerase reverse transcriptase." Nat. Struct. Mol. Biol. **13**(3): 218-25.

Jacobs, S. A., E. R. Podell, D. S. Wuttke and T. R. Cech (2005). "Soluble domains of telomerase reverse transcriptase identified by high-throughput screening." Protein Sci. **14**(8): 2051-8.

Jarstfer, M. B. and T. R. Cech (2002). "Effects of nucleotide analogues on Euplotes aediculatus telomerase processivity: evidence for product-assisted translocation." Biochemistry **41**(1): 151-61.

Kelleher, C., M. T. Teixeira, K. Forstemann and J. Lingner (2002). "Telomerase: biochemical considerations for enzyme and substrate." Trends Biochem. Sci. **27**(11): 572-9.

Keppler, B. R., A. T. Grady and M. B. Jarstfer (2006). "The biochemical role of the heat shock protein 90 chaperone complex in establishing human telomerase activity." J. Biol. Chem. **281**(29): 19840-8.

Keppler, B. R. and M. B. Jarstfer (2004). "Inhibition of telomerase activity by preventing proper assemblage." Biochemistry **43**(2): 334-43.

Kiefer, J. R., C. Mao, J. C. Braman and L. S. Beese (1998). "Visualizing DNA replication in a catalytically active Bacillus DNA polymerase crystal." Nature **391**(6664): 304-7.

Kim, S. H., P. Kaminker and J. Campisi (1999). "TIN2, a new regulator of telomere length in human cells." Nat. Genet. **23**(4): 405-12.

Knappik, A. and A. Pluckthun (1994). "An improved affinity tag based on the FLAG peptide for the detection and purification of recombinant antibody fragments." Biotechniques **17**(4): 754-61.

Kohlstaedt, L. A., J. Wang, J. M. Friedman, P. A. Rice and T. A. Steitz (1992). "Crystal structure at 3.5 A resolution of HIV-1 reverse transcriptase complexed with an inhibitor." Science **256**(5065): 1783-90.

Kreiter, M., V. Irion, J. Ward and G. Morin (1995). "The fidelity of human telomerase." Nucleic Acids Symp. Ser. (33): 137-9.

Kunkel, T. A. (2004). "DNA replication fidelity." J. Biol. Chem. **279**(17): 16895-8.

Kunkel, T. A. and K. Bebenek (2000). "DNA replication fidelity." Annu. Rev. Biochem. **69**: 497-529.

Kyrion, G., K. A. Boakye and A. J. Lustig (1992). "C-terminal truncation of RAP1 results in the deregulation of telomere size, stability, and function in Saccharomyces cerevisiae." Mol. Cell. Biol. **12**(11): 5159-73.

Laemmli, U. K. (1970). "Cleavage of structural proteins during the assembly of the head of bacteriophage T4." Nature **227**(5259): 680-5.

Lai, C. K., J. R. Mitchell and K. Collins (2001). "RNA binding domain of telomerase reverse transcriptase." Mol. Cell. Biol. **21**(4): 990-1000.

Lai, C. K., M. C. Miller and K. Collins (2002). "Template boundary definition in Tetrahymena telomerase." Genes Dev. **16**(4): 415-20.

Lai, C. K., M. C. Miller and K. Collins (2003). "Roles for RNA in telomerase nucleotide and repeat addition processivity." Mol. Cell **11**(6): 1673-83.

Lee, S. R., J. M. Wong and K. Collins (2003). "Human telomerase reverse transcriptase motifs required for elongation of a telomeric substrate." J. Biol. Chem. **278**(52): 52531-6.

Leeper, T., N. Leulliot and G. Varani (2003). "The solution structure of an essential stem-loop of human telomerase RNA." Nucleic Acids Res. **31**(10): 2614-21.

Leeper, T. C. and G. Varani (2005). "The structure of an enzyme-activating fragment of human telomerase RNA." RNA **11**(4): 394-403.

Legassie, J. D. and M. B. Jarstfer (2006). "The unmasking of telomerase." Structure **14**(11): 1603-9.

Lendvay, T. S., D. K. Morris, J. Sah, B. Balasubramanian and V. Lundblad (1996). "Senescence mutants of Saccharomyces cerevisiae with a defect in telomere replication identify three additional EST genes." Genetics **144**(4): 1399-412.

Li, B., S. Oestreich and T. de Lange (2000). "Identification of human Rap1: implications for telomere evolution." Cell **101**(5): 471-83.

Licht, J. D. and K. Collins (1999). "Telomerase RNA function in recombinant Tetrahymena telomerase." Genes Dev. **13**(9): 1116-25.

Lin, J., H. Ly, A. Hussain, M. Abraham, S. Pearl, Y. Tzfati, T. G. Parslow and E. H. Blackburn (2004). "A universal telomerase RNA core structure includes structured motifs required for binding the telomerase reverse transcriptase protein." Proc. Natl. Acad. Sci. U. S. A. **101**(41): 14713-8.

Lingner, J., T. R. Cech, T. R. Hughes and V. Lundblad (1997). "Three Ever Shorter Telomere (EST) genes are dispensable for in vitro yeast telomerase activity." Proc. Natl. Acad. Sci. U. S. A. **94**(21): 11190-5.

Lingner, J., J. P. Cooper and T. R. Cech (1995). "Telomerase and DNA end replication: no longer a lagging strand problem?" Science **269**(5230): 1533-4.

Lingner, J., L. L. Hendrick and T. R. Cech (1994). "Telomerase RNAs of different ciliates have a common secondary structure and a permuted template." Genes Dev. **8**(16): 1984-98.

Lingner, J., T. R. Hughes, A. Shevchenko, M. Mann, V. Lundblad and T. R. Cech (1997). "Reverse transcriptase motifs in the catalytic subunit of telomerase." Science **276**(5312): 561-7.

Livengood, A. J., A. J. Zaug and T. R. Cech (2002). "Essential regions of Saccharomyces cerevisiae telomerase RNA: separate elements for Est1p and Est2p interaction." Mol. Cell. Biol. **22**(7): 2366-74.

Lue, N. F. (2004). "Adding to the ends: what makes telomerase processive and how important is it?" Bioessays **26**(9): 955-62.

Ly, H., L. Xu, M. A. Rivera, T. G. Parslow and E. H. Blackburn (2003). "A role for a novel 'trans-pseudoknot' RNA-RNA interaction in the functional dimerization of human telomerase." Genes Dev. **17**(9): 1078-83.

Mason, D. X., E. Goneska and C. W. Greider (2003). "Stem-loop IV of tetrahymena telomerase RNA stimulates processivity in trans." Mol. Cell. Biol. **23**(16): 5606-13.

Mathews, D. H., M. D. Disney, J. L. Childs, S. J. Schroeder, M. Zuker and D. H. Turner (2004). "Incorporating chemical modification constraints into a dynamic programming algorithm for prediction of RNA secondary structure." Proc. Natl. Acad. Sci. U. S. A. **101**(19): 7287-92.

Maxam, A. M. and W. Gilbert (1977). "A new method for sequencing DNA." Proc. Natl. Acad. Sci. U. S. A. **74**(2): 560-4.

McCall, M., T. Brown and O. Kennard (1985). "The crystal structure of d(G-G-G-G-C-C-C-C). A model for poly(dG).poly(dC)." J. Mol. Biol. **183**(3): 385-96.

McCormick-Graham, M. and D. P. Romero (1995). "Ciliate telomerase RNA structural features." Nucleic Acids Res. **23**(7): 1091-7.

Meier, U. T. (2005). "The many facets of H/ACA ribonucleoproteins." Chromosoma **114**(1): 1-14.

Merino, E. J., K. A. Wilkinson, J. L. Coughlan and K. M. Weeks (2005). "RNA structure analysis at single nucleotide resolution by selective 2'-hydroxyl acylation and primer extension (SHAPE)." J. Am. Chem. Soc. **127**(12): 4223-31.

Michiels, P. J., A. A. Versleijen, P. W. Verlaan, C. W. Pleij, C. W. Hilbers and H. A. Heus (2001). "Solution structure of the pseudoknot of SRV-1 RNA, involved in ribosomal frameshifting." J. Mol. Biol. **310**(5): 1109-23.

Miller, M. C. and K. Collins (2002). "Telomerase recognizes its template by using an adjacent RNA motif." Proc. Natl. Acad. Sci. U. S. A. **99**(10): 6585-90.

Miller, M. C., J. K. Liu and K. Collins (2000). "Template definition by Tetrahymena telomerase reverse transcriptase." EMBO J. **19**(16): 4412-22.

Minchenkova, L. E., A. K. Schyolkina, B. K. Chernov and V. I. Ivanov (1986). "CC/GG contacts facilitate the B to A transition of DNA in solution." J. Biomol. Struct. Dyn. **4**(3): 463-76.

Mitchell, J. R. and K. Collins (2000). "Human telomerase activation requires two independent interactions between telomerase RNA and telomerase reverse transcriptase." Mol. Cell **6**(2): 361-71.

Mollenbeck, M., J. Postberg, K. Paeschke, M. Rossbach, F. Jonsson and H. J. Lipps (2003). "The telomerase-associated protein p43 is involved in anchoring telomerase in the nucleus." J. Cell Sci. **116**(Pt 9): 1757-61.

Moore, M. J. and P. A. Sharp (1992). "Site-specific modification of pre-mRNA: the 2'-hydroxyl groups at the splice sites." Science **256**(5059): 992-7.

Moriarty, T. J., R. J. Ward, M. A. Taboski and C. Autexier (2005). "An anchor site-type defect in human telomerase that disrupts telomere length maintenance and cellular immortalization." Mol. Biol. Cell **16**(7): 3152-61.

Mortimer, S. A. and K. M. Weeks (2007). "A fast-acting reagent for accurate analysis of RNA secondary and tertiary structure by SHAPE chemistry." J. Am. Chem. Soc. **129**(14): 4144-5.

Moyzis, R. K., J. M. Buckingham, L. S. Cram, M. Dani, L. L. Deaven, M. D. Jones, J. Meyne, R. L. Ratliff and J. R. Wu (1988). "A highly conserved repetitive DNA sequence, (TTAGGG)n, present at the telomeres of human chromosomes." Proc. Natl. Acad. Sci. U. S. A. **85**(18): 6622-6.

Nakamura, T. M., G. B. Morin, K. B. Chapman, S. L. Weinrich, W. H. Andrews, J. Lingner, C. B. Harley and T. R. Cech (1997). "Telomerase catalytic subunit homologs from fission yeast and human." Science **277**(5328): 955-9.

Nakano, S., T. Kanzaki and N. Sugimoto (2004). "Influences of ribonucleotide on a duplex conformation and its thermal stability: study with the chimeric RNA-DNA strands." J. Am. Chem. Soc. **126**(4): 1088-95.

Nixon, P. L., A. Rangan, Y. G. Kim, A. Rich, D. W. Hoffman, M. Hennig and D. P. Giedroc (2002). "Solution structure of a luteoviral P1-P2 frameshifting mRNA pseudoknot." J. Mol. Biol. **322**(3): 621-33.

Nugent, C. I., T. R. Hughes, N. F. Lue and V. Lundblad (1996). "Cdc13p: a single-strand telomeric DNA-binding protein with a dual role in yeast telomere maintenance." Science **274**(5285): 249-52.

O'Connor, C. M. and K. Collins (2006). "A novel RNA binding domain in tetrahymena telomerase p65 initiates hierarchical assembly of telomerase holoenzyme." Mol. Cell. Biol. **26**(6): 2029-36.

O'Connor, C. M., C. K. Lai and K. Collins (2005). "Two purified domains of telomerase reverse transcriptase reconstitute sequence-specific interactions with RNA." J. Biol. Chem. **280**(17): 17533-9.

Olovnikov, A. M. (1971). "[Principle of marginotomy in template synthesis of polynucleotides]." Dokl. Akad. Nauk. S.S.S.R. **201**(6): 1496-9.

Oulton, R. and L. Harrington (2004). "A human telomerase-associated nuclease." Mol. Biol. Cell **15**(7): 3244-56.

Pilet, J., J. Blicharski and J. Brahms (1975). "Conformations and structural transitions in polydeoxynucleotides." Biochemistry **14**(9): 1869-76.

Prathapam, R., K. L. Witkin, C. M. O'Connor and K. Collins (2005). "A telomerase holoenzyme protein enhances telomerase RNA assembly with telomerase reverse transcriptase." Nat. Struct. Mol. Biol. **12**(3): 252-7.

Prescott, J. and E. H. Blackburn (1997). "Telomerase RNA mutations in Saccharomyces cerevisiae alter telomerase action and reveal nonprocessivity in vivo and in vitro." Genes Dev. **11**(4): 528-40.

Richards, R. J., C. A. Theimer, L. D. Finger and J. Feigon (2006). "Structure of the Tetrahymena thermophila telomerase RNA helix II template boundary element." Nucleic Acids Res. **34**(3): 816-25.

Richards, R. J., H. Wu, L. Trantirek, C. M. O'Connor, K. Collins and J. Feigon (2006). "Structural study of elements of Tetrahymena telomerase RNA stem-loop IV domain important for function." RNA **12**(8): 1475-85.

Rivera, M. A. and E. H. Blackburn (2004). "Processive utilization of the human telomerase template: lack of a requirement for template switching." J. Biol. Chem. **279**(51): 53770-81.

Romero, D. P. and E. H. Blackburn (1991). "A conserved secondary structure for telomerase RNA." Cell **67**(2): 343-53.

Romi, E., N. Baran, M. Gantman, M. Shmoish, B. Min, K. Collins and H. Manor (2007). "High-resolution physical and functional mapping of the template adjacent DNA binding site in catalytically active telomerase." Proc. Natl. Acad. Sci. U. S. A. **104**(21): 8791-6.

Saenger, W. (1984). Principles of nucleic acid structure. New York, Springer-Verlag.

Sarma, M. H., G. Gupta and R. H. Sarma (1986). "500-MHz 1H NMR study of poly(dG).poly(dC) in solution using one-dimensional nuclear Overhauser effect." Biochemistry **25**(12): 3659-65.

Shakirov, E. V., Y. V. Surovtseva, N. Osbun and D. E. Shippen (2005). "The Arabidopsis Pot1 and Pot2 proteins function in telomere length homeostasis and chromosome end protection." Mol. Cell. Biol. **25**(17): 7725-33.

Shay, J. W. and W. E. Wright (2006). "Telomerase therapeutics for cancer: challenges and new directions." Nat. Rev. Drug Discov. **5**(7): 577-84.

Shay, J. W., Y. Zou, E. Hiyama and W. E. Wright (2001). "Telomerase and cancer." Hum Mol. Genet. **10**(7): 677-85.

Shefer, K., Y. Brown, V. Gorkovoy, T. Nussbaum, N. B. Ulyanov and Y. Tzfati (2007). "A triple helix within a pseudoknot is a conserved and essential element of telomerase RNA." Mol. Cell. Biol. **27**(6): 2130-43.

Smith, S., I. Giriat, A. Schmitt and T. de Lange (1998). "Tankyrase, a poly(ADP-ribose) polymerase at human telomeres." Science **282**(5393): 1484-7.

Smogorzewska, A., B. van Steensel, A. Bianchi, S. Oelmann, M. R. Schaefer, G. Schnapp and T. de Lange (2000). "Control of human telomere length by TRF1 and TRF2." Mol. Cell. Biol. **20**(5): 1659-68.

Sperger, J. M. and T. R. Cech (2001). "A stem-loop of Tetrahymena telomerase RNA distant from the template potentiates RNA folding and telomerase activity." Biochemistry **40**(24): 7005-16.

Stefl, R., L. Trantirek, M. Vorlickova, J. Koca, V. Sklenar and J. Kypr (2001). "A-like guanine-guanine stacking in the aqueous DNA duplex of d(GGGGCCCC)." J. Mol. Biol. **307**(2): 513-24.

Stone, M. D., M. Mihalusova, M. O'Connor C, R. Prathapam, K. Collins and X. Zhuang (2007). "Stepwise protein-mediated RNA folding directs assembly of telomerase ribonucleoprotein." Nature **446**(7134): 458-61.

Strahl, C. and E. H. Blackburn (1994). "The effects of nucleoside analogs on telomerase and telomeres in Tetrahymena." Nucleic Acids Res. **22**(6): 893-900.

Su, L., L. Chen, M. Egli, J. M. Berger and A. Rich (1999). "Minor groove RNA triplex in the crystal structure of a ribosomal frameshifting viral pseudoknot." Nat. Struct. Biol. **6**(3): 285-92.

Taggart, A. K. and V. A. Zakian (2003). "Telomerase: what are the Est proteins doing?" Curr. Opin. Cell Biol. **15**(3): 275-80.

ten Dam, E., A. van Belkum and K. Pleij (1991). "A conserved pseudoknot in telomerase RNA." Nucleic Acids Res. **19**(24): 6951.

Tesmer, V. M., L. P. Ford, S. E. Holt, B. C. Frank, X. Yi, D. L. Aisner, M. Ouellette, J. W. Shay and W. E. Wright (1999). "Two inactive fragments of the integral RNA cooperate to assemble active telomerase with the human protein catalytic subunit (hTERT) in vitro." Mol. Cell. Biol. **19**(9): 6207-16.

Theimer, C. A., C. A. Blois and J. Feigon (2005). "Structure of the human telomerase RNA pseudoknot reveals conserved tertiary interactions essential for function." Mol. Cell **17**(5): 671-82.

Theimer, C. A. and J. Feigon (2006). "Structure and function of telomerase RNA." Curr. Opin. Struct. Biol. **16**(3): 307-18.

Theimer, C. A., L. D. Finger and J. Feigon (2003). "YNMG tetraloop formation by a dyskeratosis congenita mutation in human telomerase RNA." RNA **9**(12): 1446-55.

Theimer, C. A., L. D. Finger, L. Trantirek and J. Feigon (2003). "Mutations linked to dyskeratosis congenita cause changes in the structural equilibrium in telomerase RNA." Proc. Natl. Acad. Sci. U. S. A. **100**(2): 449-54.

Tzfati, Y., T. B. Fulton, J. Roy and E. H. Blackburn (2000). "Template boundary in a yeast telomerase specified by RNA structure." Science **288**(5467): 863-7.

Tzfati, Y., Z. Knight, J. Roy and E. H. Blackburn (2003). "A novel pseudoknot element is essential for the action of a yeast telomerase." Genes Dev. **17**(14): 1779-88.

Ueda, C. T. and R. W. Roberts (2004). "Analysis of a long-range interaction between conserved domains of human telomerase RNA." RNA **10**(1): 139-47.

Vicens, Q., A. R. Gooding, A. Laederach and T. R. Cech (2007). "Local RNA structural changes induced by crystallization are revealed by SHAPE." RNA **13**(4): 536-48.

Wang, H., D. Gilley and E. H. Blackburn (1998). "A novel specificity for the primer-template pairing requirement in Tetrahymena telomerase." EMBO J. **17**(4): 1152-60.

Wang, L., S. R. Dean and D. E. Shippen (2002). "Oligomerization of the telomerase reverse transcriptase from Euplotes crassus." Nucleic Acids Res. **30**(18): 4032-9.

Ware, T. L., H. Wang and E. H. Blackburn (2000). "Three telomerases with completely non-telomeric template replacements are catalytically active." EMBO J. **19**(12): 3119-31.

Watson, J. D. (1972). "Origin of concatemeric T7 DNA." Nat. New Biol. **239**(94): 197-201.

Weeks, K. M. (1997). "Protein-facilitated RNA folding." Curr. Opin. Struct. Biol. **7**(3): 336-42.

Wenz, C., B. Enenkel, M. Amacker, C. Kelleher, K. Damm and J. Lingner (2001). "Human telomerase contains two cooperating telomerase RNA molecules." EMBO J. **20**(13): 3526-34.

Wilkinson, K. A., E. J. Merino and K. M. Weeks (2005). "RNA SHAPE chemistry reveals nonhierarchical interactions dominate equilibrium structural transitions in tRNA(Asp) transcripts." J. Am. Chem. Soc. **127**(13): 4659-67.

Wilkinson, K. A., E. J. Merino and K. M. Weeks (2006). "Selective 2'-hydroxyl acylation analyzed by primer extension (SHAPE): quantitative RNA structure analysis at single nucleotide resolution." Nat. Protoc. **1**(3): 1610-6.

Witkin, K. L. and K. Collins (2004). "Holoenzyme proteins required for the physiological assembly and activity of telomerase." Genes Dev. **18**(10): 1107-18.

Witkin, K. L., R. Prathapam and K. Collins (2007). "Positive and negative regulation of Tetrahymena telomerase holoenzyme." Mol. Cell. Biol. **27**(6): 2074-83.

Wolin, S. L. and E. J. Wurtmann (2006). "Molecular chaperones and quality control in noncoding RNA biogenesis." Cold Spring Harb. Symp. Quant. Biol. **71**: 505-11.

Xia, J., Y. Peng, I. S. Mian and N. F. Lue (2000). "Identification of functionally important domains in the N-terminal region of telomerase reverse transcriptase." Mol. Cell. Biol. **20**(14): 5196-207.

Xin, H., D. Liu, M. Wan, A. Safari, H. Kim, W. Sun, M. S. O'Connor and Z. Songyang (2007). "TPP1 is a homologue of ciliate TEBP-beta and interacts with POT1 to recruit telomerase." Nature **445**(7127): 559-62.

Yang, Q., Y. L. Zheng and C. C. Harris (2005). "POT1 and TRF2 cooperate to maintain telomeric integrity." Mol. Cell. Biol. **25**(3): 1070-80.

Ye, A. J. and D. P. Romero (2002). "Phylogenetic relationships amongst tetrahymenine ciliates inferred by a comparison of telomerase RNAs." Int. J. Syst. Evol. Microbiol. **52**(Pt 6): 2297-302.

Zappulla, D. C. and T. R. Cech (2004). "Yeast telomerase RNA: a flexible scaffold for protein subunits." Proc. Natl. Acad. Sci. U. S. A. **101**(27): 10024-9.

Zappulla, D. C. and T. R. Cech (2006). "RNA as a flexible scaffold for proteins: yeast telomerase and beyond." Cold Spring Harb. Symp. Quant. Biol. **71**: 217-24.

Zappulla, D. C., K. Goodrich and T. R. Cech (2005). "A miniature yeast telomerase RNA functions in vivo and reconstitutes activity in vitro." Nat. Struct. Mol. Biol. **12**(12): 1072-7.

Zaug, A. J. and T. R. Cech (1995). "Analysis of the structure of Tetrahymena nuclear RNAs in vivo: telomerase RNA, the self-splicing rRNA intron, and U2 snRNA." RNA **1**(4): 363-74.

Zuker, M. (1989). "On finding all suboptimal foldings of an RNA molecule." Science **244**(4900): 48-52.